

**ACTIVE PRESSURE DISTRIBUTION
FOR
WALLS RETAINING COHESIONLESS SOILS**

A DISSERTATION

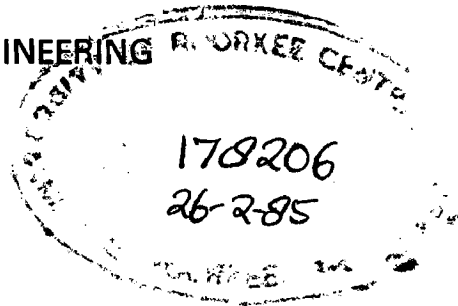
*Submitted in partial fulfilment of the
requirements for the award of the Degree*

of

MASTER OF ENGINEERING

in

EARTHQUAKE ENGINEERING



By

G. K. PANIGRAHY



**DEPARTMENT OF EARTHQUAKE ENGINEERING
UNIVERSITY OF ROORKEE
ROORKEE-247667 (INDIA)**

July, 1984

(i)

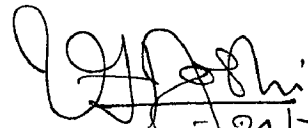
C E R T I F I C A T E

Certified that the dissertation entitled 'ACTIVE PRESSURE DISTRIBUTION FOR WALLS RETAINING COHESIONLESS SOILS' which is being submitted by G.K.Panigrahy in partial fulfilment for the award of the degree of Master of Engineering in Earthquake Engineering, of the University of Roorkee, Roorkee, is a record of student's own work carried out by him under my supervision and guidance. The matter embodied in this dissertation has not been submitted for the award of any other degree or diploma.

This is to further certify that he has worked for an effective period of about five months from January 1984 to July 1984, for preparing the dissertation for Master of Engineering Degree at the University.

Roorkee

Dated July 24, 1984



- 24/7/84

(Dr. V. H. Joshi)
Reader of Soil Dynamics,
Deptt. of Earthquake Engineering
University of Roorkee
Roorkee

A C K N O W L E D G E M E N T S

I wish to express my deep sense of gratitude to Dr. V.H. Joshi, Reader in Soil Dynamics, Department of Earthquake Engineering, for all the help and expert guidance provided by him during the preparation of this Thesis. The valuable hours of discussion, that I had with him have really helped in enlightening my thoughts in the right direction for completion of the work in its present perspective. Work carried out under his guidance would always remain as a deep experience in my memory.

Sincere gratitude is extended to Prof. L.S. Srivastava, Prof. P.N. Agrawal, and Dr. G.I. Prajapati for all the facilities provided during this course of work.

I wish to express my gratitude to Deputy Secretary, Irrigation and Power, Govt. of Orissa for deputing me to this work.

I wish to express my gratefulness to my parents for taking pain to bear the domestic problems during the work.

I would like to express my greatest appreciation to Mrs. Supria Panigrahy for her patience and encouragement during the work.

Sincere thanks are due to Mr. B.K.R. Patnaik, Mr. V.V. Apparao, Mr. Copi Krishna, Mr. J.K. Patnaik, Mr. N. Mohapatro, Mr. K.K. Gupta and Mr. B.K. Sahoo for the help extended to me during the work.

Lastly, I would like to thank the staff of Computer Centre for the facilities given and Mr. Prakash Lal for typing the manuscript and Mr. S.C. Sharma for preparing the drawings.

G.K. PANIGRAHY

A B S T R A C T

Classical earth pressure theories of Coulomb and Rankine for static case and of Mononobe-Okabe for dynamic case consider only force equilibrium condition and neglect moment equilibrium condition. Hence they fail to predict pressure distribution. The method proposed by Prakash and Basavanna can predict static and dynamic active pressure distribution but the assumptions involved do not appear to be reasonable. Since laboratory investigations indicate a non-linear pressure variation with depth even for static case and especially for dynamic case, there is need for development of a better method for this purpose.

The numerical method proposed by Joshi and Prajapati (1982) computes distribution of soil reaction for Mononobe-Okabe rupture wedge by considering equilibrium of discrete wedges. The tangent of the orientation of earth forces with horizontal at vertical interfaces within the rupture wedge is assumed to vary proportionally to distance of the interface from the upper end of rupture surface. With this the point of action of soil reaction is obtained which is useful in computing point of action of earth force using moment equilibrium condition. This method has been adopted for this investigation. The results are presented in terms of dimensionless factors.

The computed pressure distributions for static and dynamic cases are in reasonable agreement with reported experimental results. Use of wall batters leaning away from fill leads to higher forces and overturning moments. Therefore, the walls with vertical back or with slight batter leaning towards the fill should be favoured. Angle of wall friction is related to not only angle of shearing resistance of fill materials but more significantly to angle of wall back and angle of surcharge. The stability of the surcharge slope should be considered in evaluating limiting angle of surcharge. This limiting value if evaluated by using Mononobe-Okabe formula may fail to comply with moment equilibrium. A remedy is suggested to overcome this problem. The point of application of earth force as per IS : 1893-1975 shows tendencies opposite to those predicted by better theoretical methods.

The method used in this investigation is simple and yet effective. It is believed that this method could greatly be used to design and field engineers in design of retaining structures. This is a welcome development for a developing country like India with acute shortage of highly trained technical personnel and sophisticated computing facilities.

NOTATIONS

A	Constant
B	Constant
C_a	Coefficient of active earth pressure by proposed method.
C_{da}	depth factor = X/H
C_{fa}	force factor = $2E_a / \gamma H^2$
C_{fah}	$C_{fa} \times \cos \eta$
C_{ha}	Point of action factor = H_p/H
C_{ma}	moment factor = $6 M_p / \gamma H^3$
C_{moa}	mobilization factor = $P_x / \gamma X$
C_{pra}	pressure factor = $P_x / \gamma H$
C_{prah}	pressure factor due to horizontal component of $P_x = C_{pra} \times \cos \eta$
E_a	active earth force on the retaining structure
H	height of the retaining wall
H_c	depth of tension cracks = $\sqrt{N_c} \quad 4C/\gamma$
H_p	vertical distance from the base of the wall to point of application of E_a
H_t	vertical distance from the top of the wall to point of action of E_a
I	No. of discrete wedges adopted
K_a	coefficient of active earth force by Coulomb/ Mononobe-Okabe/Janbus theory.
K_o	Coefficient of at rest earth pressure
M_p	moment of earth force E_a about the base of the wall
N	power factor

N_{ϕ}	$\tan^2 (45 + \phi/2)$
P_x	pressure behind the wall back at a depth X below the top of the wall
R	soil reaction
S	stress due to soil reaction along the rupture surface
W	weight of the soil in the rupture wedge
W_w	weight of the retaining wall
X	vertical distance from the top of the wall
α	angle of wall back with horizontal
α_h	horizontal seismic coefficient
α_v	vertical seismic coefficient
β	angle of surcharge with horizontals
β_{ℓ}	limiting value of β
γ	unit weight of the soil
δ	angle of wall friction
δ_c	critical angle of wall friction
δ_{cmax}	maximum value of δ_c for a given value of ϕ
$\delta_{cmax\alpha}$	maximum value of δ_{cmax} for a given value of α
$\delta_{c\phi}$	δ_c at a value of ϕ
ϕ	angle of shearing resistance of soil
ϕ_b	angle of friction at the base of the retaining wall
μ	angle between E_a and R
η	angle of E_a with horizontal
η_i	angle of interslice earth force with horizontal at the vertical interface I

e	$\tan^{-1} [\alpha_h / (1 + \alpha_v)]$
ρ	angle of failure surface with the horizontal
ρ_{cr}	critical value of ρ
λ	angle of R with horizontal
ψ	angle between earth force and weight of the wedge

LIST OF FIGURES

FIGURE No.	T I T L E	PAGE NO.
3.1.1	Coulomb's active failure wedge	21
3.1.2	Janbu's active failure wedge	21
3.1.3	Dimensionless static active earth force, C_{fa} , by Coulomb's theory and by Janbu's method of slices	24
3.2.1	Dimensionless dynamic active earth force by Mononobe-Okabe method and by experimentation (Ishii et al, 1960)	27
3.2.2	Dimensionless dynamic active earth force by Mononobe-Okabe method and by experimentation (Jacobsen, 1951)	27
3.3.1	Schematic diagram of soil-wall system for the proposed method of analysis	30
4.4.1	Variation of C_{ma} , C_{ha} and C_{fah} with α	39
4.4.2	Variation of volume of failure wedge with α	42
4.4.3	Distribution of pressure factor, C_{pra} , for various values of α	45
4.4.4	Variation of C_a and N with α	46
4.5.1	Variation of C_{ma} , C_{ha} and C_{fah} with β	48
4.5.2	Variation of C_{ha} with β for various values of ϕ and δ	50
4.5.3	Variation of C_{ha} with β for various values of ϕ for $\alpha_h = 0.1$	51
4.5.4	Variation of pressure factor, C_{pra} , for various values of β	52
4.5.5	Variation of C_a and N with β	54

4.5.6	Values of limiting and allowable β for various values of ϕ and α_h	55
4.6.1	Variation of C_{fa} and μ with δ	58
4.6.2	Distribution of C_{pra} along wall back and pressure due to soil reaction along rupture surface for various values of δ	60
4.6.3	Variation of pressure factor, C_{pra} , for various values of δ	61
4.6.4	Variation of C_{ma} , C_{ha} and C_{fah} with δ	62
4.6.5	Variation of C_a and N with δ	65
4.7.1	Variation of δ_c with ϕ for various values of α	67
4.7.2	Variation of δ_c with α	68
4.7.3	Variation of μ with δ for various values of β	70
4.7.4	Variation of δ_c with ϕ for various values of β	71
4.7.5	Variation of δ_c with ϕ for various values of α	73
4.7.6	Variation of δ_c with α_h for various values of ϕ and α	74
4.7.7	Variation of δ_c with α for various values of ϕ and α_h	75
4.7.8	Variation of δ_c with β for various values of ϕ and α_h	77
4.8.1	Variation of C_{ma} , C_{ha} and C_{fah} with ϕ	81
4.8.2	Variation of pressure factor, C_{pra} , for various values of ϕ	82
4.8.3	Variation of C_a and N with ϕ	83

4.9.1	Variation of C_{ma} , C_{ha} and C_{fah} with α_h for various values of α	85
4.9.2	Variation of C_{ma} , C_{ha} and C_{fah} with α_h for various values of δ	86
4.9.3	Variation of C_{ma} , C_{ha} and C_{fah} with α_h for various values of ϕ	87
4.9.4	Variation of C_{ha} with α_h and α_v for $\beta = 0^\circ$	88
4.9.5	Variation of C_{ha} with α_h and α_v for $\beta = 5^\circ$	90
4.9.6	Variation of C_{ha} with α_h and α_v for $\beta = 10^\circ$	91
4.9.7	Variation of C_{pra} for various values of α_h and α_v	92
4.10.1	Distribution of Acceleration within the Rupture Wedge for active case	95
4.10.2	Variation of C_{ha} with α_h and α_v by different methods	97
4.10.3	Variation of C_{prah} with depth factor C_{da} for static case by different proposals	99

LIST OF TABLES

Table No.	Title	Page No.
3.3.1	Dimensionless Factors	33
4.2.1	Percentage errors with number of discretization	36
4.4.1	Static force factor, C_{fa} , for various values of α	38
4.4.2	Effect of the angle of wall back	41
4.4.3	Percentage increase in weight of the rupture wedge with respect to that for vertical wall	43
4.5.1	Effect of angle of surcharge, β	48A
4.5.2	Values of limiting and allowable β for various values of ϕ and α_h	56
4.6.1	Effect of angle of wall friction, δ	63
4.7.1	Values of δ_c for various values of α and α_h	78
4.7.2	Values of δ_c for various values of β and α_h	78
4.8.1	Effect of angle of shearing resistance, ϕ	80
4.10.1	Distribution of acceleration within the rupture wedge for active case	94

C O N T E N T S

CHAPTER	TITLE	PAGE NO.
	CERTIFICATE	i
	ACKNOWLEDGEMENTS	ii
	ABSTRACT	iii
	NOTATIONS	v
	LIST OF FIGURES	viii
	LIST OF TABLES	xi
1	INTRODUCTION	
	1.1 Preamble	1
	1.2 Scope	3
2	REVIEW OF LITERATURE	
	2.1 General	6
	2.2 Analytical Methods for Static Active Earth Pressures	6
	2.3 Analytical Methods for Dynamic Active Earth Pressures	8
	2.4 Displacement Method of Analysis of Retaining Structures	16
	2.5 Experimental Investigations	17
3	METHODS OF ANALYSIS	
	3.1 Coulomb's Theory for Rigid Retaining Wall	20
	3.2 Theory of Mononobe-Okabe for Dynamic Active Earth Force	25
	3.3 Numerical Method of Analysis Proposed by Joshi and Prajapati	28

4

RESULTS OF THE INVESTIGATION

4.1	Details of the Soil-Wall System Analysed	34
4.2	Degree of Discretization	35
4.3	Orientation of Earth Force at Vertical Interface of Discrete Wedges	37
4.4	Effect of the Angle of Wall Back	38
4.5	Effect of Angle of Surcharge	47
4.6	Effect of the Angle of Wall Friction	57
4.7	Critical Angle of Wall Friction	64
4.8	Effect of Angle of Shearing Resistance	76
4.9	Effect of Seismic Coefficient	79
4.10	Advantages and Limitations of this Investigation	93

5

CONCLUSIONS AND SUGGESTIONS FOR FURTHER
RESEARCH

5.1	Conclusions	104
5.2	Suggestions for Further Research	108

REFERENCES	109
------------	-----

BIODATA	114
---------	-----

CHAPTER - .I

INTRODUCTION

1.1 PREAMBLE

The study of earth pressures dates back to 1776 when Coulomb proposed his famous theory of earth pressures for retaining walls. Nearly a hundred years later Rankine proposed his theory for retaining walls with smooth back. Both these theories do not consider moment equilibrium condition. Therefore, the distribution of earth pressure behind retaining wall has to be assumed. The hydrostatic variation of pressure is commonly assumed. For the dynamic case, Mononobe-Okabe (1929) extended the Coulomb's theory which also neglects moment equilibrium condition and fails to provide pressure distribution.

There are many experimental investigation reported for static and dynamic active earth pressures. The pressure distribution is non-linear for both cases, particularly for the dynamic case. Prakash and Basavanna (1969) proposed a theory to predict pressure distribution using Mononobe-Okabe rupture wedge. However, this theory makes certain assumptions which are not appropriate. Besides, it is not applicable when the surface of the fill is uneven and carries concentrated or distributed surcharge loads. It is also not applicable when the fill is partially submerged.

A numerical method has been proposed by Joshi and Prajapati (1982) for obtaining static and dynamic earth pressure distribution. It considers the Mononobe-Okabe rupture wedge discretized into many smaller sub-wedges. The interslice earth forces are assumed to be parallel to the fill surface at the upper end of the rupture wedge and making a known angle of δ to the normal to the back of the wall. The tangent of the angle of inter slice force for in between vertical faces is assumed to vary proportionally to the horizontal distance between the inter slice face from the upper end of the rupture plane. The equilibrium of the discrete wedges leads to pressure distribution due to soil reaction along the rupture surface. Knowing this, the moment equilibrium condition can be used to determine the point of application of earth force. The earth pressure distribution along the wall back is obtained by using the relation :

$$P_x = \gamma C_a X^N$$

where

P_x = pressure at a depth X below the top of the wall

γ = unit weight of back fill

C_a = active earth pressure coefficient

N = constant (power factor)

N and C_a can be evaluated knowing the magnitude and point of application of earth force, E_a .

This method is quite general in application. It can consider irregular fill surfaces, concentrated and uniformly distributed load as well as partially submerged fills.

1.2 SCOPE

Retaining walls and other retaining structures are most commonly encountered civil engineering structures. They are often small and simple structures, designed and constructed under the supervision of engineers who may not be specialists in the area of earth pressure. Therefore, these problems may not always get the best attention. Any improvement in the design of such structures, therefore, will be reflected in large savings on the national basis. For this purpose, the proposed practice should be simple and easy to use. As far as possible it is desirable to carry out the design calculations using hand calculations or mini computers, wherever available. The numerical method proposed by Joshi and Prajapati (1982) is ideally suited for these needs. Besides, it is also capable of considering a general case of earth retaining structures for static as well as dynamic conditions. Therefore, this method of analysis has been adopted for this investigation.

Only cohesionless soils with angle of shearing resistance in the range of 20° to 40° have been considered in this analysis. Plane surface of surcharge only has been considered. Concentrated and uniformly distributed loads on the fill surface have not been considered. Similarly partially submerged fills and fills subjected to seepage forces have also not been

considered. The analysis is based on pseudostatic approach for the dynamic case, because, the results of experimental investigations by Jacobsen (1951) and Ishii et al.(1960) have indicated that Mononobe-Okabe rupture wedge predicts the dynamic earth force with reasonable accuracy.

Joshi and Prajapati (1982) have reported the results of very limited parametric studies in their presentation. Therefore, it is proposed to carry out extensive parametric studies to investigate the influence of various parameters on the static and dynamic earth pressure distribution behind retaining structures. The parameters studied in this investigation are :

1. Degree of discretization
2. Orientation of inter slice earth force
3. Angle of wall back, α
4. Surcharge angle, β
5. Angle of wall friction, δ
6. Angle of shearing resistance, ϕ
7. Horizontal seismic coefficient, α_h
8. Vertical seismic coefficient, α_v

The results of this investigation have been presented in the form of a set of dimensionless parameters so that they are independent of the size of the retaining structure and the units adopted in the analysis. In the light of the results

of this investigation, the Indian Standard Code of Practice (IS : 1893 -1975) has been critically examined and suggestions for improved practice have been presented.

As far as possible the experimental evidence reported by other investigators have been used to compare the results of this investigation and for supporting the assumptions made in this analysis.

CHAPTER II

REVIEW OF LITERATURE

2.1 GENERAL

The theories proposed by Coulomb (1776) and Rankine (1857) are considered to be the classical earth pressure theories. These are the most commonly used in engineering practice even today. The Coulomb's theory modified by Mononobe and Okabe (1929) for the dynamic case using the principles of pseudostatic analysis is the most popularly used theory for estimating dynamic earth forces even to-day. The experimental evidences appear to support these theories as far as estimation of magnitude of earth force is considered. In this presentation, as far as possible, the emphasis is on review of literature pertaining to static and dynamic active earth forces and pressures.

2.2 ANALYTICAL METHODS FOR STATIC ACTIVE EARTH PRESSURES

Coulomb's theory is based on consideration of extremum methods. It maximises the active earth forces on the wall by varying the angle of the assumed plane surface of failure with the horizontal. This evaluates the angle of critical rupture surface for a given wall friction angle. The critical value of wall friction angle is obtained by minimising the earth forces obtained with the critical rupture planes cited above. The assumption of plane rupture surface appears to be acceptable

as indicated by experimental and theoretical investigations reported, even though the actual rupture surface is somewhat curved. This theory fails to obtain points of application of soil reaction and earth force, because, there is only moment equilibrium condition available to evaluate these two unknowns. Therefore, the earth pressure problem is statically indeterminate. Rankine (1857) assumed that the introduction of smooth wall back does not effect the state of stress when the soil is in Rankine's active state. For this case, the pressure distribution will be hydrostatic.

Jenbu (1957) considered a combination of log spiral at the lower portion and Rankine's active state rupture plane for the upper portion of the rupture surface for cohesionless soil for computing active earth force. He further subdivides the rupture wedge sitting on the log spiral portion into a number of slices. The interslice earth forces on vertical interslice faces are considered to act at the lower one third point of the respective interfaces. The soil reaction is assumed to act at the centre of the base of the slice. The magnitude and direction of the unknown interslice forces and the magnitude of the soil reaction for each slice are obtained by using the three equilibrium conditions. The results of his investigations appear to suggest that the estimates of earth force obtained by using the curved rupture surface suggested are not appreciably different from those obtained by using plane rupture surfaces. Besides, the assumption of existence of

Rankine active zone in the rupture wedge bounded by Rankine rupture plane is not reasonable, because, this is possible only if Rankine's rupture planes in the complimentary directions exist. No experimental evidence is available regarding the existence of this complimentary failure surface. The method also does not predict the distribution of earth pressure behind the wall back.

2.3 ANALYTICAL METHODS FOR DYNAMIC ACTIVE EARTH PRESSURES

The first theoretical study in this field dates back to 1916 when Sano introduced seismic coefficient method for cohesionless soil. He suggested reduction in value of angle of shearing resistance, ' ϕ ' by $\tan^{-1} [\alpha_h / (1 - \alpha_v)]$. This pseudo-reduction in ϕ is contrary to the experimental findings of dynamic tests on cohesionless materials and ϕ appears to have negligible variation under different types of dynamic loadings.

The above cited fallacy was removed by the Mononobe-Okabe theory (1929) which is a modification of Coulomb's theory for dynamic case using the pseudostatic method of analysis. This theory does not consider moment equilibrium condition and arbitrarily assumes hydrostatic dynamic pressure distribution. However, the magnitude of dynamic earth force predicted by this theory has been supported by experimental investigations reported by many investigators. The experimental investigations suggest that the dynamic pressure distribution is

distinctly nonlinear with depth which is contrary to that assumed in this theory.

The dynamic earth pressure coefficient for active case as per Mononobe-Okabe formula is given by :

$$K_a = \frac{(1 \pm \alpha_v) \sec \theta \sin^2 (\alpha + \phi - \theta)}{\sin^2 \alpha \sin(\alpha - \delta - \theta) \left[1 + \sqrt{\frac{\sin(\phi + \delta) \sin(\phi - \beta - \theta)}{\sin(\alpha + \beta) \sin(\alpha - \delta - \theta)}} \right]^2} \quad (2.1.0)$$

where $\theta = \tan^{-1} \frac{\alpha_h}{1 \pm \alpha_v}$

α_h = horizontal seismic coefficient

α_v = vertical seismic coefficient

ϕ = angle of shearing resistance

δ = wall friction angle

β = angle of surcharge

α = angle of wall back with horizontal

For obtaining real solutions, the quantity under the radical sign should not be negative. This gives rise to the relationship :

$$\sin(\phi - \beta - \theta) \leq 0 \quad (2.1.1)$$

or $\phi - \beta - \theta \leq 0$

or $\beta \leq \phi - \theta$

This expression gives the limiting value of β for dynamic case. If a particular value of β is considered then this expression also represents the limiting value of θ as :

$$\theta = \phi - \beta \quad (2.1.2)$$

$$\alpha_h = (1 \pm \alpha_v) \tan (\phi - \beta) \quad (2.1.3)$$

However, it may be observed that these equations are based on force equilibrium conditions only. Therefore, it is quite possible that these relationships may not satisfy moment equilibrium condition. As such there may be situations where permissible value of β or θ may have to be less than the values given by the above equations.

Richards and Elms (1979) have reported that the use of Mononobe-Okabe theory is reasonable if inertia of the wall is also duly accounted for. They have considered the equilibrium of the wall acted upon by the dynamic active earth force predicted by Mononobe-Okabe theory, inertia forces due to mass of wall and the base resistance. Using force equilibrium conditions, they have developed an expression for weight of the wall in terms of dynamic earth pressure coefficient, properties of the soil wall system and seismic coefficient. However, they have not considered passive soil resistance on the open side of the wall and the moment equilibrium condition. Both these limitations render their recommendations to be of limited use for practical purposes.

Kapila (1962) modified Culmann's method of static case for the dynamic condition by considering the inertia forces. This method is otherwise similar to Mononobe-Okabe theory.

Arya and Gupta (1966) considered the horizontal seismic coefficient to vary linearly from base to the top of the retaining wall. Since the design seismic coefficient is based on maximum acceleration at ground level, its effective value is only be $2/3$ of this acceleration. This discrepancy could result into unsafe estimation of earth force. Besides, no justification for linear variation of the seismic coefficient has been given by these authors. Prakash and Saran (1966) have given dimensionless earth pressure factors for obtaining static and dynamic earth force for a $c - \phi$ soil. The gravity effects, surcharge load effects and the effect of cohesive force are considered separately and principle of superposition is utilised for obtaining the expression for active earth force. The effect of tension cracks has also been considered by truncating the plane failure surface at the point where it meets a vertical crack of depth, H_c , below the surface of the fill where $H_c = (4c/\gamma) \sqrt{N_\phi}$. The dimensionless factors may be read from charts for various values of cohesion of soil, c , angle of shearing resistance, ϕ , angle of wall friction, δ , ratio of H_c to depth of fill, the horizontal and vertical seismic coefficients, and the surcharge load on the surface of the fill. This theory does not predict pressure distribution. It does not consider moment equilibrium condition. The principle of superposition results into independent maximisation of earth force. The assumption of the depth of tension cracks, H_c , cited above for the dynamic case is questionable, because, the soil may not be capable of withstanding such cracks under

the increased lateral forces due to dynamic conditions.

Madhav and Rao (1969) presented design curves for earth pressure coefficient in terms of soil properties, angle of wall friction, angle of wall back, angle of surcharge and the seismic coefficients using pseudostatic analysis. The direction of resultant inertia force was optimised to obtain maximum earth force. They recommended that the worst combination of the vertical and horizontal seismic coefficient should be considered for design purposes. Prakash and Basavanna (1969) pointed out that if the pressure due to soil reaction and the earth force vary linearly then the resultant earth force, soil reaction and the weight of the rupture wedge are not concurrent. This means that the moment equilibrium condition is not satisfied. This is true even for the rupture wedge of Mononobe-Okabe theory for dynamic case. To overcome this deficiency they have proposed a method of analysis which considers all the three equilibrium conditions of an element of soil parallel to the surface of the fill. They have suggested that the distribution of earth pressure is similar to that of the soil reaction along the rupture surface. For determining rupture surface, the pressure on the wall and the moments were separately maximized. Since these two approaches did not give identical results, the maximum moment was considered for retaining wall in computing pressure. The results of their theoretical investigation have been presented in the form of dimensionless coefficients.

Basavanna (1970) modified the earlier work of Prakash and Basavanna where it was assumed that full friction along rupture surface is mobilised even when component of body forces parallel and perpendicular to the fill surface were acting separately. This discrepancy was eliminated and another set of coefficients was presented. They are not applicable for $C - \phi$ soils and for soils with irregular surface of fill carrying concentrated or distributed loads. They also assumed that the vertical stress within the rupture wedge is given by the vertical column of soil at that point. This is not correct, because, each vertical column of soil standing on the rupture surface transfers a portion of the vertical force associated with that slice to the adjacent column of soil on the wall side. This invariably leads to a vertical stress larger than that due to vertical soil column at the point under consideration within the rupture wedge. Besides, this theory cannot be used for partially submerged fills.

Nandkumaran and Joshi (1973) considered that if a failure wedge is developed under static active condition, a new failure wedge is not likely to be developed under dynamic condition. This was substantiated by the experimental investigations carried out by Nandkumaran. Using this proposition, the earth force on the wall for dynamic condition was obtained by using pseudostatic analysis. By further assuming that no tension can develop on the rupture surface, and by superposition of the dynamic increment on the static forces the magnitude

and point of application of dynamic pressures has been determined. It was found that the point of application of dynamic increment is influenced by the geometry of the problem and the design seismic coefficient. In general, the point of application of the dynamic increment lies within the middle third segment of the wall back.

Joshi and Prajapati (1982) have proposed a numerical method for obtaining distribution of pressure due to soil reaction by considering equilibrium of discrete wedges. The failure wedge considered is that proposed by Mononobe-Okabe. Knowing the pressure distribution due to soil reaction, the point of application of the soil reaction can be obtained. Now it is possible to use the moment equilibrium condition to evaluate the point of application of the earth force. Knowing the magnitude and point of application of earth force, the distribution of pressure along the wall back for the static and dynamic conditions may be obtained by the expression :

$$P_x = \gamma C_a X^N$$

It appears that this theory is reasonable, because, the earth force predicted by Mononobe-Okabe theory is in good agreement with the experimental results reported by many investigators. This theory is free from the draw backs associated with the assumptions of Prakash and Basavanna (1969) and Basavanna(1970). The additional advantage of this method is that it can consider partially submerged fills, fills with irregular surface and

concentrated or distributed loads. However, they have presented the results of only a limited parametric studies in their publication.

Matsuo and Ohara (1960) computed active earth pressures by considering an elastic backfill under plane strain condition. This theory computes the earth forces separately for the cases of moving wall and rigid wall. The net force is obtained by the sum of the forces for these two cases. The results of their investigation indicate good agreement with those by Mononobe-Okabe theory. However, Scott (1973) states that the theory gives pressures and moments much larger than those by Mononobe-Okabe theory.

Ishii et al. (1960) developed a theory for dynamic earth forces which is similar to that of Matsuo and Ohara. For the case of fixed wall the soil is assumed to be visco-elastic and for the moving wall the soil is assumed to be elastic but the weight of the wall is also considered.

Aggour and Brown (1973) have used finite element idealization for wall soil system subjected to sinusoidal ground motion. Contact between wall and soil is assumed throughout the duration of shaking. The parameters studied in this investigation are : flexibility of wall, soil modulus and length and shape of back-fill. They concluded that the pressure near the top of a flexible wall is smaller than that for a rigid wall. Besides, dynamic pressures were found to depend very much on static pressures.

Nadim and Whitman (1983) carried out investigations using finite element method of analysis with slip elements to represent interface between wall and the fill and also the rupture surface for the study of dynamic earth pressures. Sinusoidal base excitation was adopted. The results indicate that the wall moves nearly in step wise fashion.

2.4 DISPLACEMENT METHOD OF ANALYSIS OF RETAINING STRUCTURES

In engineering practice, the criteria of satisfactory performance is generally based on displacements or deformations. Only for relatively brittle materials, the concept of factor of safety based on ultimate and allowable loads, may be meaningful. Therefore, for the case of retaining structures, it is more logical to relate the earth force to wall movement for both static and dynamic conditions. Methods have been proposed by some investigators for this purpose. (Newmark; 1965, Nandakumaran; 1973, Richards and Elms; 1979, Joshi and Mukherjee; 1981, and Prakash and Puri; 1981) .

The scope of this investigation is to compute the maximum value of dynamic active earth force. It is presumed that sufficient wall motion takes place to develop static or dynamic active state behind the retaining wall. Therefore, the displacement method of analysis of retaining structures is not discussed in detail over here.

2.5 EXPERIMENTAL INVESTIGATIONS

Experimental investigations are mainly to evaluate the results of the earth pressure theories. Besides, they will be helpful in formation of better theoretical models since experimentation gives reasonable idea about the mechanics involved.

Mononobe and Matsuo have tested sand inside a box mounted on horizontal shake table producing sinusoidal excitation. Maximum pressure measured by hydraulic gages indicated that observed pressures were in good agreement with those predicted by Mononobe-Okabe theory.

Matsuo (1941) used similar set-up. He observed that dynamic component of earth force acts at $2/3$ height of the wall.

Jacobsen (1951) tested three foot high retaining wall model in a box mounted on shake table using sand as the fill material. His results showed that measured earth force agreed reasonably with that predicted by Mononobe-Okabe formula. However, dynamic component was found to act at upper third point of the wall. The restraint provided by dynamo-meters used to measure the earth force might have some effect on the test results.

Matsuo and Ohara (1960) performed test on 1.5 m high concrete wall of 0.9 m thickness in a pit. Vibrations were generated externally by 1 Hp oscillator mounted on a burried trough 4.5 m away from the wall and another on the wall

top. Pressure cells were used to measure pressures. The dynamic pressures were observed to act at 1/3rd point near the top.

Ishii, et al (1960) conducted tests on 70 cm high wall in a box, 400 cm long. The wall was also provided with foundation soil. Types of movements of walls considered are : translation, rotation about bottom, combination of both and no motion of the wall. Period of the sinusoidal table motion was 0.3 sec. Table acceleration upto 1000 gals at 100 gals intervals were adopted. They observed that total dynamic earth force consisted of a non-fluctuating component and an oscillating component. The sum of the two compare well with that of Mononobe-Okabe. The oscillator component of the force is relatively very small. Rupture surfaces were visible only for accelerations greater than 500 gals. The distribution of acceleration within the soil fill indicate that the acceleration near the wall are comparable to those near the centre of the box. Besides, the acceleration near the wall at various depth differ by only 10 to 15 percent which is in reasonable agreement with the observations reported by Seed and Whitman (1970).

Murphy (1960) conducted tests on rubber models of retaining walls. He found that slip surface for dynamic case is much flatter than that for static case.

Nandakumaran (1973), carried out test on retaining wall models with cohesionless fill. He observed that if a failure surface is developed under static condition, then the dynamic loading causes further displacements of this static rupture wedge instead of developing new flatter rupture surfaces. He concluded that the pressures give better tally when correlated with velocity rather than acceleration. He used impact loading with pendulum weight for dynamic loading. Dynamic loading was also produced by dropping the weight on the ground at some distance away from the test wall. He observed that the pressure distribution for dynamic case is curvilinear but the resultant was considerably below upper middle third of the wall. However, it may be noticed that he used very high levels of horizontal accelerations of the order of 4g.

Sim and Berrill (1979) conducted shake table test on gravity retaining wall model. They have reported that the walls translate outward in step-wise fashion as predicted by the analytical model proposed by Richards and Elms.

From this review, it appears to be reasonable to presume that the dynamic earthforce observed from the tests agree well with that predicted by Mononobe-Okabe theory. Besides, it appears that the point of application of the dynamic earth force acts between the upper and lower middle third points. Very few attempts have been made to obtain pressure distribution behind the retaining wall. Therefore, it may be stated that there is an urgent need for developing a simple and effective method for this purpose.

CHAPTER III

METHOD OF ANALYSIS

3.1 COULOMBS THEORY FOR RIGID RETAINING WALL

The theory of earth pressure proposed by Coulomb(1776) is by far the most popularly used. Even though, two centuries have passed after it was proposed, not much has been done to improve this proposition as far as the estimation of magnitude of earth force is considered.

The assumptions made in Coulomb's theory are as follows :

1. The backfill is homogeneous isotropic and either completely submerged or dry.
2. The wall yields sufficiently so that the backfill reaches the active state.
3. The slip surface is a plane passing through the heel of the wall and the shearing resistance along this plane is fully mobilized.
4. The back of the wall is rough. The earth force makes an angle δ with the normal to the wall back.

For obtaining the expression for active earth force on the wall back, an arbitrary plane failure making an angle of θ with the horizontal is assumed as shown in Fig.3.1.1. The forces keeping the rupture wedge in equilibrium are : the weight of the wedge, W , soil reaction, R , and the active earth force, E_a .

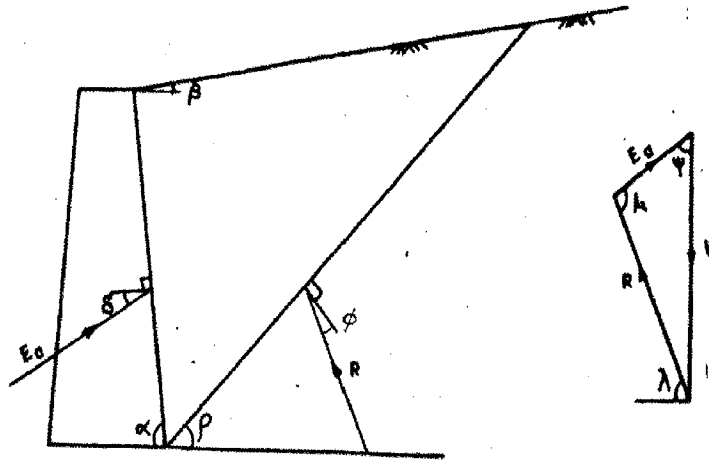


FIG. 3.1.1 - COULOMB'S ACTIVE FAILURE WEDGE

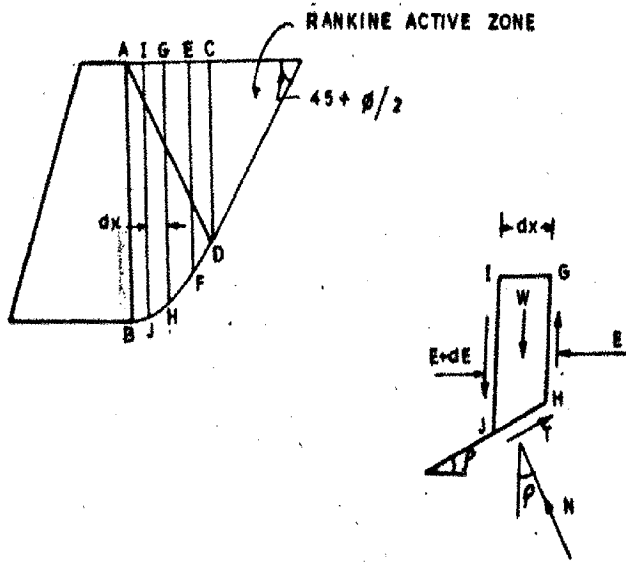


FIG. 3.1.2 - JANBU'S ACTIVE FAILURE WEDGE

The magnitude and direction of W and the directions of E_a and R are known. Hence, the magnitudes of E_a and R can be evaluated by considering the equilibrium of the rupture wedge.

Coulomb's theory utilises the extremum method. For a given value of δ and other parameters, the value of ρ is varied to maximise the earth force on the wall. This force is the active earth force and the corresponding value of ρ is the angle of critical failure surface. However, these values of ρ and E_a are true for an assumed value of δ or the corresponding angle ψ defined as $(\alpha - \delta)$. Therefore, to get unique value of E_a and ρ , it is necessary to minimise the value of E_a to obtain the critical value of δ . These conditions may be expressed as

$$\frac{\partial E_a}{\partial \rho} + \frac{\partial E_a}{\partial \psi} = 0 \quad (3.1.1)$$

Equation 3.1.1 can be solved in stages. In the first stage E_a is maximised by changing the values of ρ to obtain critical values, ρ_{cr} and E_{acr} for an assumed value of δ . In the second stage the value of E_a is minimised with respect to δ using the values of E_a and ρ obtained above to find out δ_c and the corresponding values of E_a and ρ will satisfy the Eqn.3.1.1.

The earth force is expressed as :

$$E_a = \frac{1}{2} \gamma K_a H^2 \quad (3.1.2)$$

where γ = unit weight of soil

K_a = coefficient of active earth force

H = height of wall

The coefficient of earth force is given by

$$K_a = \frac{\sin^2(\alpha + \phi)}{\sin^2\alpha \sin(\alpha - \delta) \left[1 + \frac{\sin(\phi + \delta) \sin(\phi - \beta)}{\sin(\alpha - \delta) \sin(\alpha + \beta)} \right]^2} \quad (3.1.3)$$

Coulomb in his original presentation did not propose earth pressure distribution. He only obtained expression for the magnitude of earth force.

Muller and Breslau (1916) carried out tests on 60 cm high retaining walls and concluded that the rupture slightly curved at the lower end and that the earth force was comparable to that predicted by Coulomb's theory. Fulton (1920), Franzius (1924), Terzaghi (1928-29), Johnson (1953) and many others have also reported similar observations based on their test results.

As explained in Chapter 11, the results of the analytical investigation carried out by Janbu (1957) using a combination of log spiral for the lower portion and Rankine's plane surface for the upper portion of the rupture failure surface (Fig. 3.1.2) have indicated that the magnitude of the earth force predicted by his method agrees reasonably with that of Coulomb which may be observed from Fig. 3.1.3. It may also be observed from this figure that the magnitudes of active earth force predicted by the two methods are identical for a smooth wall. For wall with $\tan \delta = \tan \phi / 2$, the discrepancy between the two is 8.8 percent and for a wall with $\delta = \phi$,

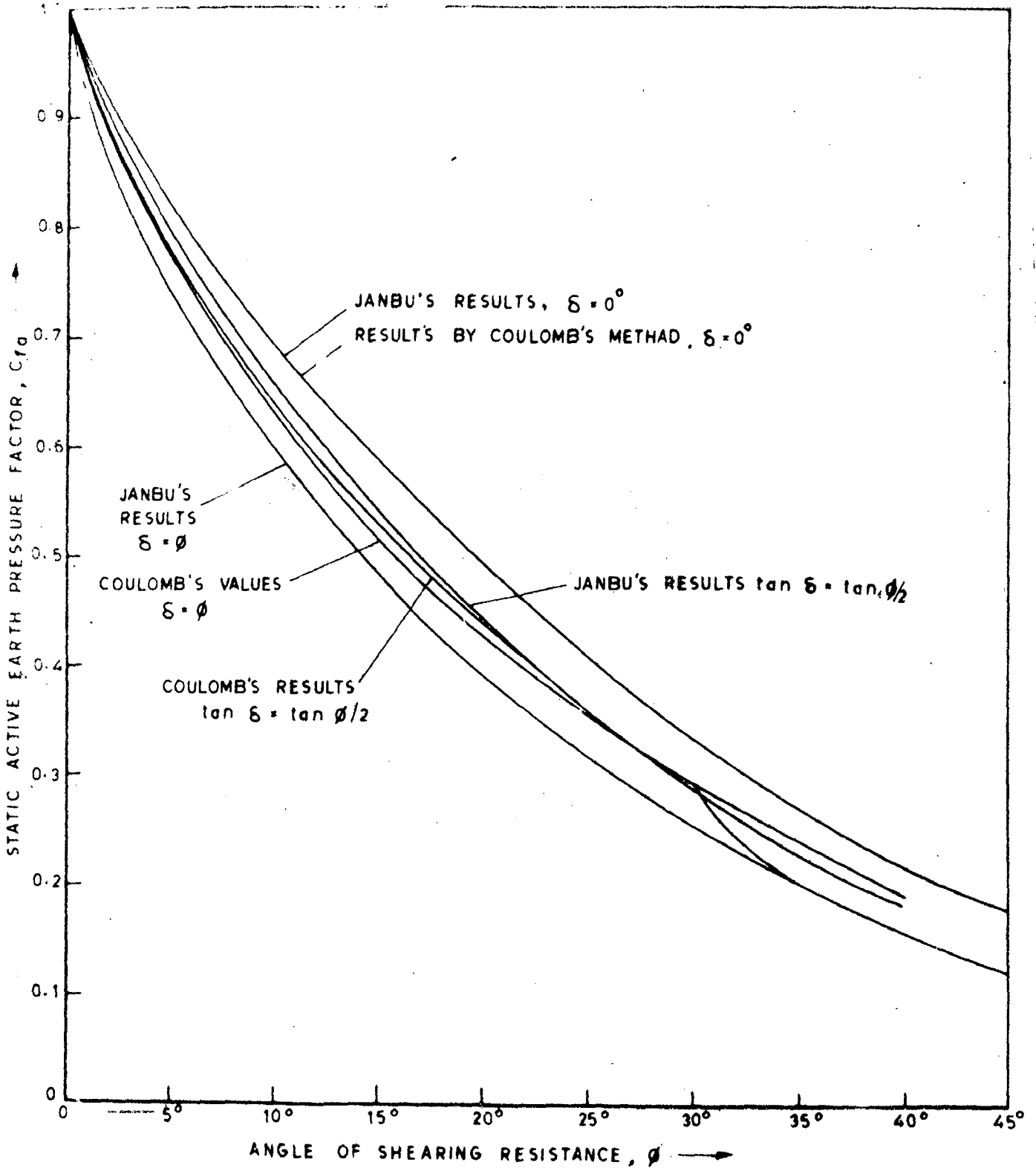


FIG. 3.1.3 - FORCE FACTOR, C_{fa} FOR STATIC ACTIVE CASE BY COULOMB AND BY JANBU (1957)

the discrepancy is 13.5 percent with the value associated with plane surface of failure being higher for both cases. This indicates that the use of plane surface of failure for active case is quite reasonable and leads to some what conservative estimates of active earth force for the static case.

3.2 THEORY OF MONONOBE-OKABE FOR DYNAMIC ACTIVE EARTH FORCE

The Coulomb's theory was extended for dynamic earth force by Mononobe and Okabe (1929). They have considered the equilibrium of failure wedge for the dynamic case by incorporating the vertical and horizontal inertial forces using principles of pseudostatic analysis. The active earth force predicted by this theory is expressed as :

$$E_a = \frac{1}{2} K_{ad} \gamma H^2 \quad (3.2.1)$$

and the coefficient of dynamic earth force K_{ad} is given by

$$K_a = \frac{(1 \pm \alpha_v) \sec \theta \sin^2 (\alpha + \phi - \theta)}{\sin^2 \alpha \cdot \sin(\alpha - \delta - \theta) \left[1 + \sqrt{\frac{\sin(\alpha + \delta) \sin(\phi - \beta - \theta)}{\sin(\alpha + \beta) \sin(\alpha - \delta - \theta)}} \right]^2} \quad (3.2.2)$$

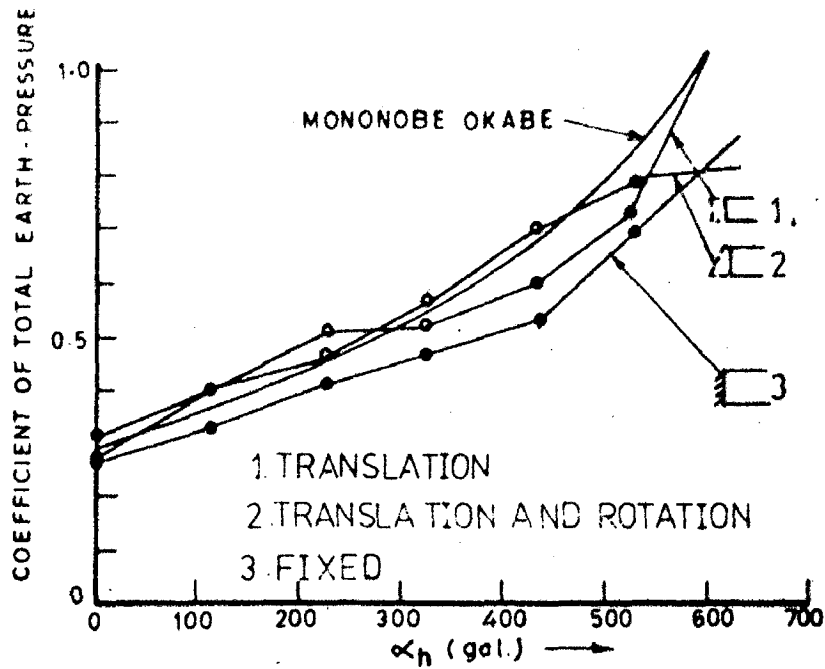
where $\tan \theta = \frac{\alpha_h}{1 \pm \alpha_v} \quad (3.2.3)$

In this presentation, the vertical inertia force is directed downward when seismic coefficient α_v is positive and the horizontal inertia force is directed towards the wall when seismic coefficient, α_h , is positive.

Ishii et al (1960) carried out extensive experimental investigations using laboratory tests. Even though they did not observe development of rupture surface for horizontal accelerations upto 500 gals, the values of dynamic earth force tallies well with that predicted by Mononobe-Okabe theory. It is clear from Fig.3.2.1 in which the experimental values of dimensionless earth force for a fixed wall, wall having translatory ^{ve}moment and combined translation and rotation are compared with those predicted by Mononobe-Okabe theory.

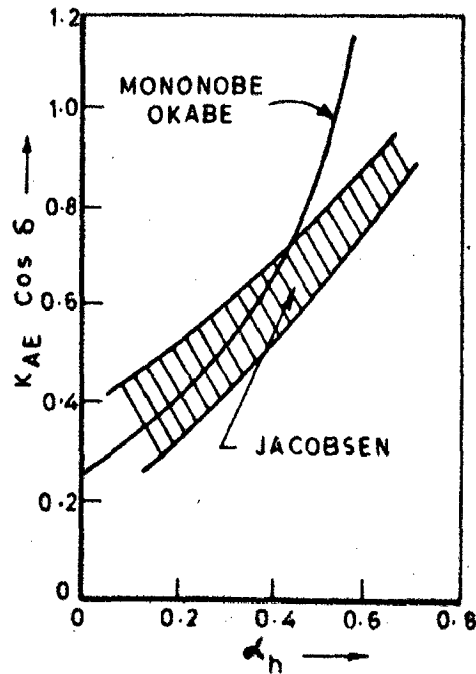
Experiments were also carried out by Jacobsen (1951). The values of the dimensionless earth forces obtained by him experimentally fall within a narrow shaded band shown in Fig. 3.2.2. It may be observed that the corresponding values predicted by Mononobe-Okabe theory also fall within the same band. Similar observation were reported by Matsuo (1941) and Mononobe and Matsuo (Nandakumaran, 1973).

From this discussion it may be concluded that even though the rupture surface may not be formed visibly for horizontal acceleration coefficient less than 0.5, the Mononobe-Okabe theory predicts the dynamic active earth pressure reasonably well. On similar lines, the plane rupture surface assumed for the Coulomb's case is considered to be reasonable for the static active case. Therefore, in this investigation the plane rupture surface predicted by Coulomb's theory for static case and Mononobe-Okabe theory for dynamic case have been adopted.



EXPERIMENTATION (ISHII ETAL, 1960)

FIG. 3.2.1 - DIMENSIONLESS DYNAMIC ACTIVE EARTH FORCE



EXPERIMENTATION (JACOBSEN, 1951)

FIG. 3.2.2 - DIMENSIONLESS DYNAMIC ACTIVE EARTH FORCE

3.3 NUMERICAL METHOD OF ANALYSIS PROPOSED BY JOSHI AND PRAJAPATI

Joshi and Prajapati (1982) have proposed a numerical method of analysis for obtaining distribution of earth pressure behind a retaining wall for static and as well as dynamic cases using the rupture wedge predicted by Coulomb's theory and Mononobe-Okabe's theory respectively. The assumptions made in this investigation are as follows :

1. The backfill is a cohesionless material.
2. Rupture surface is a plane passing through the heel of the wall.
3. Angle of wall friction, δ , is known.
4. The wall is a rigid body.
5. Displacement conditions required for active state behind the wall are realised.
6. For dynamic case it is further assumed that pseudo-static analysis is adequate.
7. Seismic coefficient for the entire failure wedge remains the same and is a known quantity.
8. The direction of interslice earth force on a vertical interface within the failure wedge varies from angle, δ , normal to the wall back to the direction parallel to the earth fill surface at the top end of the rupture surface.

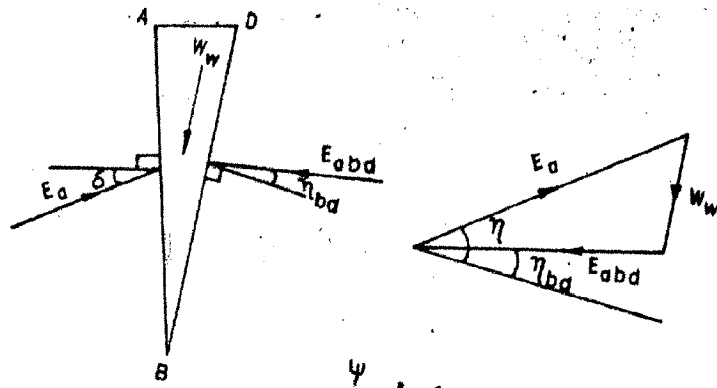
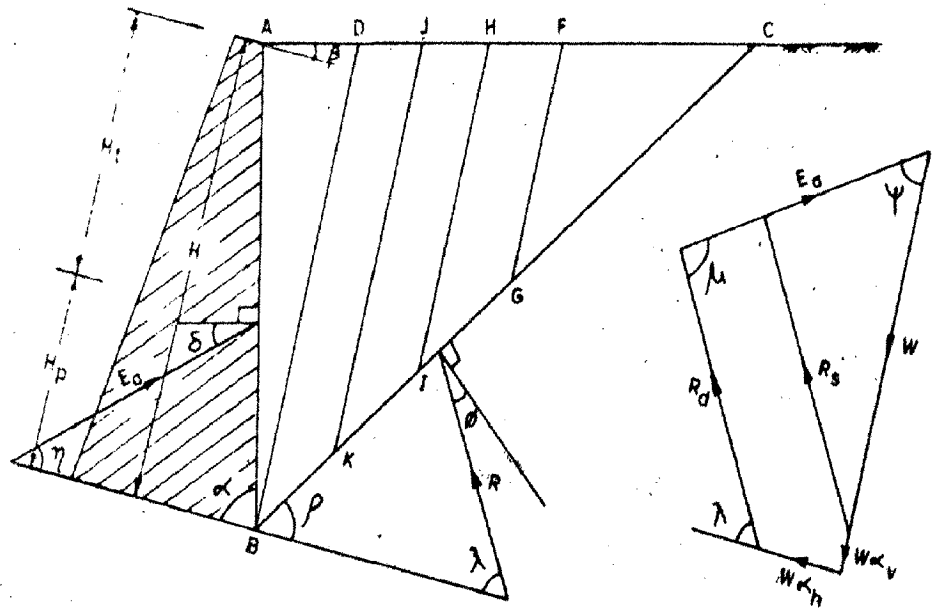
For this case the magnitude and direction of the weight of the wedge, the vertical and horizontal inertia forces as well as the directions of earth force and the soil

reactions are known. Therefore, the magnitudes of earth force and soil reaction can be evaluated from equilibrium conditions. The failure wedge may be discretized as shown in Fig.3.3.1 into a number of smaller wedges, with vertical interfaces. For the wall with angle of wall back, α , less than 90° , the equilibrium of the triangular wedge ABD will evaluate the magnitude and direction of the inter slice force K_{bd} and its direction with horizontal η_{bd} . The angle of interface earth force, E_{ih} , on the interface IH may be obtained as :

$$\tan \eta_{ih} = \tan \beta + (\tan \eta_{bd} - \tan \beta) CH/CD$$

Consider equilibrium of the first discrete wedge CFG. All the forces acting on this wedge are known in magnitude and direction except the soil reaction R_{gc} and interface earth force E_{gf} for which only the direction is known. Their magnitudes can be obtained by considering the equilibrium of this discrete wedge. For a sufficiently small size of the wedge, the pressure due to soil reaction along the CG may be assumed to vary linearly with reasonable accuracy, and thus the intensity of pressure due to soil reaction, S_g , at point G on the rupture surface may be obtained.

On similar lines by considering the equilibrium of the next discrete wedge CIH, it is possible to evaluate the magnitude of the soil reaction, R_{ic} , and hence, the incremental soil reaction, R_{ig} , acting along the segment of rupture surface IG. Knowing the intensity of pressure due to soil reaction, S_g , that at



$$\begin{aligned} \psi &= (\alpha - \delta) \\ \lambda &= (90 - \rho + \theta) \\ \eta &= (90 - \alpha + \delta) \\ \mu &= (\eta + \lambda) \end{aligned}$$

FIG. 3.3.1 - SCHEMATIC DIAGRAM OF SOIL WALL SYSTEM FOR THE PROPOSED METHOD OF ANALYSIS

point I can be evaluated by assuming linear variation of pressure intensity along IG. On similar lines, the pressure intensities all along the rupture surface may be obtained by considering the equilibrium of the successive discrete wedges. With the help of this information the point of application of the soil reaction, R, can be obtained. It is now possible to consider the moment equilibrium condition for the entire failure wedge ABC to evaluate the point of application of the earth force E_a .

The earth pressure P_x at a depth x below the top of the wall may be expressed as

$$P_x = \gamma C_a X^N \quad (3.3.1)$$

where

C_a = coefficient of earth pressure

N = constant

Knowing the magnitude and point of application of E_a , the expressions for C_a and N are obtained as follows:

$$N = (2H_T - H \cos \delta) / (H \cos \delta - H_T) \quad (3.3.2)$$

$$C_a = E_a(N+1) / (H^{N+1}) \quad (3.3.3)$$

The power factor, N , governs the rate of increase of earth pressure with increasing depth. If N is greater than unity, the rate of increase in pressure increases with depth. It varies linearly with depth if N is unity. For N less than unity and greater than zero the intensity of pressure keeps increasing with depth below the wall top through out. If N is

equal to zero then the pressure remains constant throughout. For negative values of N, the pressure at first increases with depth to reach a peak and then decreases with further increase in depth.

Coefficient of earth pressure, C_a , has dimensions which can be evaluated by putting the dimensions of various quantities defining pressure as follows :

$$P_x = \gamma C_a X^N \quad (3.3.4)$$

i.e.

$$ML^{-1} T^{-2} = (MLT^{-2} L^{-3})(C_a)L^N \quad (3.3.5)$$

or $C_a = L^{1-N} \quad (3.3.6)$

Therefore, C_a has the units of $L^{(1-N)}$

However, it may be noted that the value of C_a does not change with depth of the earth fill. It's values are expressed in meter to the power of $(1-N)$ for various cases. In this chapter, for all practical purposes, this parameter may be considered to be a constant for a given set of data. To convert it from metric units to feet units, it may be multiplied by $0.328^{(1-N)}$. The results of this investigation have been presented in the form of dimensionless factors given in Table 3.3.1.

TABLE 3.3.1 : DIMENSIONLESS FACTORS

Sl.No.	Factor	Symbol	Definition
1	Depth factor	C_{da}	X/H
2	Pressure factor	C_{pra}	$P_x/(\gamma H)$
3	Mobilization factor	C_{moa}	$P_x/(\gamma X)$
4	Point of action factor	C_{ha}	H_p/H
5	Force Factor	C_{fa}	$2E_a/(\gamma H^2)$
6.	Moment factor	C_{ma}	$6E_a/(\gamma H^3)$
7.	Power factor	N	-

The discussion given in this chapter covers the details of the method of analysis adopted for this investigation. The details of the soil wall system, the material properties and the details of the proposed parametric studies have been already explained in Chapter I. The analysis has been carried out using DEC-2050 computer available with the Computer Center, University of Roorkee.

CHAPTER - IV

RESULTS OF THE INVESTIGATION

4.1 DETAILS OF THE SOIL WALL SYSTEM ANALYSED

The schematic diagram of the soil wall system considered for this investigation is shown in Fig.3.3.1. A rigid retaining wall of 3 m height retaining dry homogeneous and isotropic cohesionless backfill of unit weight 1.9 t/m^3 has been considered.

The various parameters and the range of their variation considered are as follows :

1. Degree of discretization of the failure wedge.
2. Orientation of earth forces at vertical interfaces of discrete wedges.
3. Angle of wall back, $\alpha = 70^\circ, 80^\circ, 90^\circ, 100^\circ, 110^\circ$.
4. Angle of surcharge, $\beta = 0^\circ, 5^\circ, 10^\circ, 15^\circ, 20^\circ$.
5. Angle of wall friction, $\delta = 0^\circ, 5^\circ, 7.5^\circ, 10^\circ, 15^\circ, 20^\circ, 25^\circ, 30^\circ, 35^\circ, 40^\circ$.
6. Angle of shearing resistance of the backfill, $\phi = 20^\circ, 25^\circ, 30^\circ, 35^\circ, 40^\circ$.
7. Horizontal seismic coefficient, $\alpha_h = 0.0, 0.05, 0.1, 0.15, 0.2, 0.3$.
8. Vertical seismic coefficient, $\alpha_v = 0.0, 0.05, 0.1, 0.15, -0.05, -0.1, -0.15$.

The results of the investigation have been presented in the form of non-dimensional factors listed in Table 3 3.1.

4.2 DEGREE OF DISCRETIZATION

The degree of discretization depends upon the number of discrete wedges considered in the analysis. The larger the number, the greater the degree of accuracy of the results in the analysis. However, the larger the number of discrete wedges considered, the greater the computational effort required for the solution. Therefore, it is desirable to arrive at the optimum discretization giving reasonably accurate results at relatively small computational effort. For this purpose the analysis was carried out for the case of $\phi = 32.5^\circ$, $\delta = 15^\circ$, $\beta = 0^\circ$, $\alpha = 90^\circ$ using 5, 10, 15, 20, 25 and 30 wedges for static and dynamic cases with $\alpha_h = 0.1$ and 0.2. The parameters which are greatly influenced by the degree of discretization are the stress intensities due to soil reaction along the rupture surface, the point of action factor, C_{ha} , and the moment factor, C_{ma} . Therefore, the percentage errors in computed values of these parameters using different degrees of discretization have been listed in the Table 4.2.1 with the results obtained from the analysis using 30 discrete wedges as the basis of comparison. It is clear from this table that the largest percentage error for any of these parameters is much less than 0.01 percent even when only five discrete wedges are considered for the analysis. The order of error is the same even for the dynamic case with

TABLE 4.2.1 : EFFECT OF DEGREE OF DISCRETIZATION

$H = 3 \text{ m}$, $\gamma = 1.41 \text{ t/m}^3$, $\alpha = 90^\circ$, $\beta = 0^\circ$, $\delta = 7.5^\circ$,
 $\phi = 32.5^\circ$, $\alpha_v = 0$

α_h	I	S	Percentage Error into 10^{-4}	C_{ha}	Percentage Error into 10^{-4}	C_{ma}	Percentage Error into 10^{-4}
0.0	5	0.3554385	17.60	0.3137861	-80.0	0.2592489	-80.0
	10	0.3547982	-0.68	0.3138112	1.0	0.2592697	0.80
	20	0.3548182	-0.11	0.3138110	0.00	0.2592695	0.00
	30	0.3548222	-	0.3138110	-	0.2592695	-
0.1	5	0.3883909	17.86	0.3779610	-0.67	0.3805420	-0.66
	10	0.3876772	-0.55	0.3779865	0.01	0.3805675	0.01
	20	0.3876953	-0.08	0.3779863	0.00	0.3805673	0.00
	30	0.3876984	-	0.3779863	-	0.3805673	-
0.2	5	0.4251075	18.06	0.4406465	-6.0	0.5419228	-6.00
	10	0.4243238	-0.41	0.4406784	0.45	0.5419559	0.55
	20	0.4243383	-0.07	0.4406732	0.23	0.5419557	0.20
	30	0.4243412	-	0.4406732	-	0.5419556	-

I = Number of discrete wedges.

S = stress due to soil reaction at the base of the wall.

$\alpha_h = 0.1$ and 0.2 . Therefore, ten discrete wedges have been considered for the proposed investigation which is more than adequate.

4.3 ORIENTATION OF EARTH FORCES AT VERTICAL INTERFACES OF DISCRETE WEDGES

The orientation of the earth forces at the vertical interfaces varies from β at the top end of the rupture surface to η_{bd} at the vertical interface through the base of the wall. The angle η_{ih} of the earth force at the interface IH (Fig 3.3.1) is given by :

$$\tan \eta_{ih} = \tan \beta + (\tan \eta_{bd} - \tan \beta) \times \left(\frac{CH}{CD}\right)^Z \quad (4.3.1)$$

where $Z = \text{constant}$.

Since the value of η_{ih} is supposed to be known to make the problem statically determinate, it is proposed to investigate the influence of different patterns of variations of the orientation of interstice force on the computed results.

Three types of variations of this parameter have been investigated assuming the value of power, Z , being equal to one, two and three.

For a vertical wall with level fill of $\phi = 30^\circ$ and $\delta = 10^\circ$, the value of point of action factor, C_{ha} , for static case is obtained for the three cases as 0.3184013, 0.3259314 and 0.3310168 respectively. The percentage error in C_{ha} for the case of $Z = 2$ with respect to that for $Z = 1$ is 2.3649715 and the corresponding percentage error for the case of $Z = 3$ is 3.9621383 only. This indicates that the pattern of

variation of orientation of earth force at vertical interface has relatively insignificant influence on the distribution of earth pressure. Therefore, in this investigation the value of Z is considered to be unity.

4.4 EFFECT OF THE ANGLE OF WALL BACK, α

It is common practice to provide a gentle batter to the wall back making the wall lean away from the fill. It is generally believed that this will be helpful in improving the stability of the retaining wall for a given set of parameters. The most commonly used batter is 10° with the vertical. Batters making the wall lean towards the fill are relatively uncommon.

TABLE 4.4.1 STATIC FORCE FACTOR FOR VARIOUS VALUES OF α

α	70°	80°	90°	100°	110°	120°
C_{fa}	0.47635	0.37840	0.30140	0.23716	0.19274	0.12676

The values of the force factor, C_{fa} , for static case with angle of wall back, α , are shown in Table 4.4.1. It is evident that C_{fa} is the largest for $\alpha = 70^\circ$ and smallest for $\alpha = 120^\circ$. The variation of C_{fa} , C_{ma} and C_{ha} with angle of wall back for $\alpha_h = 0.0, 0.1, 0.2$, are shown in Fig. 4.4.1. It is clear from this figure that the moment factor as well as force factor decrease considerably with increasing angle of wall back. However, the point of action factor, C_{ha} , is

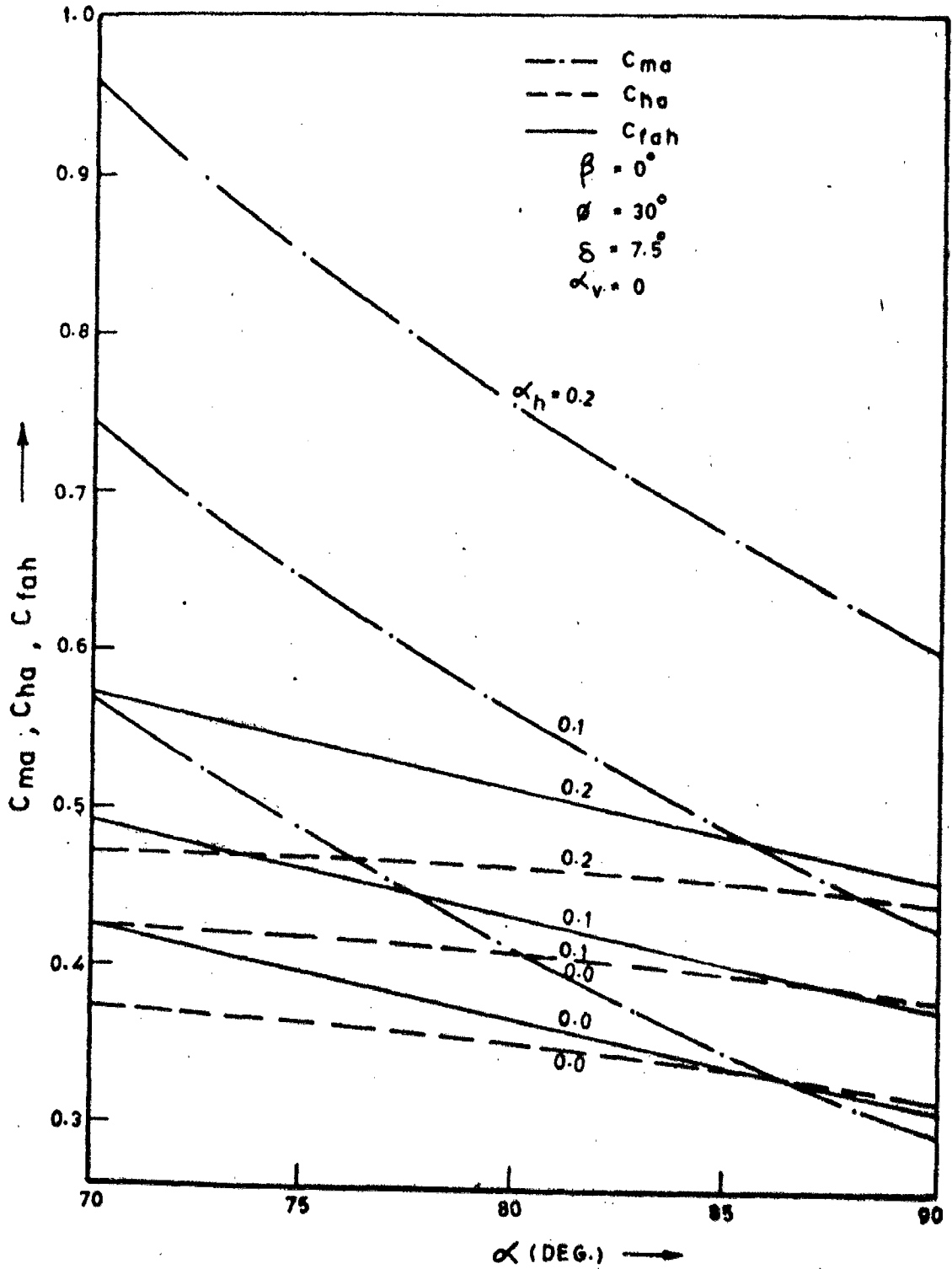


FIG. 4.4.1- VARIATION OF C_{ma} , C_{ha} , C_{tah} WITH α

not equally sensitive to changes in angle of wall back even though its values continuously decrease with increasing angle of wall back. Similar observations may be made from the results given in Table 4.4.2, for a backfill with $\phi = 30^\circ$, $\delta = 7.5^\circ$, $\beta = 0^\circ$, $\alpha_h = 0.0, 0.1, 0.2$ and $\alpha_v = 0$.

The angle of rupture plane ρ for different angles of wall back are shown in Fig.4.4.2 for soil with $\phi = 30^\circ$, $\beta = 0^\circ$, $\delta = 7.5^\circ$ with $\alpha_h = 0.0, 0.1$ and 0.2 and $\alpha_v = 0$. It may be observed from this figure that the value of ρ and the weight of the rupture wedge increase as α decreases. The percentage increase in weight of rupture wedge for various values of α with respect to that for $\alpha = 90^\circ$ are listed in Table 4.4.2. The force polygons, centres of gravity and the soil reactions for the various cases are shown in Fig.4.4.2 from which it may be observed that it is basically due to increased weight of the rupture wedge that the values of the force factor, C_{fa} , increases with decreasing angle of wall back. The moment due to weight of the rupture wedge sharply decreases with α , because, its lever arm decreases much faster than the increase in the weight of the wedge.

On the other hand, the magnitude, lever-arm and the moment about the base of the retaining wall of the soil reaction does not change appreciably with α . The moments due to soil reaction and rupture wedge normalized with respect to $(\gamma H^3/6)$ for different values of α for the static case are also shown in Fig.4.4.2. As a result, a larger proportion of

TABLE 4.4.2 : EFFECT OF THE ANGLE OF WALL BACK, α ,
 $\beta = 0^\circ$, $\phi = 30^\circ$, $\delta = 7.5^\circ$, $\alpha_v = 0$, ρ (IN DEG.)

α	90°	85°	80°	75°	70°	
$\alpha_h = 0$	C_{fah}	0.3105	0.34035	0.3697	0.3985	0.4267
	ρ	58.303	60.523	62.708	64.853	66.948
	C_{ha}	0.3184	0.3375	0.3529	0.3651	0.3745
	C_{ma}	0.2960	0.3513	0.4132	0.4850	0.5703
	N	1.1998	1.0140	0.8792	0.7807	0.7093
	Ca	0.2766	0.3457	0.4160	0.4887	0.5659
$\alpha_h = 0.05$	C_{fah}	0.3408	0.3707	0.4000	0.4287	0.4567
	ρ	55.905	57.983	60.0097	61.975	63.865
	C_{ha}	0.3490	0.3667	0.3810	0.39202	0.4003
	C_{ma}	0.3569	0.4158	0.4826	0.56014	0.6523
	N	0.9121	0.7679	0.66228	0.58548	0.5312
	Ca	0.3620	0.4331	0.50519	0.58003	0.6598
$\alpha_h = 0.1$	C_{fah}	0.3743	0.4043	0.43365	0.46233	0.4903
	ρ	53.2903	55.2044	57.0476	58.805	60.4584
	C_{ha}	0.3795	0.39576	0.4085	0.41813	0.42476
	C_{ma}	0.4262	0.48932	0.5610	0.64431	0.74314
	N	0.67282	0.56050	0.47865	0.42065	0.38213
	Ca	0.452238	0.52365	0.59606	0.67175	0.75309
$\alpha_h = 0.15$	C_{fah}	0.4116	0.44176	0.47127	0.5001	0.52825
	ρ	50.4311	52.1572	53.7902	55.3107	56.6935
	C_{ha}	0.4102	0.4249	0.4360	0.4437	0.44826
	C_{ma}	0.5066	0.57403	0.6507	0.7396	0.8450
	N	0.46827	0.38134	0.31954	0.27836	0.25480
	Ca	0.54661	0.61667	0.68850	0.76451	0.84724
$\alpha_h = 0.2$	C_{fah}	0.4534	0.48387	0.5137	0.54296	0.5716
	ρ	47.2944	48.8074	50.20303	51.4569	52.5376
	C_{ha}	0.4418	0.4546	0.46366	0.4691	0.4710
	C_{ma}	0.60085	0.6727	0.7543	0.8489	0.9607
	N	0.28861	0.22272	0.17848	0.15281	0.14367
	Ca	0.64373	0.71171	0.78265	0.85920	0.94404

TABLE 4.4.2 : EFFECT OF THE ANGLE OF WALL BACK, α ,
 $\beta = 0^\circ$, $\phi = 30^\circ$, $\delta = 7.5^\circ$, $\alpha_v = 0$, ρ (IN DEG.)

α	90°	85°	80°	75°	70°	
$\alpha_h = 0$	C_{fah}	0.3105	0.34035	0.3697	0.3985	0.4267
	ρ	58.303	60.523	62.708	64.853	66.948
	C_{ha}	0.3184	0.3375	0.3529	0.3651	0.3745
	C_{ma}	0.2960	0.3513	0.4132	0.4850	0.5703
	N	1.1998	1.0140	0.8792	0.7807	0.7093
	C_a	0.2766	0.3457	0.4160	0.4887	0.5659
$\alpha_h = 0.05$	C_{fah}	0.3408	0.3707	0.4000	0.4287	0.4567
	ρ	55.905	57.983	60.0097	61.975	63.865
	C_{ha}	0.3490	0.3667	0.3810	0.39202	0.4003
	C_{ma}	0.3569	0.4158	0.4826	0.56014	0.6523
	N	0.9121	0.7679	0.66228	0.58548	0.5312
	C_a	0.3620	0.4331	0.50519	0.58003	0.6598
$\alpha_h = 0.1$	C_{fah}	0.3743	0.4043	0.43365	0.46233	0.4903
	ρ	53.2903	55.2044	57.0476	58.805	60.4584
	C_{ha}	0.3795	0.39576	0.4085	0.41813	0.42476
	C_{ma}	0.4262	0.48932	0.5610	0.64431	0.74314
	N	0.67282	0.56050	0.47865	0.42065	0.38213
	C_a	0.452238	0.52365	0.59606	0.67175	0.75309
$\alpha_h = 0.15$	C_{fah}	0.4116	0.44176	0.47127	0.5001	0.52825
	ρ	50.4311	52.1572	53.7902	55.3107	56.6935
	C_{ha}	0.4102	0.4249	0.4360	0.4437	0.44826
	C_{ma}	0.5066	0.57403	0.6507	0.7396	0.8450
	N	0.46827	0.38134	0.31954	0.27836	0.25480
	C_a	0.54661	0.61667	0.68850	0.76451	0.84724
$\alpha_h = 0.2$	C_{fah}	0.4534	0.48387	0.5137	0.54296	0.5716
	ρ	47.2944	48.8074	50.20303	51.4569	52.5376
	C_{ha}	0.4418	0.4546	0.46366	0.4691	0.4710
	C_{ma}	0.60085	0.6727	0.7543	0.8489	0.9607
	N	0.28861	0.22272	0.17848	0.15281	0.14367
	C_a	0.64373	0.71171	0.78265	0.85920	0.94404

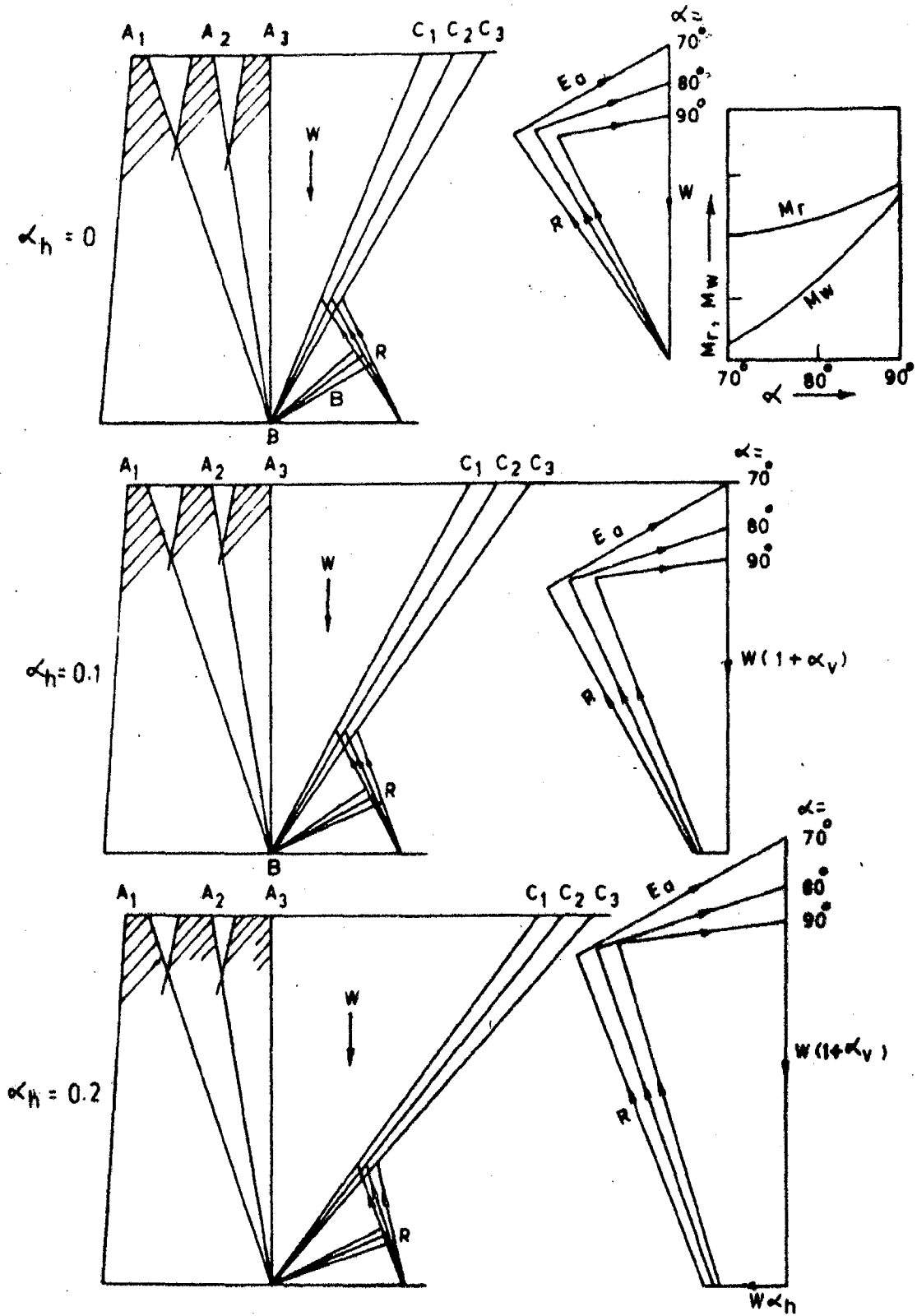


FIG. 4.4.2 - VARIATION OF FAILURE WEDGE

TABLE 4.4.3 PERCENTAGE INCREASE IN WEIGHT OF THE RUPTURE WEDGE WITH RESPECT TO THAT FOR VERTICAL WALL
 ($\alpha_v = 0$, $\phi = 30^\circ$, $\beta = 0^\circ$, $\delta = 7.5^\circ$)

α_h	0.0		0.1		0.2	
α	W	δW	W	δW	W	δW
90°	2.7789	-	3.3554	-	4.1533	-
80°	8.1153	12.10	3.7105	10.58	4.5425	09.37
70°	3.5529	27.85	4.1882	24.82	5.0862	22.46

N.B.: W = Weight of rupture wedge in tonnes

$\delta W = \%$ increase in the weight of the wedge with respect to that for vertical wall.

a unbalanced moment due to soil reaction has to be counter-balanced by moment due to E_a . This results into increase in C_{ha} with decreasing α . Similar observations may be made for the dynamic case also.

The distributions of static earth pressure factor along the wall back for various values of α are shown in Fig.4.4.3, from which it is clear that the curve is convex downward for vertical wall and it gradually becomes convex upward for $\alpha = 70^\circ$. This is in agreement with increase in point of action factor with decreasing α cited earlier. From the same figure similar observations may be made for dynamic case also.

The values of coefficient of active earth pressure, C_a , and the power factor, N , for these cases are shown in Fig.4.4.4. It may be observed from this figure that the value of C_a decreases with increasing value of α almost linearly for static as well as dynamic conditions. This may be of some help in interpolating the values of C_a for various values of α for a given problem. The power factor, N , on the other hand increases with increasing α indicating more distinct non-linear variation of pressure with depth for the smaller values of α particularly for the dynamic case. This is in agreement with the explanation cited in this section earlier.

From this discussion, it may be concluded that if the angle of wall back is less than 90° the earth force as well as the net overturning moment about the base of the wall increase considerably with decreasing α . This is not a desirable

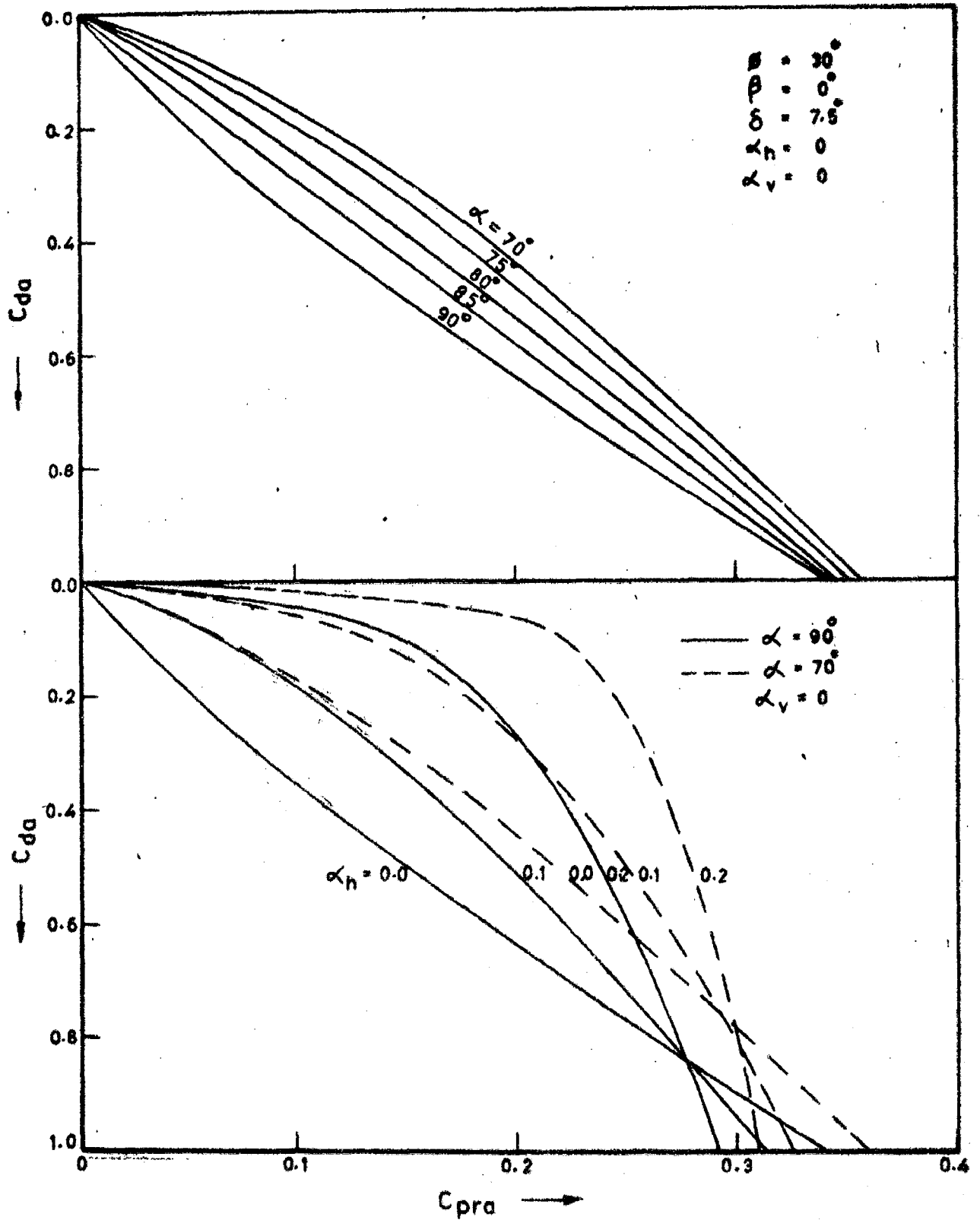


FIG. 4.4.3 - VARIATION OF C_{pra} WITH DEPTH FACTOR FOR VARIOUS VALUES OF α

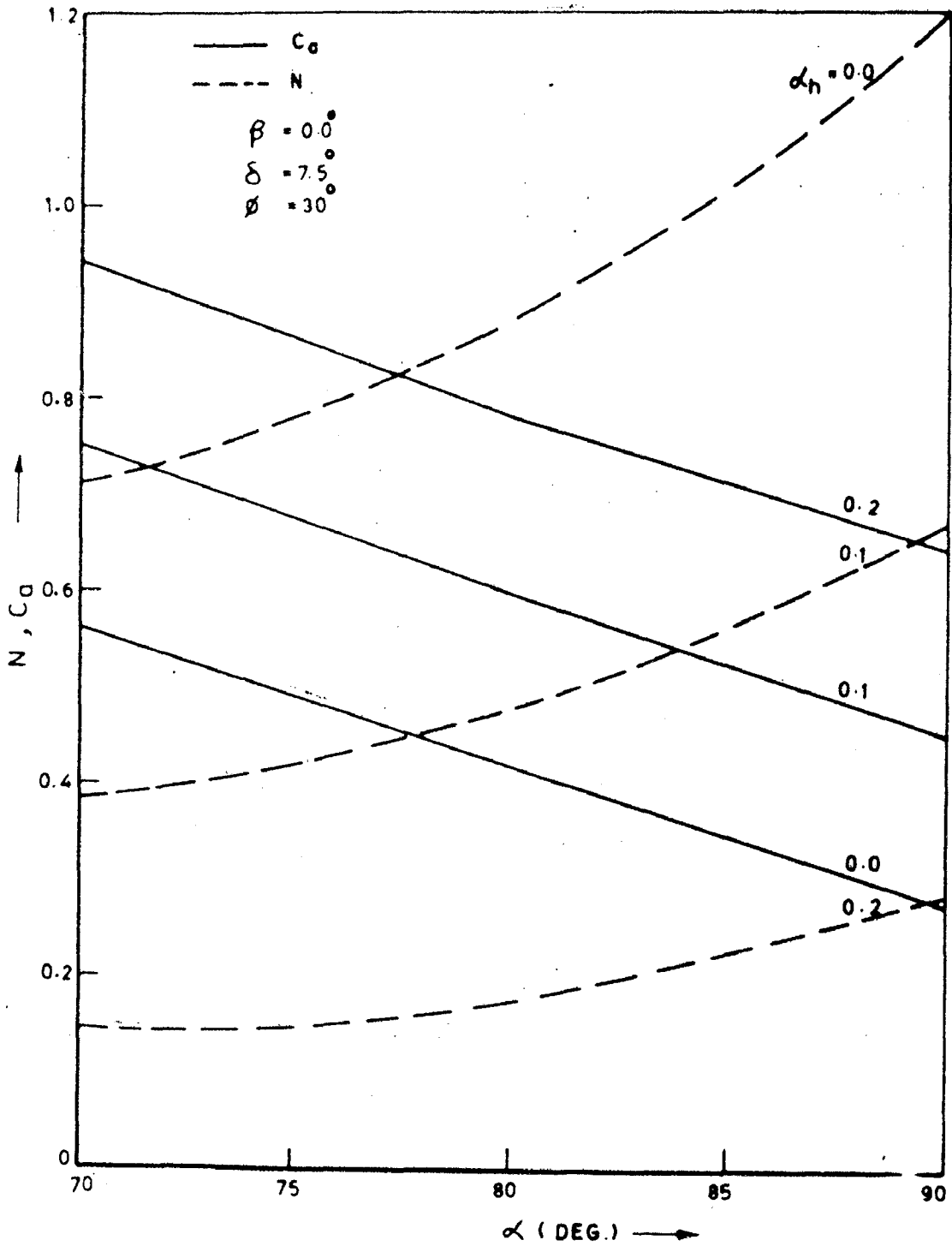


FIG. 4.4.4 - VARIATION OF C_d AND N WITH α FOR VARIOUS VALUES OF α_h

feature. Wall batters leaning away from the fill adversely influence the stability of the wall which is contrary to the common belief. Therefore, as far as possible retaining structures with vertical wall back should be favoured.

4.5 EFFECT OF ANGLE OF SURCHARGE

In engineering practice there are many situations where the earthfill retained by the structure has a sloping surcharge. Therefore, it is important to study the influence of such surcharge on the earth pressure distribution. Figure 3.3.1 shows the rupture wedge for a sloping surcharge. It may be observed that the size of the rupture wedge will be considerably larger for such a case than for a level fill. Therefore, it is obvious that the earth force for a given height of retaining wall will increase with increasing β .

Figure 4.5.1 shows variation of C_{ma} , C_{ha} , C_{fah} with β for different values of α_h . From this figure, it may be observed that all these factors increase with β . Similar observations may be made for dynamic case also. The various non-dimensional factors for different values of β and other parameters are listed in Table 4.5.1. The increase in C_{ma} for a given β is very significant with increasing values of α_h . The increase in E_a is basically due to increase in the weight of the rupture wedge for increasing β . This is evident from the rupture wedges ABC_1 , ABC_2 , ABC_3 and ABC_4 for $\beta = 0^\circ$, 10° , 15° , 20° respectively as shown in this figure. The

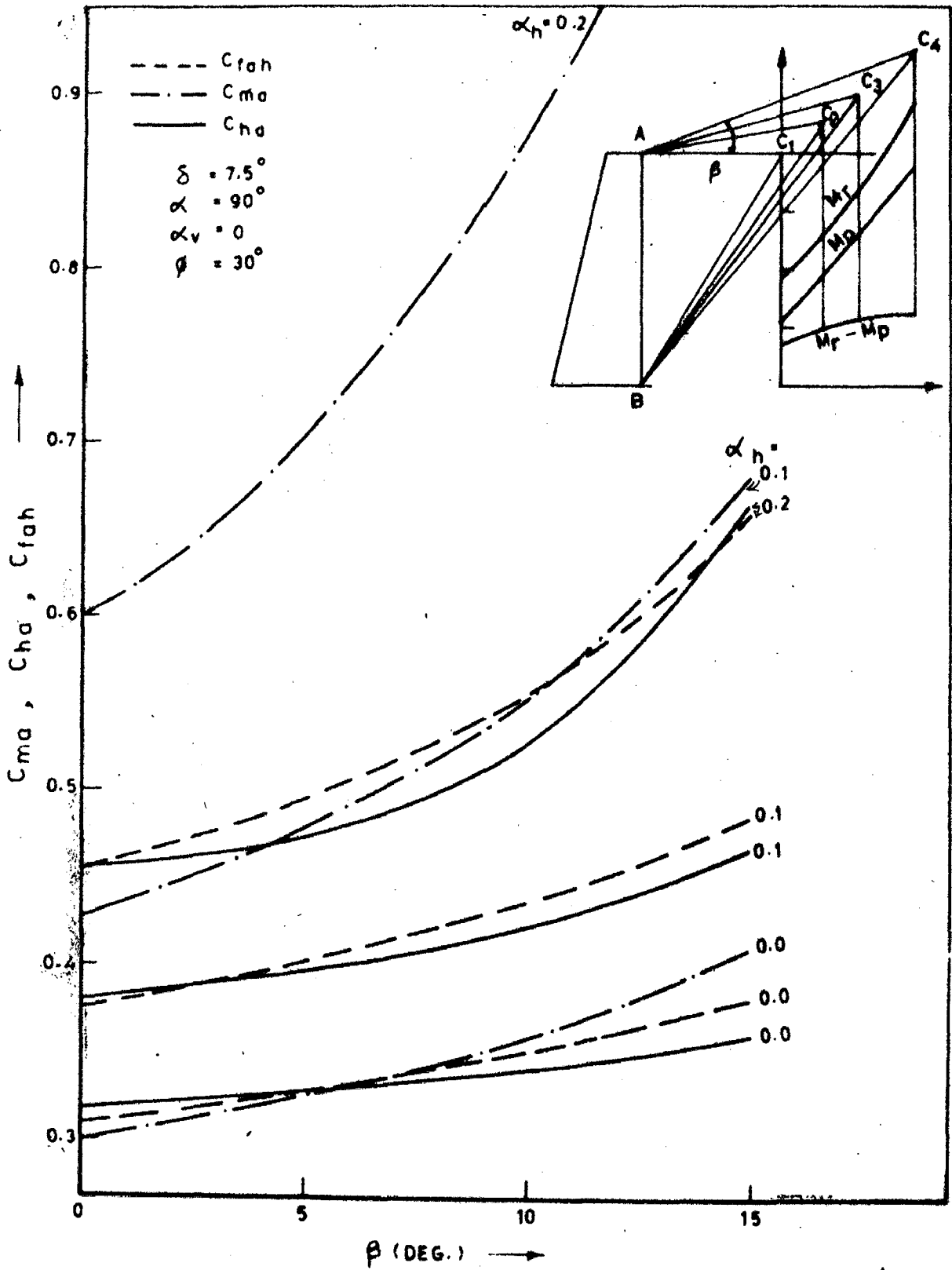


FIG. 4.5.1 - VARIATION OF C_{ma}, C_{ha}, C_{rah} WITH β (DEG.)

TABLE 4.5.1 EFFECT OF ANGLE OF SURCHARGE, ($\alpha = 90^\circ$, $\delta = 7.5^\circ$
 $\phi = 30^\circ$ AND $\alpha_v = 0^\circ$) (ρ IN DEG.)

α_h	β	0°	5°	10°	15°
0	C_{fah}	0.3105	0.3288	0.3510	0.3796
	ρ	58.3033	56.9539	55.3295	53.2701
	C_{ha}	0.3184	0.3275	0.3405	0.3602
	C_{ma}	0.2966	0.3230	0.3585	0.4102
	N	1.19980	1.10896	0.98722	0.81910
	C_a	0.2766	0.3102	0.3567	0.4248
0.1	C_{fah}	0.3743	0.4014	0.4364	0.4856
	ρ	53.2903	51.3454	48.8888	45.5242
	C_{ha}	0.3795	0.3966	0.4224	0.4669
	C_{ma}	0.4262	0.4776	0.5530	0.6801
	N	0.67282	0.55501	0.39574	0.16325
	C_a	0.4524	0.5133	0.5966	0.7143
0.2	C_{fah}	0.4534	0.4954	0.5550	0.6579
	ρ	47.2944	44.4189	40.4942	34.1406
	C_{ha}	0.4418	0.4726	0.5264	0.6625
	C_{ma}	0.6009	0.7025	0.8765	1.3076
	N	0.28861	0.13637	0.08542	0.48394
	C_a	0.6437	0.7334	0.8435	0.8741
0.05	C_{fah}	0.3408	0.3630	0.3906	0.4277
	ρ	55.9051	54.2891	52.3013	49.6961
	C_{ha}	0.3490	0.3616	0.3800	0.4094
	C_{ma}	0.3569	0.3938	0.4454	0.5252
	N	0.91207	0.80799	0.66895	0.47366
	C_a	0.36198	0.40868	0.47302	0.56666
0.15	C_{fah}	0.4116	0.4451	0.4901	0.5585
	ρ	50.4311	48.0757	44.9996	40.5113
	C_{ha}	0.4102	0.4332	0.4698	0.5418
	C_{ma}	0.5066	0.5785	0.6907	0.9077
	N	0.46827	0.33493	0.1497	0.1406
	C_a	0.54661	0.62227	0.72326	0.84746

increased length of the rupture surface and the increased weight of the rupture wedge with increasing β will result into a corresponding increase in the magnitude, lever-arm and overturning moment about base of the wall. The overturning moments due to R and weight of the wedge as well as the difference between these two moments in non-dimensional form are shown in this figure for static case. The additional over-turning moment resulting from this is to be balanced by the increased moment due to E_a which leads into shifting of the point of application of E_a farther from the base of the wall.

The variation of C_{ha} with β for different values of ϕ and δ is shown in the Fig. 4.5.2. It is interesting to note from this figure that the earth force acts always at one-third height from the base of the wall for all values of δ if $\delta = \beta$. This is true for all values of ϕ investigated. Therefore, it may be concluded that when $\delta = \beta$, ϕ value does not influence C_{ha} for static case. As shown in Fig. 5.4.3, 4.5.3 even though the variation pattern of C_{ha} with β remains the same for dynamic case, the curves do not appear to converge at a single point for $\delta = \beta$ like in static case.

The distribution of C_{pra} along the wall back for various values of β for static case are shown in Fig. 4.5.4, from which it may be observed that with increasing β , the point of action moves farther from the base. For the dynamic case also the same trend is observed. However, for $\alpha_h = 0.2$ and $\beta = 15^\circ$,

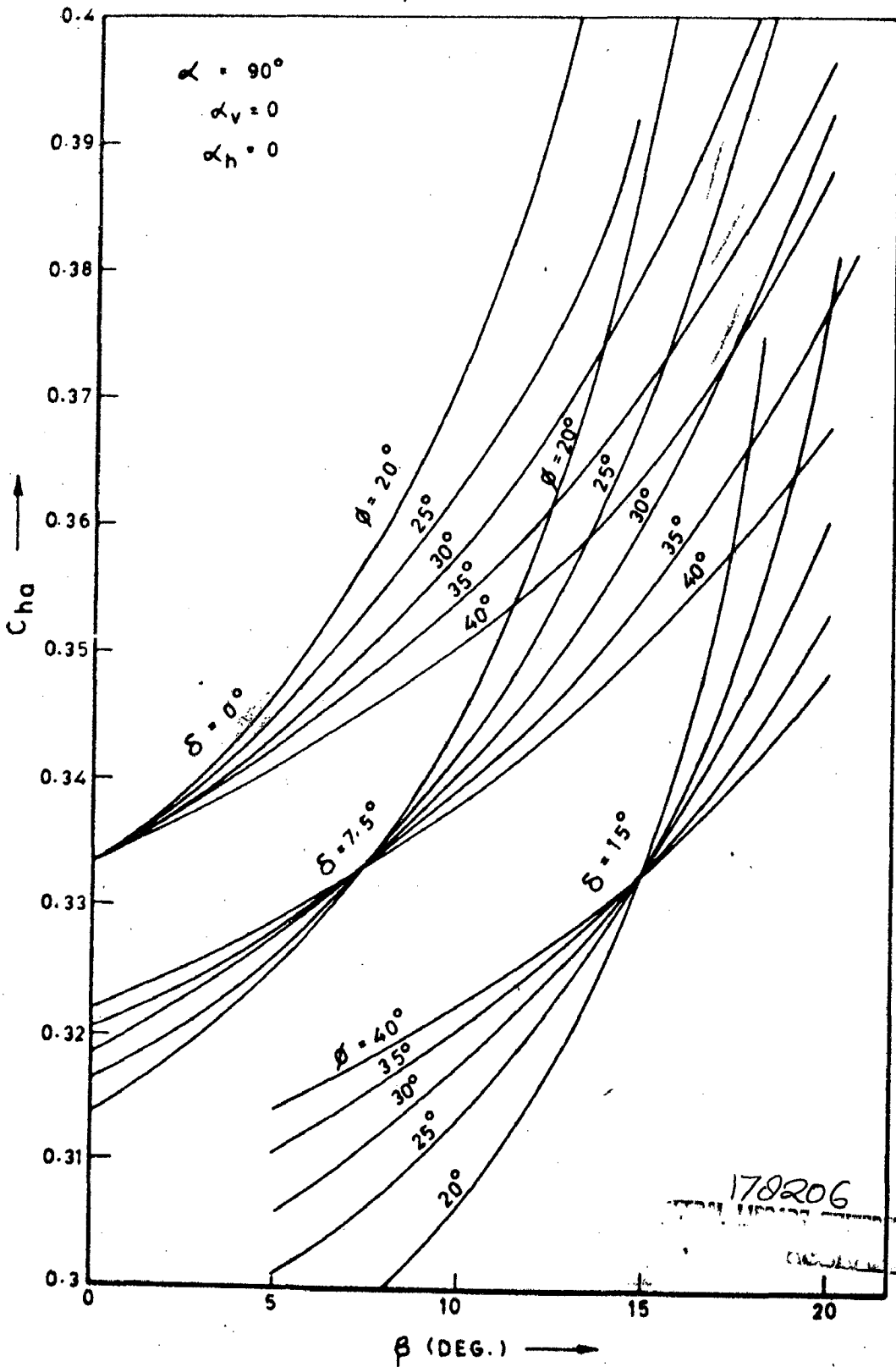


FIG.4.5.2 - VARIATION OF C_{ha} WITH β FOR DIFFERENT VALUES OF θ AND δ

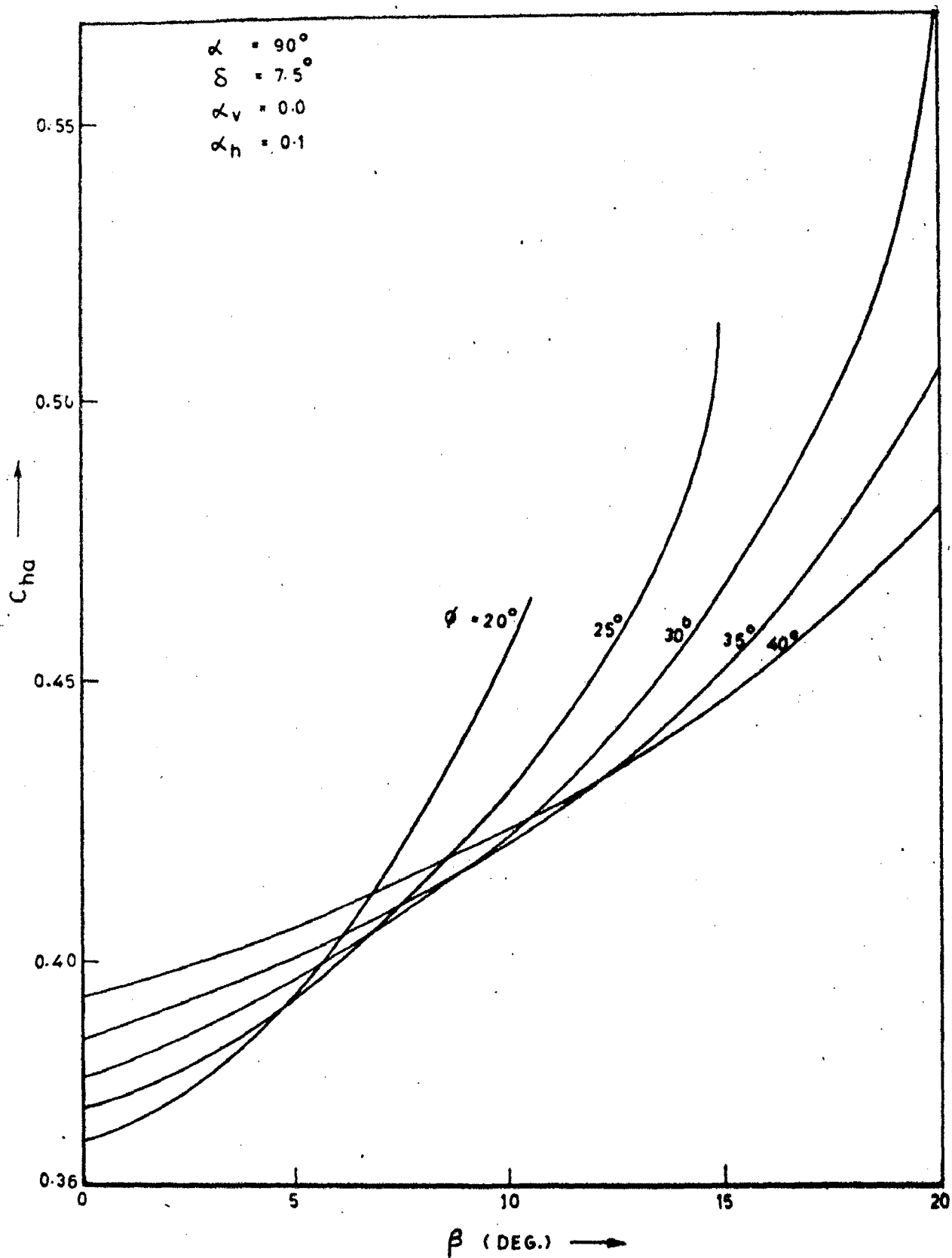


FIG. 4.5.3 - VARIATION OF C_{ha} WITH β (DEG.)

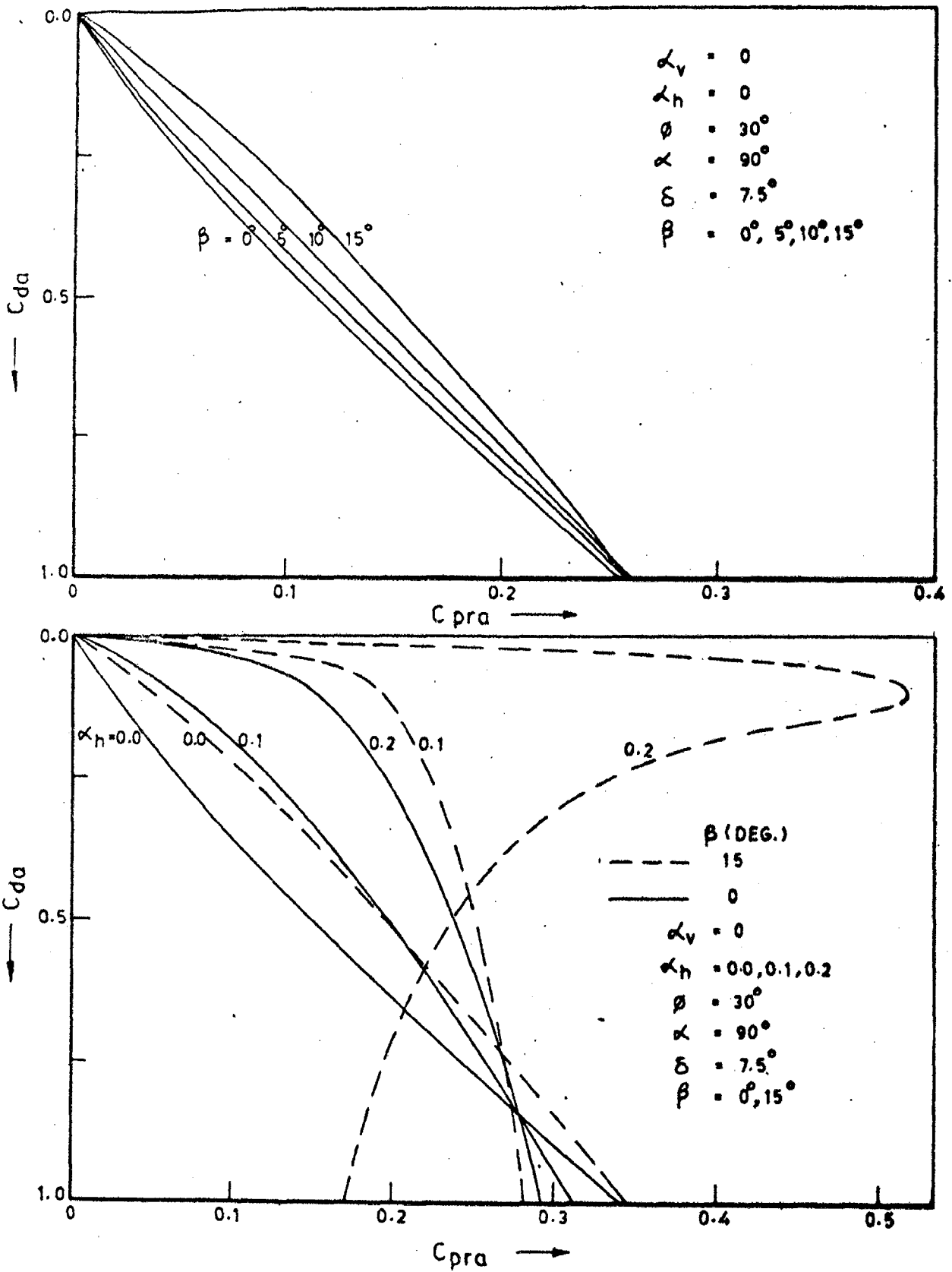


FIG. 4.5.4 - VARIATION OF C_{pra} FOR VARIOUS VALUES OF β AND α_h

C_{pra} increases sharply with depth below the top of the wall to reach a peak at $C_{da} = 0.1 H$ and then sharply decreases. This is reflected by the negative value of N . Figure 4.5.5 shows the variation of N and C_a with β for the static as well as dynamic cases. It may be noted from this figure that N values continuously decrease with β for $\alpha_h = 0.0, 0.1$ and 0.2 which is in agreement with the corresponding increase in C_{ha} . On the other hand values of C_a keep increasing with β for $\alpha_h = 0.0, 0.1$ and 0.2 . This is in agreement with continuous increase in C_{pra} for all values of β .

With increasing value of β for a given problem, the stability of the surcharge slope itself will be adversely affected, especially for the dynamic case. Equation 3.2.1 gives the expression for C_{fa} for the dynamic case by Mononobe-Okabe theory. From this expression it can be noticed that for avoiding imaginary solutions (which are not of practical interest) it is necessary to satisfy the following condition :

$$\sin (\phi - \beta - \theta) > 0 \quad (4.5.1)$$

i.e. $\phi - \beta - \theta > 0$

$$\beta < \phi - \theta$$

However, to provide for additional factor of safety, it is recommended that the actual value of β should be 5° less than $(\phi - \theta)$ for that particular problem. Figure 4.5.6 shows the variation of limiting as well as recommended values of β with α_h for different values of ϕ . Table 4.5.2 gives the limiting

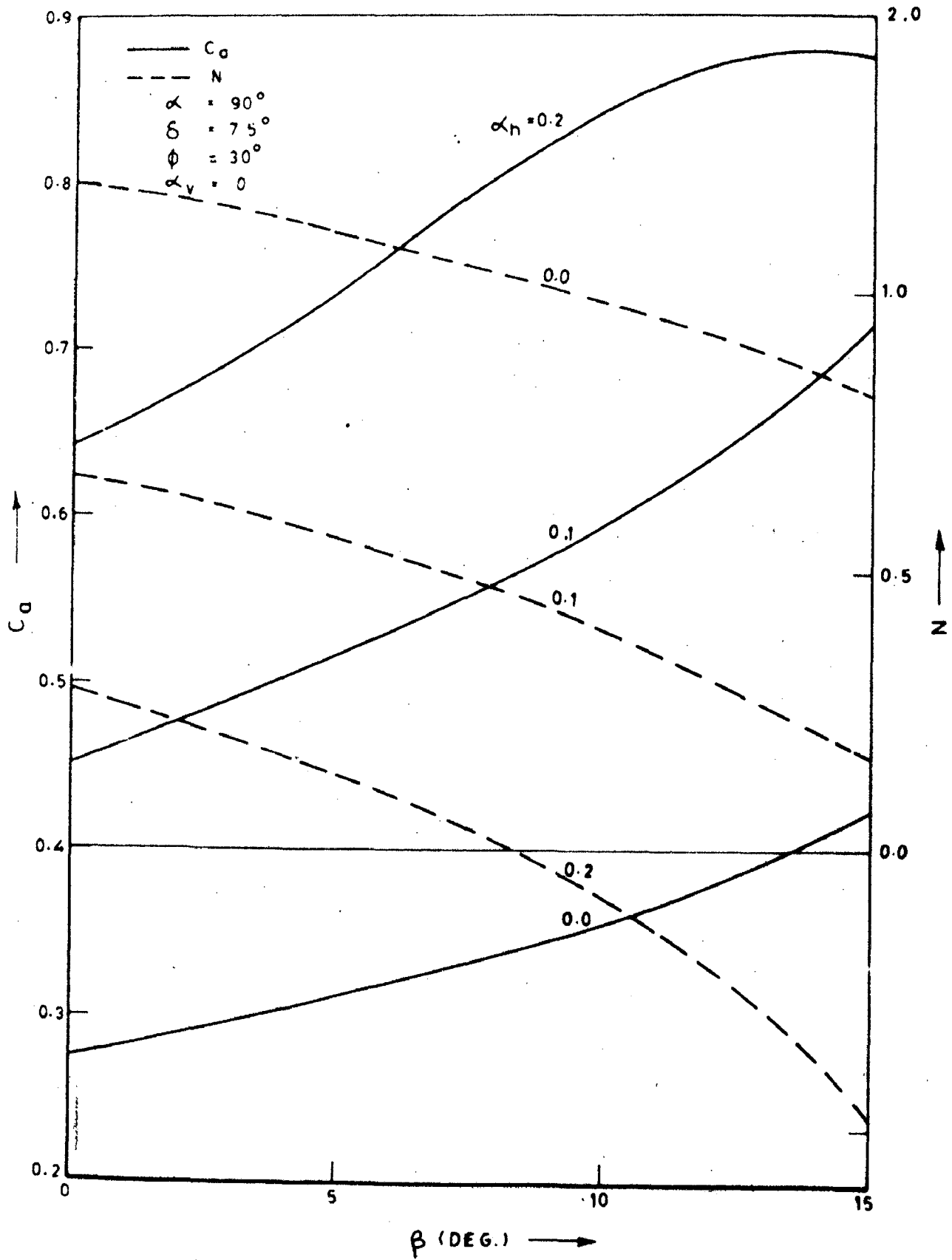


FIG. 4.5.5 - VARIATION OF C_D AND N WITH β (DEG.)

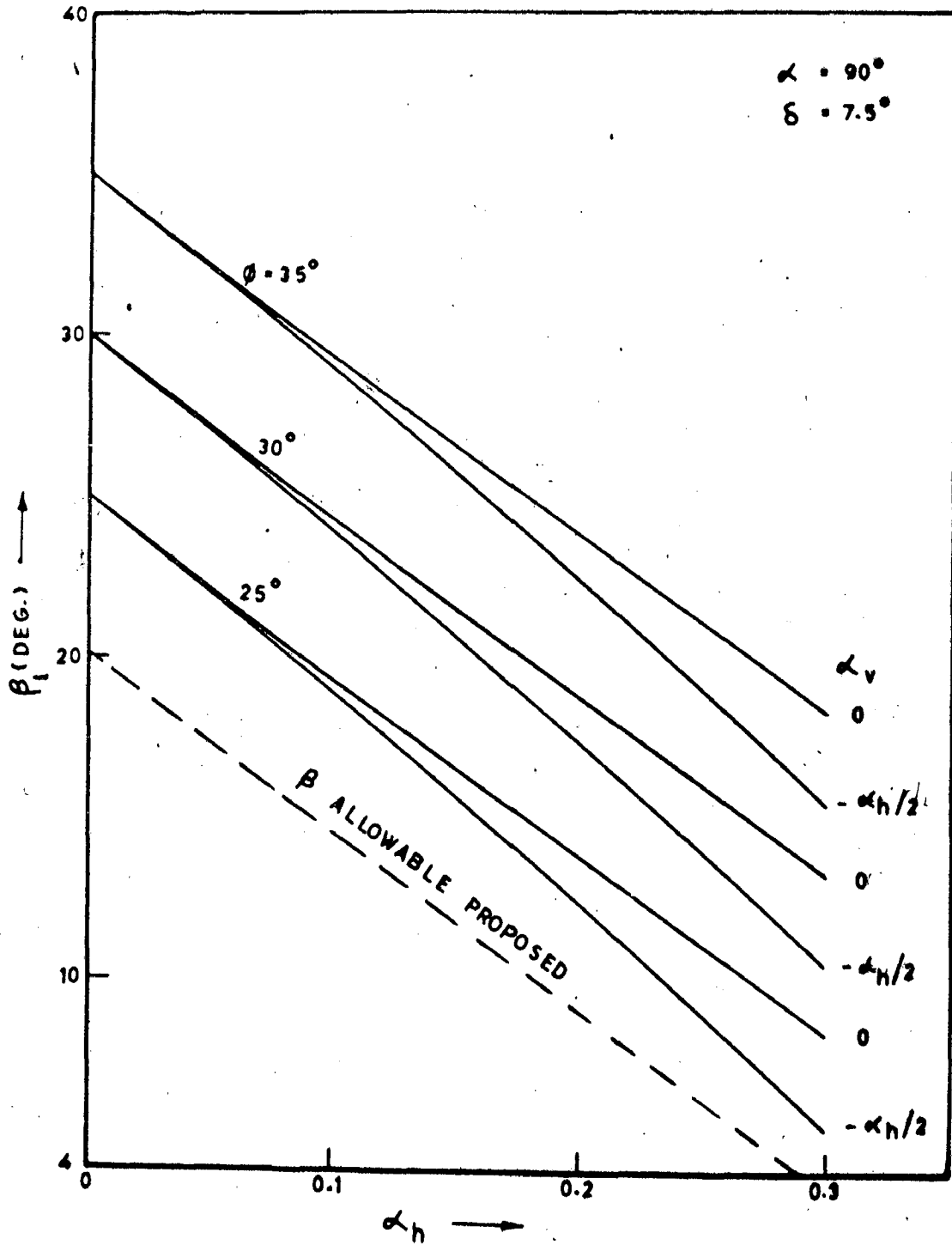


FIG. 4.5.6 - VALUES OF LIMITING β AND ALLOWABLE β FOR DIFFERENT VALUES OF α_h

TABLE No. 4.5.2 VALUES OF LIMITING β FOR VARIOUS
VALUES OF ϕ AND α_h

		β_l (IN DEG.)					
$\phi \rightarrow$	25°		30°		35°		
	$\alpha_h \downarrow$	$\alpha_v=0$	$\alpha_v=-\alpha_h/2$	$\alpha_v=0$	$\alpha_v=-\alpha_h/2$	$\alpha_v=0$	$\alpha_v=-\alpha_h/2$
0.0	25.00	25.00	30.00	30.00	35.00	35.00	
0.1	19.29	18.99	24.29	23.99	29.29	28.99	
0.2	13.69	12.47	18.69	17.47	23.69	22.47	
0.3	08.30	5.56	13.30	10.56	18.30	15.56	

values of β for various values of ϕ , α_h and α_v .

4.6 EFFECT OF THE ANGLE OF WALL FRICTION

As discussed in Sec. 3.1, the earth force on the retaining structures has to be minimised with respect to angle of wall friction. Figure 4.6.1 shows variation of C_{fa} with δ . It is clear from this figure that C_{fa} decreases with δ and reaches a minimum and then increases with δ . Therefore, it is possible to have same earth force for two different values of δ for a given problem. However, since wall friction is a resisting force, it is mobilized only to the extent it is required. Therefore, from the principles of minimum energy, only lower values of δ will be mobilized and not the higher values for a given earth force.

As such a wall friction angle greater than that for which earth force is minimum is not likely to be mobilized. If the wall undergoes sufficiently large movements to reach active state as assumed for the problem under consideration, it is reasonable to expect that the relative motion between wall and the rupture wedge at this stage is large enough to mobilize critical value of angle of wall friction. On the other hand, if wall is not allowed to move freely for this purpose, sufficient wall friction may not be developed. This results into earth force larger than the active earth force. Therefore, it makes good engineering sense to design the wall in such a way that it is not unduly constrained to stop its

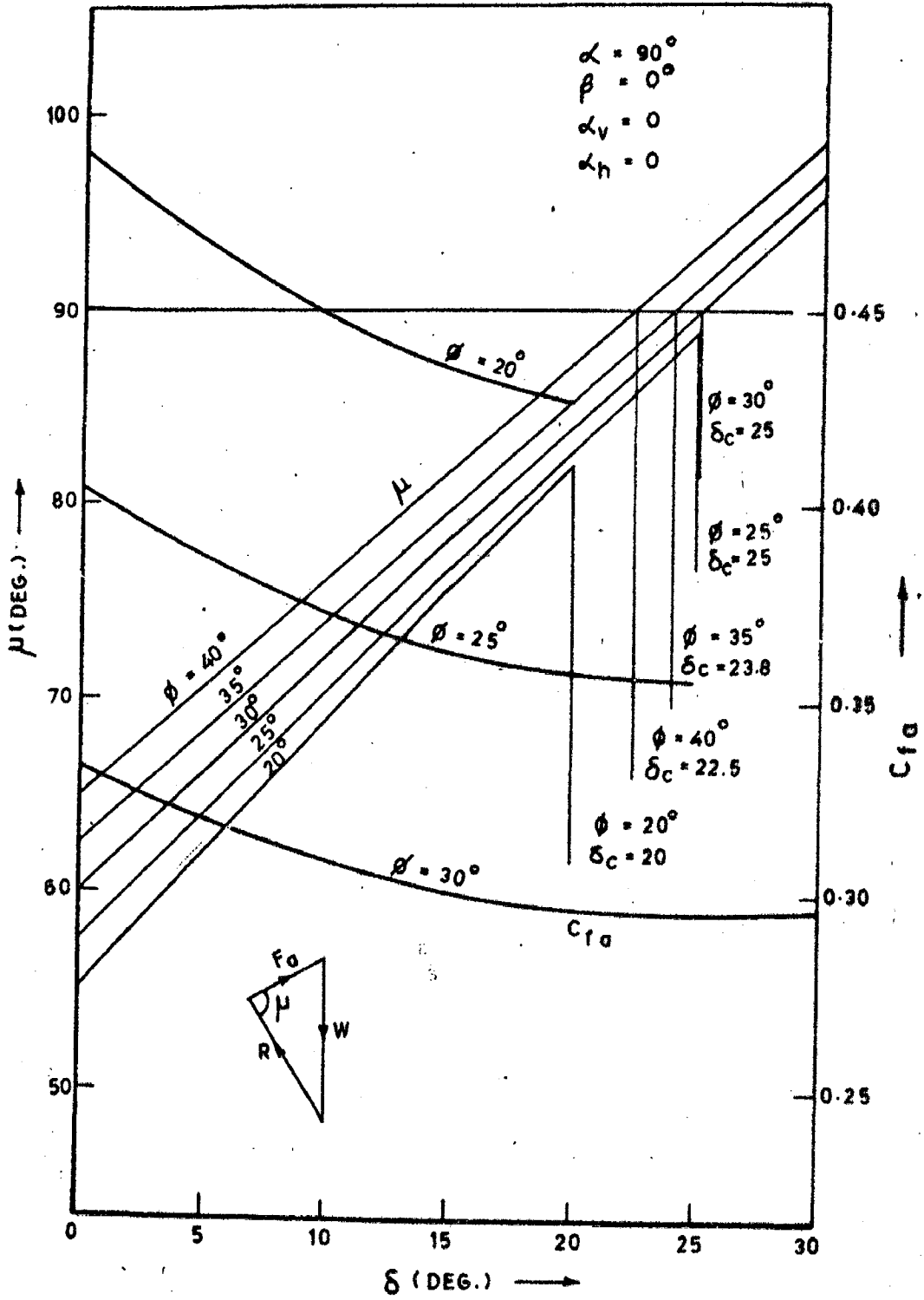


FIG. 4.6.1 - VARIATION OF C_{fa} AND μ WITH δ (DEG.)

movement required to reach active state.

Figure 4.6.2 shows distribution of pressure factor along the wall back and the stress due to soil reaction along the rupture plane for a wall with vertical back. It may be noticed that with increasing δ the angle of rupture plane, ρ , and the stress due to soil reaction, R , along the rupture plane decrease. The distribution of stress due to soil reaction along the rupture plane is very nearly linear for all values of δ .

The distribution of C_{pra} along the wall back for a smooth wall is hydrostatic and is in conformity with the Rankines theory. With increasing value of δ , the distribution of pressure factor is distinctly nonlinear and the rate of increase of pressure factor increase with depth. This brings the resultant earth force on the wall back closer to the base. Similar observations may be made from Fig.4.6.3 for the static and dynamic cases.

Figure 4.6.4 shows the variation of C_{ma} , C_{na} and C_{fah} with δ . It may be observed from this figure that with increasing δ all these factors continuously decrease. It is interesting to note that even though C_{fa} reaches a minimum and then again increases, C_{fah} continuously decreases with increasing values of δ . These observations hold good for dynamic case also.

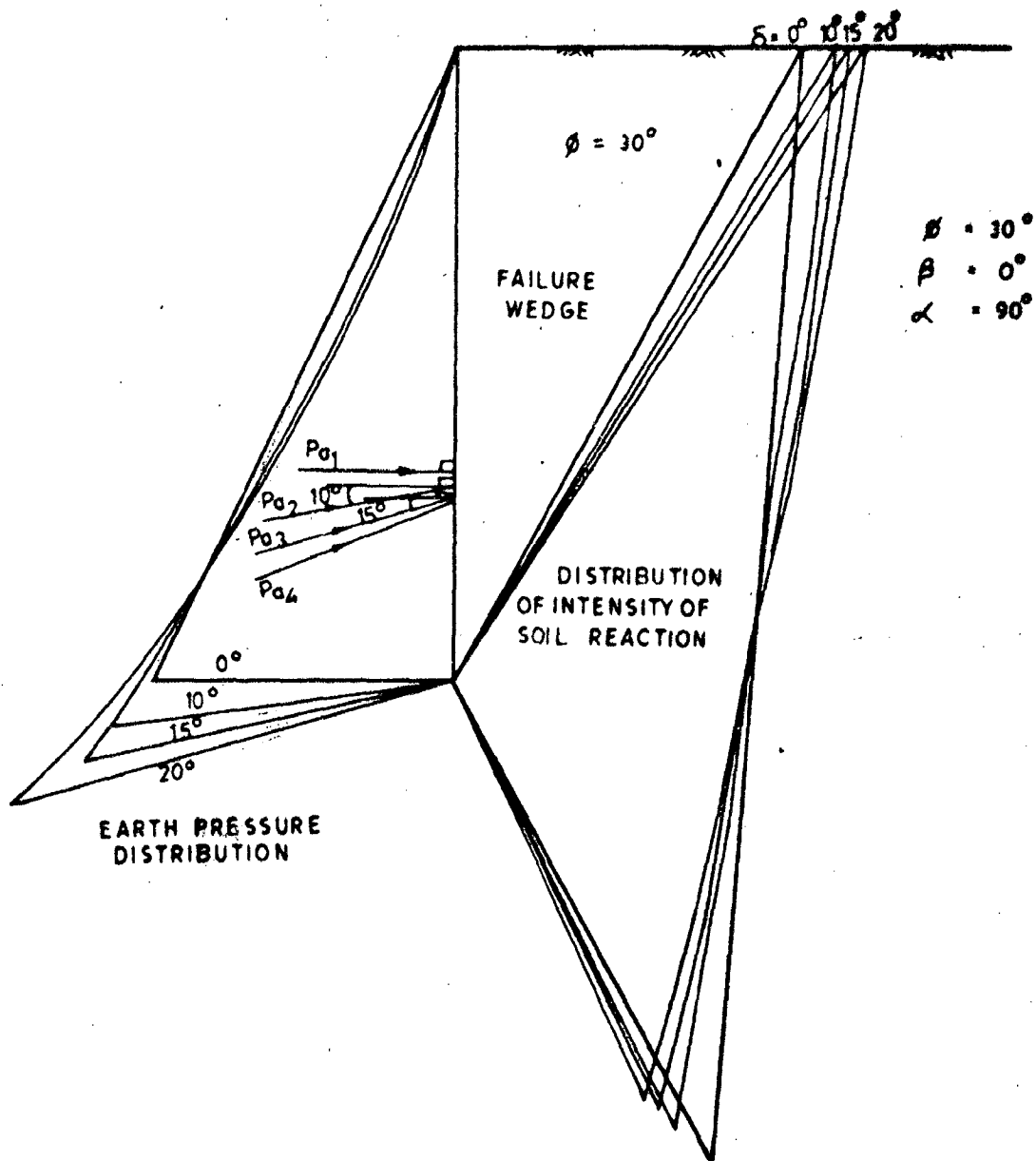


FIG. 4.6.2 - C_{pra} ALONG WALL BACK AND PRESSURE DUE TO SOIL REACTION ALONG RUPUTURE SURFACE

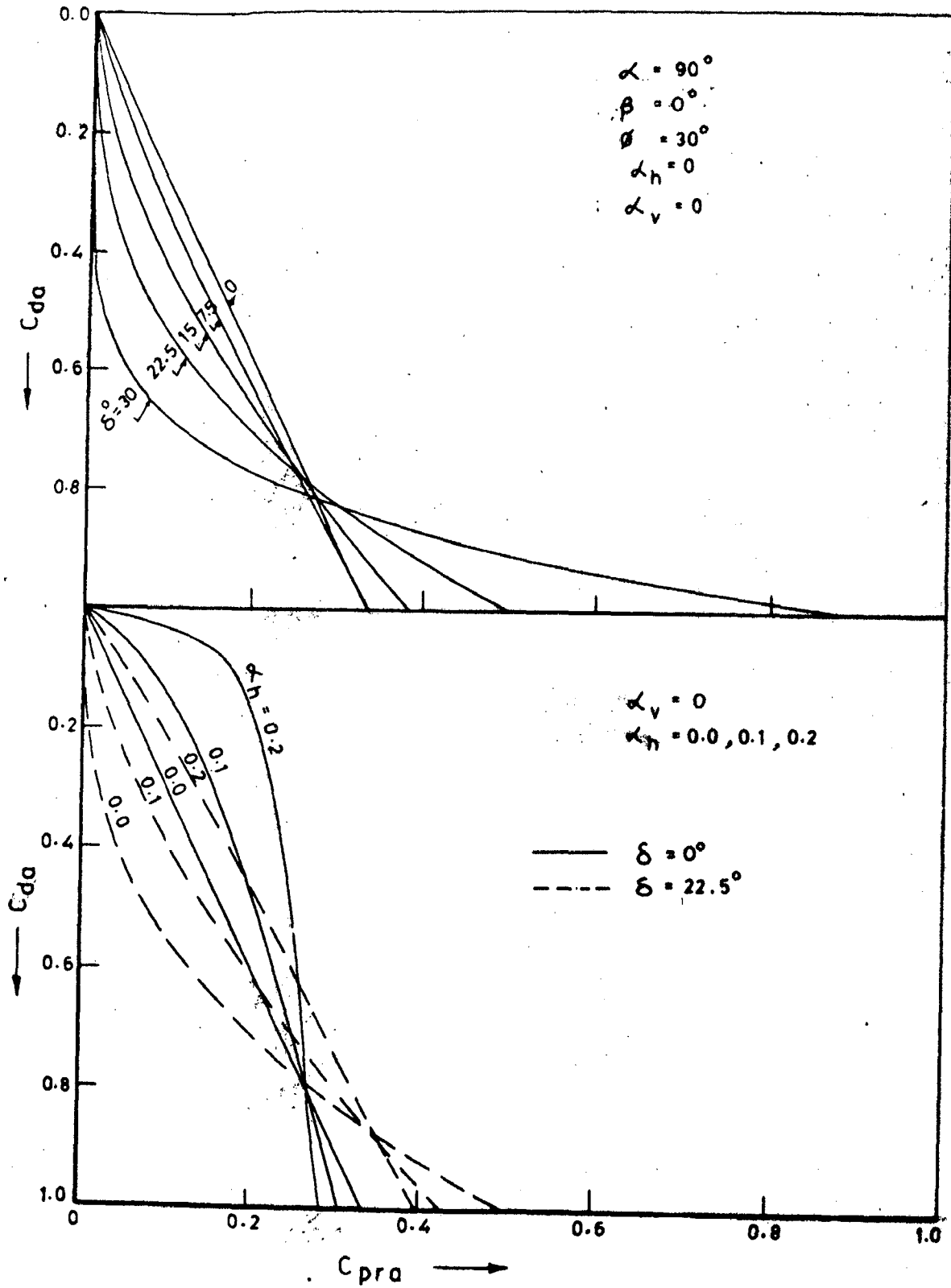


FIG. 4.6.3_ DISTRIBUTION OF C_{pra} ALONG WALL BACK FOR DIFFERENT VALUES OF δ

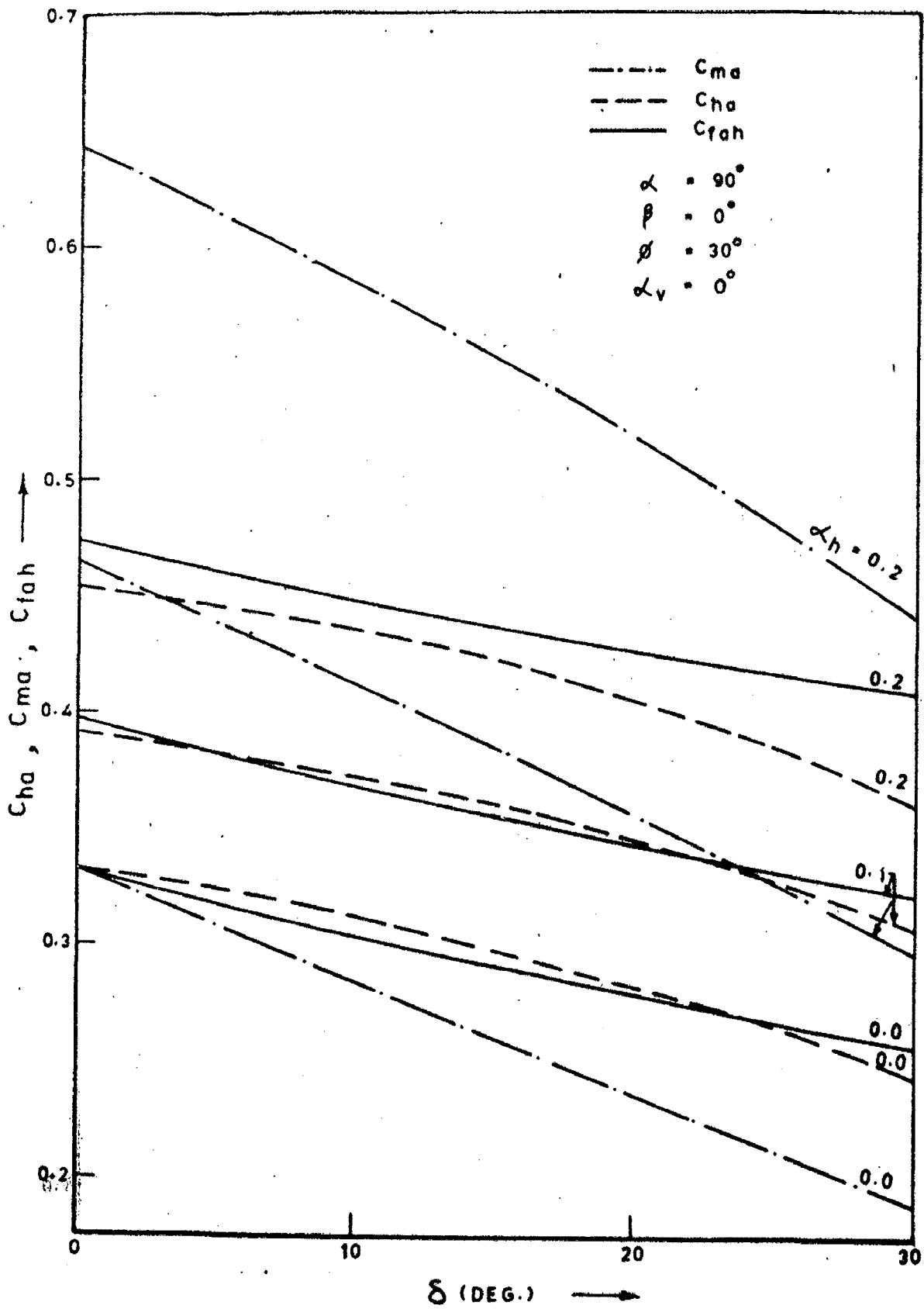


FIG. 4.6.4 - VARIATION OF C_{ma} , C_{ha} , C_{tah} WITH δ

TABLE 4.6.1 EFFECT OF ANGLE OF WALL FRICTION ($\alpha = 90^\circ$, $\delta = 0^\circ$,
 $\phi = 30^\circ$ AND $\alpha_v = 0$) (ρ IN DEG.)

α_h	β	0°	7.5°	15°	22.5°	30°
0.05	C_{fah}	0.3635	0.3408	0.3215	0.3041	0.2877
	ρ	57.7542	55.908	54.327	52.905	51.562
	C_{ha}	0.3623	0.3490	0.3308	0.3072	0.2770
	C_{ma}	0.3951	0.3569	0.3190	0.2803	0.2390
	N	0.7605	0.9121	1.2553	1.9975	4.0564
	C_a	0.4163	0.3620	0.2835	0.1649	0.0293
0.00	C_{fah}	0.3333	0.3105	0.2911	0.2737	0.2574
	ρ	60.000	58.303	56.860	55.563	54.343
	C_{ha}	0.3333	0.3184	0.2990	0.2746	0.2440
	C_{ma}	0.3333	0.2966	0.2611	0.2255	0.1884
	N	1.000	1.1998	1.6464	2.6543	5.8694
	C_a	0.3333	0.2776	0.1961	0.0879	0.0048
0.10	C_{fah}	0.3966	0.3743	0.3554	0.3383	0.3222
	ρ	55.295	53.290	51.576	50.027	48.559
	C_{ha}	0.3915	0.3795	0.3619	0.3383	0.3073
	C_{ma}	0.4658	0.4262	0.3858	0.3433	0.2971
	N	0.5540	0.6728	0.9468	1.5241	2.9955
	C_a	0.5029	0.4524	0.3796	0.2599	0.0830
0.15	C_{fah}	0.4329	0.4116	0.3935	0.3772	0.3620
	ρ	52.592	50.431	48.5810	46.908	45.317
	C_{ha}	0.4217	0.4102	0.3925	0.3680	0.3352
	C_{ma}	0.5477	0.5066	0.4633	0.4164	0.3640
	N	0.3716	0.4683	0.6952	1.1656	2.3048
	C_a	0.5922	0.5466	0.4826	0.3686	0.1647
0.20	C_{fah}	0.4733	0.4534	0.4366	0.4218	0.4081
	ρ	49.604	47.294	45.317	43.527	41.823
	C_{ha}	0.4532	0.4418	0.4230	0.3965	0.3604
	C_{ma}	0.6435	0.6009	0.5541	0.5017	0.4412
	N	0.2065	0.2886	0.4835	0.8836	1.8253
	C_a	0.6826	0.6437	0.5914	0.4886	0.2689

Figure 4.6.5 shows variation of C_a and N with δ . It may be observed that N increases with increasing δ which is in conformity with the corresponding decrease in C_{ha} . On the other hand C_a decreases with increasing δ . This decrease is relatively gradual for δ less than critical and very sharp for δ greater than δ critical, even though C_a values for δ greater than δ critical are not of much engineering interest. The value of N for δ less than δ_c increases gradually with δ and increases sharply with δ for δ greater than δ_c .

Similar observations may be made regarding C_a and N for the dynamic case also. However, with increasing α_h the value of N decreases and that of C_a increases.

4.7 CRITICAL ANGLE OF WALL FRICTION

As cited in sec. 3.1, for reaching active state behind a rough retaining wall, it is necessary to satisfy :

$$\frac{\partial E_a}{\partial \psi} = 0 \quad (4.7.1)$$

$$\frac{\partial E_a}{\partial \phi} = 0 \quad (4.7.2)$$

These equations are satisfied if δ is given by :

$$\delta = \alpha + \rho - \phi - \pi/2 \quad (4.7.3)$$

For this value of δ_c , the included angle between soil reaction and earth force, μ , is equal to 90° . However, for certain cases it is possible that this value of δ_c is greater

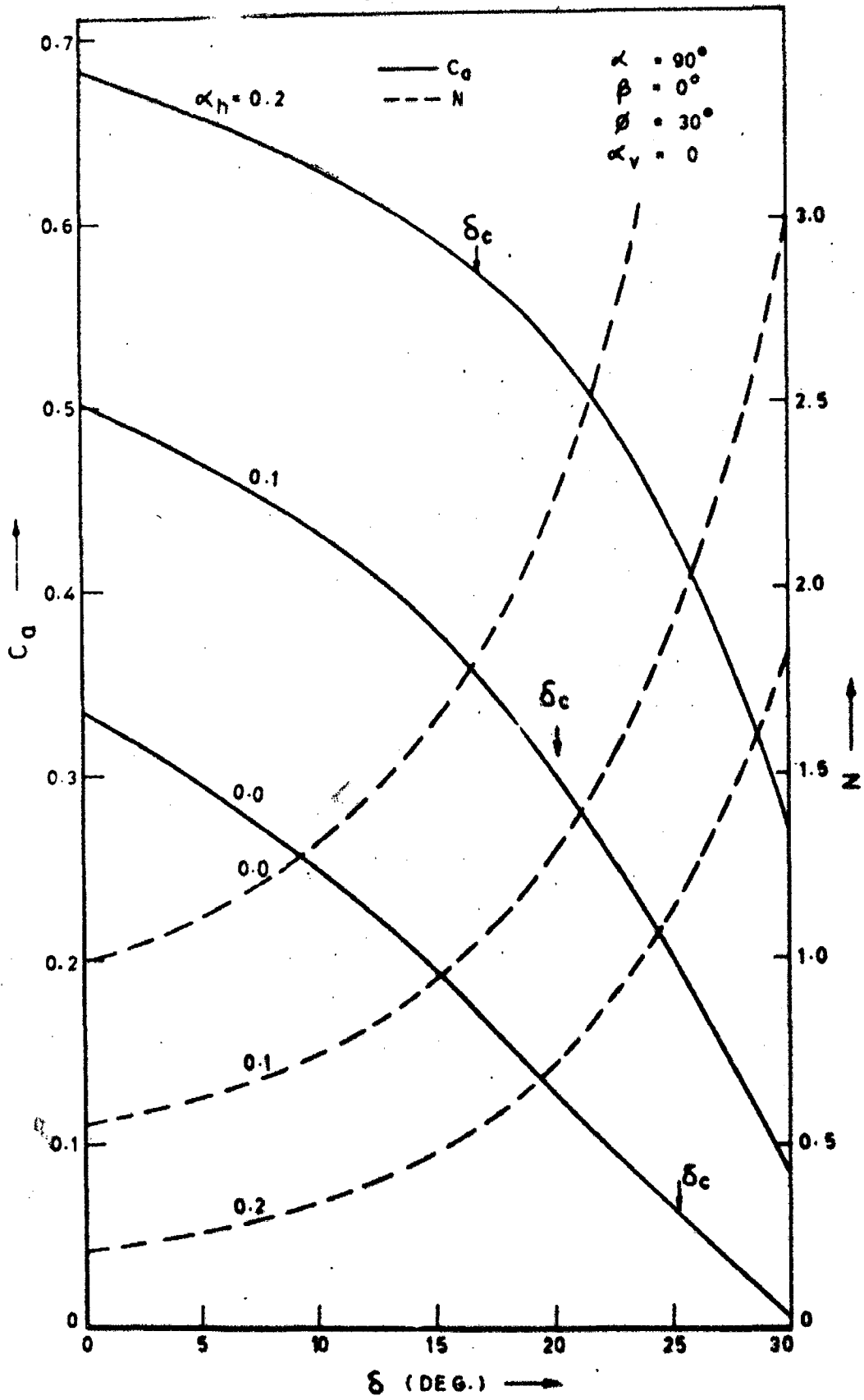


FIG. 4.6.5 - VARIATION OF C_d AND N WITH δ (DEG.)

than ϕ , which is not physically possible. Hence, for such cases the value of δ_c is equal to ϕ :

Figure 4.6.1 shows variation of μ with δ for various values of ϕ for a vertical wall. Similar plots may be obtained for other sets of data also. It is possible to read from such plots the value of δ_c at $\mu = 90^\circ$ which is the condition for reaching δ_c . The values of δ_c thus obtained for static case are shown in Fig. 4.7.1 for various values of ϕ and α . From this figure it may be observed that for every value of α , there is a maximum value of δ_c at which $\delta_c = \delta_{cmax} = \phi$. Beyond this value of δ_{cmax} , there is very little variation of δ_c for higher values of ϕ . Besides, the value of δ_{cmax} keeps increasing with α .

Figure 4.7.1 shows plots of δ given by $\delta = \phi/3$, $\delta = \phi/2$ and $\delta = 2\phi/3$. It is clear that none of these relationship for δ fit well with the values of δ_c satisfying the Eqn. 4.7.1 and thus highlight their inadequacy.

Figure 4.7.1 is useful in reading values of δ_c for wall soil system of common interest. Nevertheless, if this figure is not available it is possible to develop simple expressions for computing the same. Figure 4.7.2 shows the variation of δ_c at $\phi = 40^\circ$ and δ_{cmax} for various values of α . It is clear from this figure that the value of δ_c for $\delta_{cmax} \leq \phi \leq 40^\circ$ is more influenced by α than ϕ . Therefore, it is more logical to relate δ_c with α as well as ϕ . The value of δ_{cmax} for a given

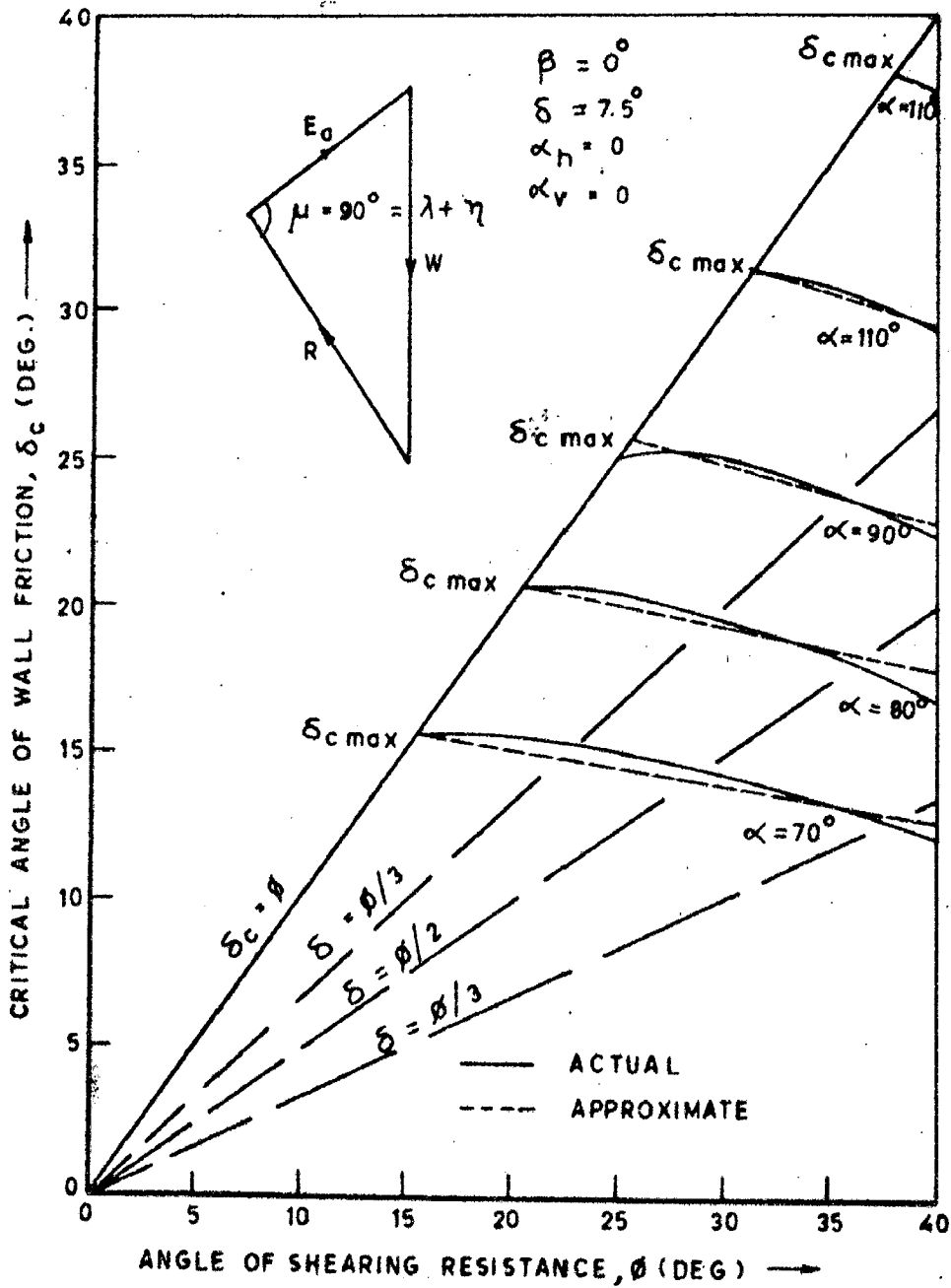


FIG. 4.7.1 - VARIATION OF CRITICAL ANGLE OF WALL FRICTION WITH ANGLE OF SHEARING RESISTANCE AND THE ANGLE OF WALL BACK

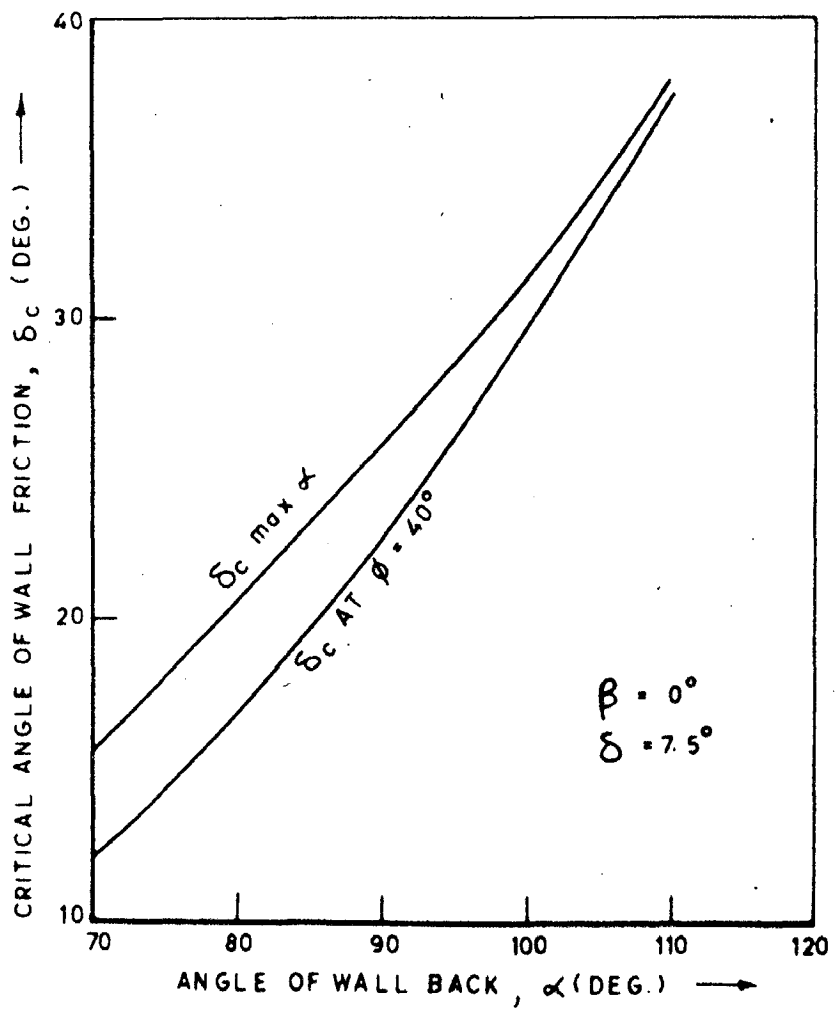


FIG. 4.7.2 - VARIATION OF δ_c WITH α

value of α may be denoted by $\delta_{c\max\alpha}$. The relationship between $\delta_{c\max}$ and α may be expressed as :

$$\delta_{c\max\alpha} = 15.5 + 0.55 (\alpha - 70) \quad (4.7.4)$$

where α is expressed in degrees. The error in computed value of $\delta_{c\max}$ varies from -0.5° to $+0.75^\circ$ which is considered to be acceptable. Furthermore, if the relationship between δ_c and ϕ (for $\delta_{c\max} \leq \phi \leq 40^\circ$) is approximated to a linear variation, for a given value of ϕ , the value of δ_c denoted by $\delta_{c\phi}$ may be expressed as :

$$\delta_{c\phi} = \delta_{c\max\alpha} - (\phi - \delta_{c\max\alpha}) (0.112245 + 0.0022(\alpha - 70)) \quad (4.7.5)$$

where all angles are expressed in degrees.

The maximum value of error in computed value of δ_c is in order of $\pm 1^\circ$ for the entire range of angles covered in this investigation which is acceptable for all engineering purposes. Figure 4.7.3 shows variation of μ with δ for different values of angle of surcharge, β , for $\phi = 30^\circ$ and $\alpha = 90^\circ$. From this figure the values of δ_c may be obtained on the lines explained earlier at $\mu = 90^\circ$. The values of δ_c obtained from similar plots for different values of ϕ are plotted in Fig.4.7.4, from which it may be observed that δ_c is strongly influenced by β also. Besides, as value of β increases the value of δ_c decreases for a given value of ϕ .

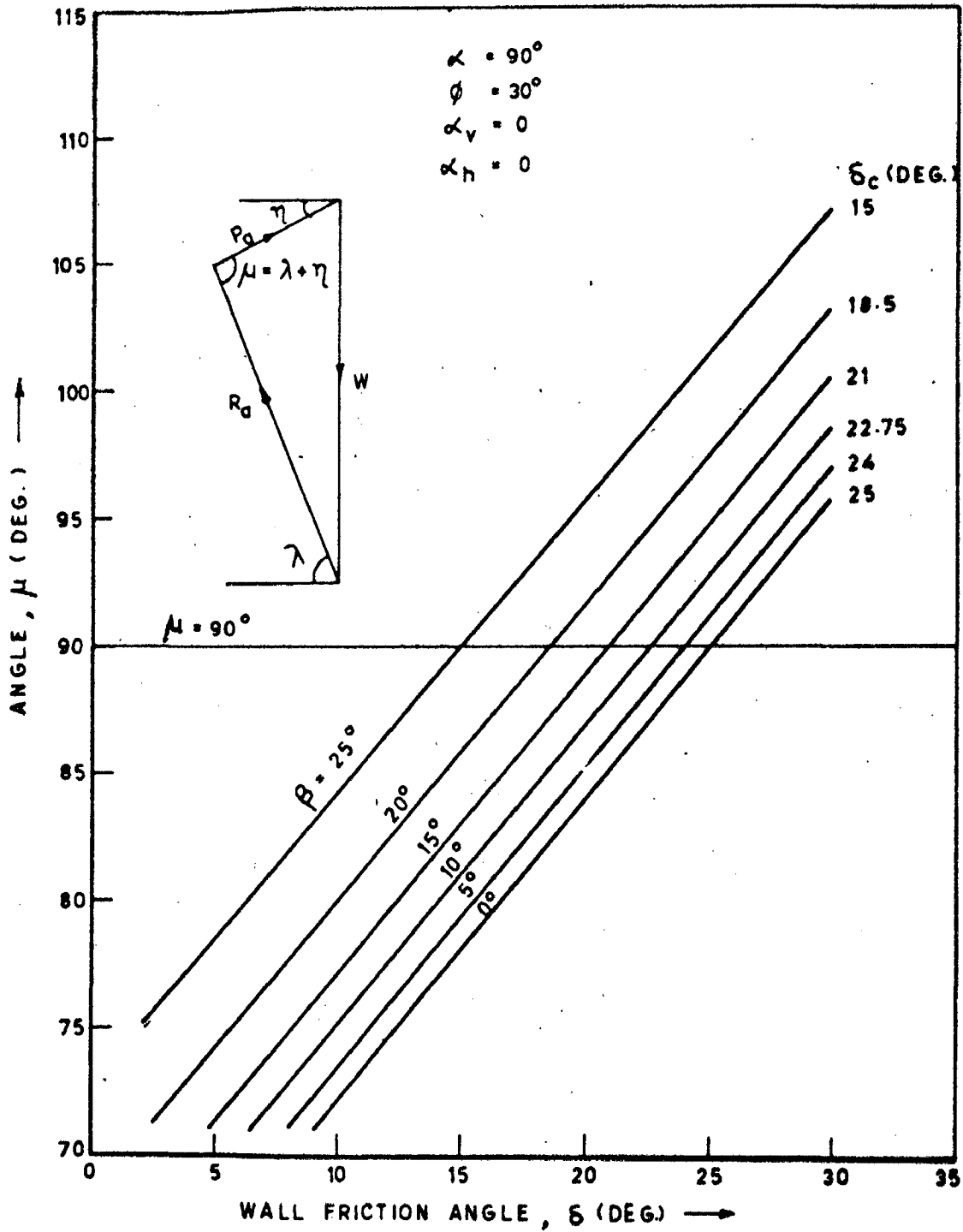


FIG. 4.7.3 - VARIATION OF μ WITH δ FOR VARIOUS VALUES OF β

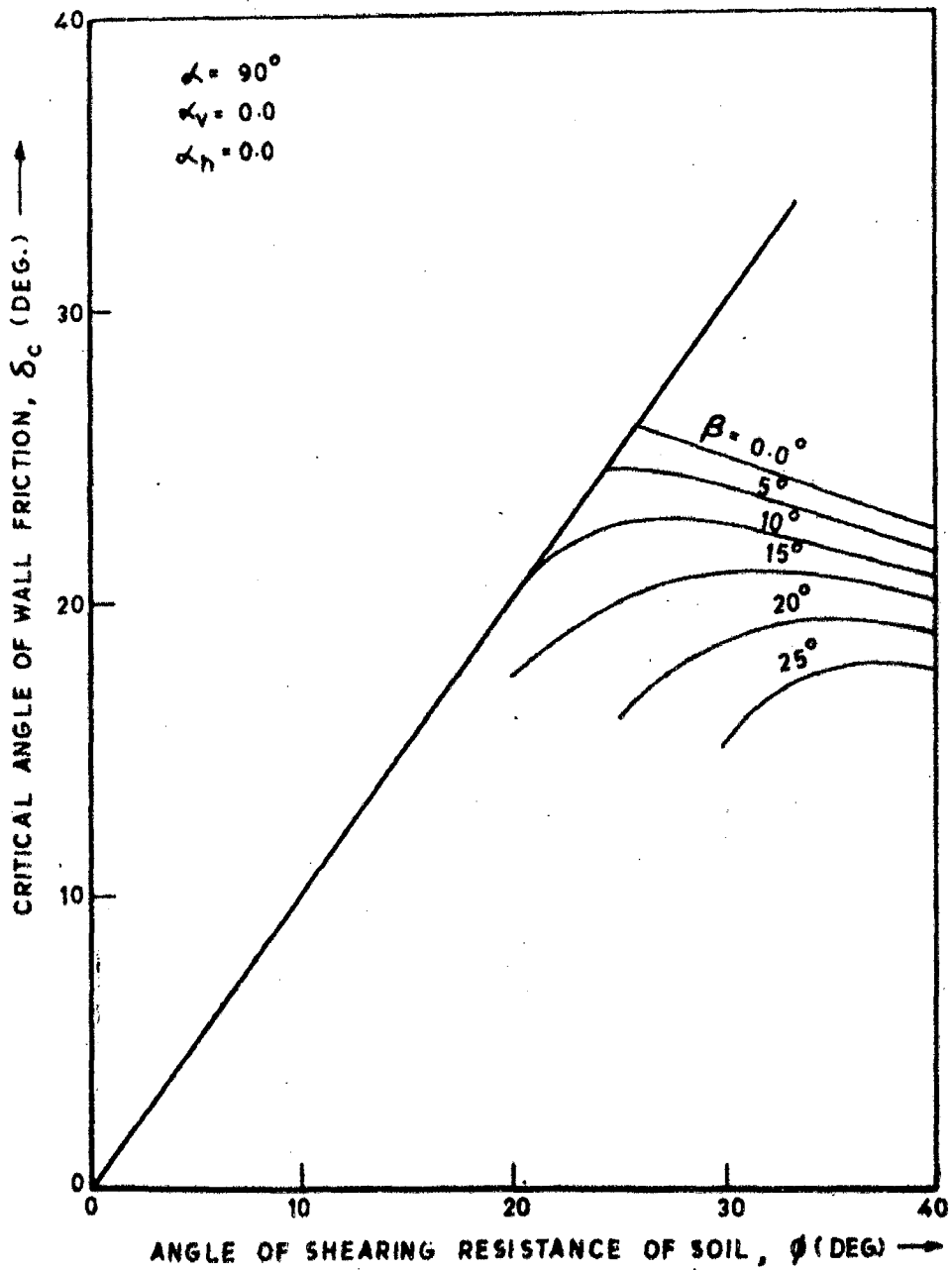


FIG. 4.7.4 - VARIATION OF δ_c WITH ϕ FOR DIFFERENT VALUES OF β

The plots of μ vs δ similar to that shown in Fig.3.6.1 may be obtained for dynamic case also with various values of α . From such plots the values of δ_c may be obtained which are plotted in Fig.4.7.5 as a function of ϕ for $\alpha = 70^\circ, 80^\circ, 90^\circ$ and $\alpha_h = 0.0, 0.1, 0.2, \beta = 0^\circ, \alpha_v = 0$. From this figure it may be observed that as the value of α_h increases the value of δ_c decreases continuously for $\alpha = 90^\circ$. However, for $\alpha = 80^\circ$ and 70° the δ_c increases from its static value for $\alpha_h = 0.1$ and then decreases for $\alpha_h = 0.2$. This variation is further emphasized in Fig. 4.7.6. From this figure it may be noticed that for vertical wall back, the value of δ_c decreases continuously with α_h for $\phi > \delta_c$. For $\alpha = 70^\circ$ and 80° the value of δ_c rises with increasing value of α_h , reaches the maximum and then decreases. This clearly indicates that the value of δ_c is strongly influenced by α_h also. Besides it is also clear from this figure that the value of δ for dynamic case is not always less than that for the static case as considered by many investigators. Figure 4.7.7 shows variation of δ_c with α for various values of ϕ and α_h from which it may be observed that though δ_c continuously increases with α for static case, it decreases with α for the dynamic cases. The value of δ_c decreases with ϕ for static case for all values of α considered. For $\alpha_h = 0.1$, the value of δ_c is 20° for all values of α , for $\phi = 20^\circ$ and its values decrease with increasing ϕ for all values of α . Similar observations can not be made for $\alpha_h = 0.2$.

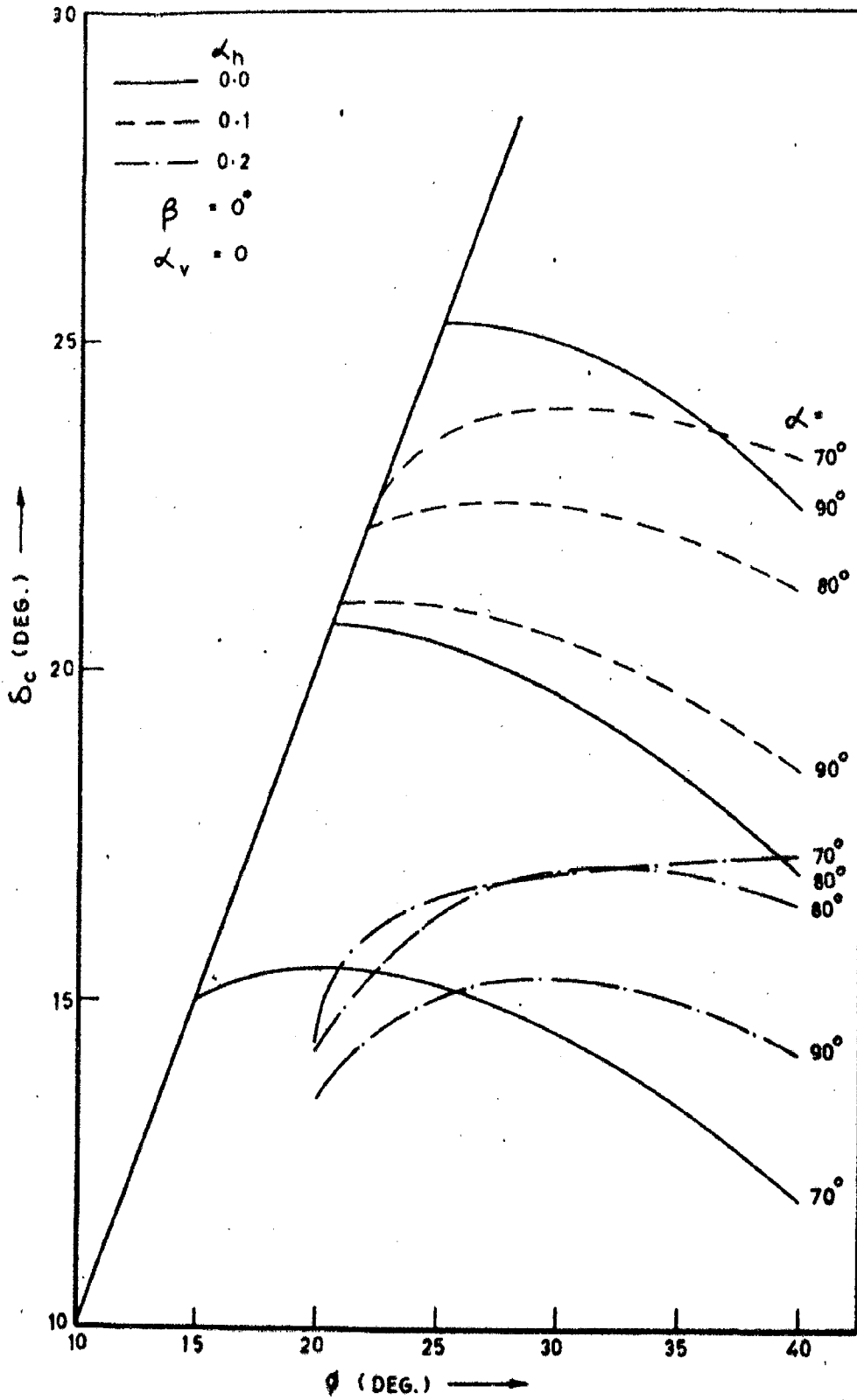


FIG. 4.7.5 - VARIATION OF δ_c WITH ϕ FOR DIFFERENT VALUES OF α

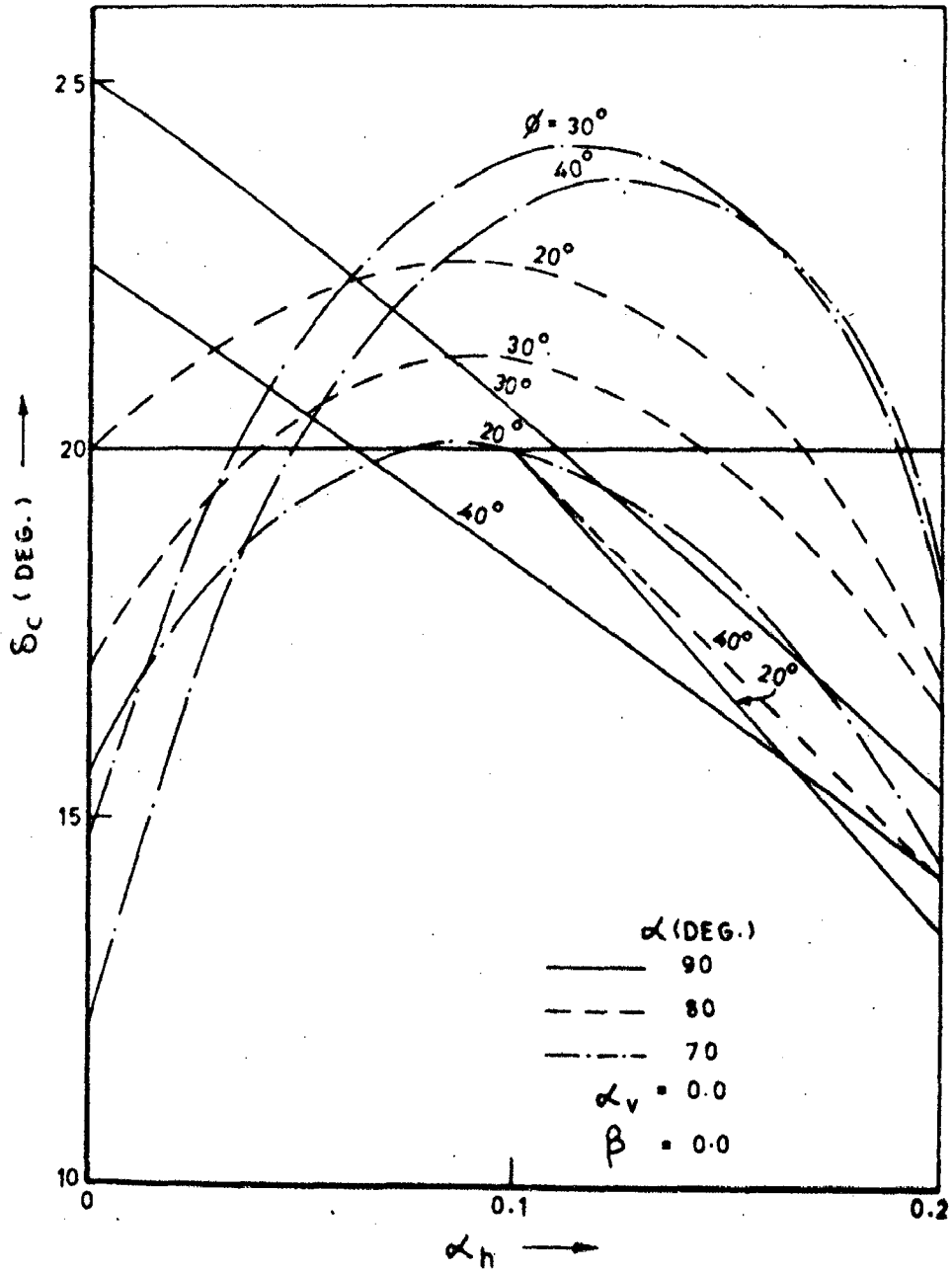


FIG. 4.7.6 - VARIATION OF δ_c WITH α_h FOR VARIOUS VALUES OF ϕ AND α

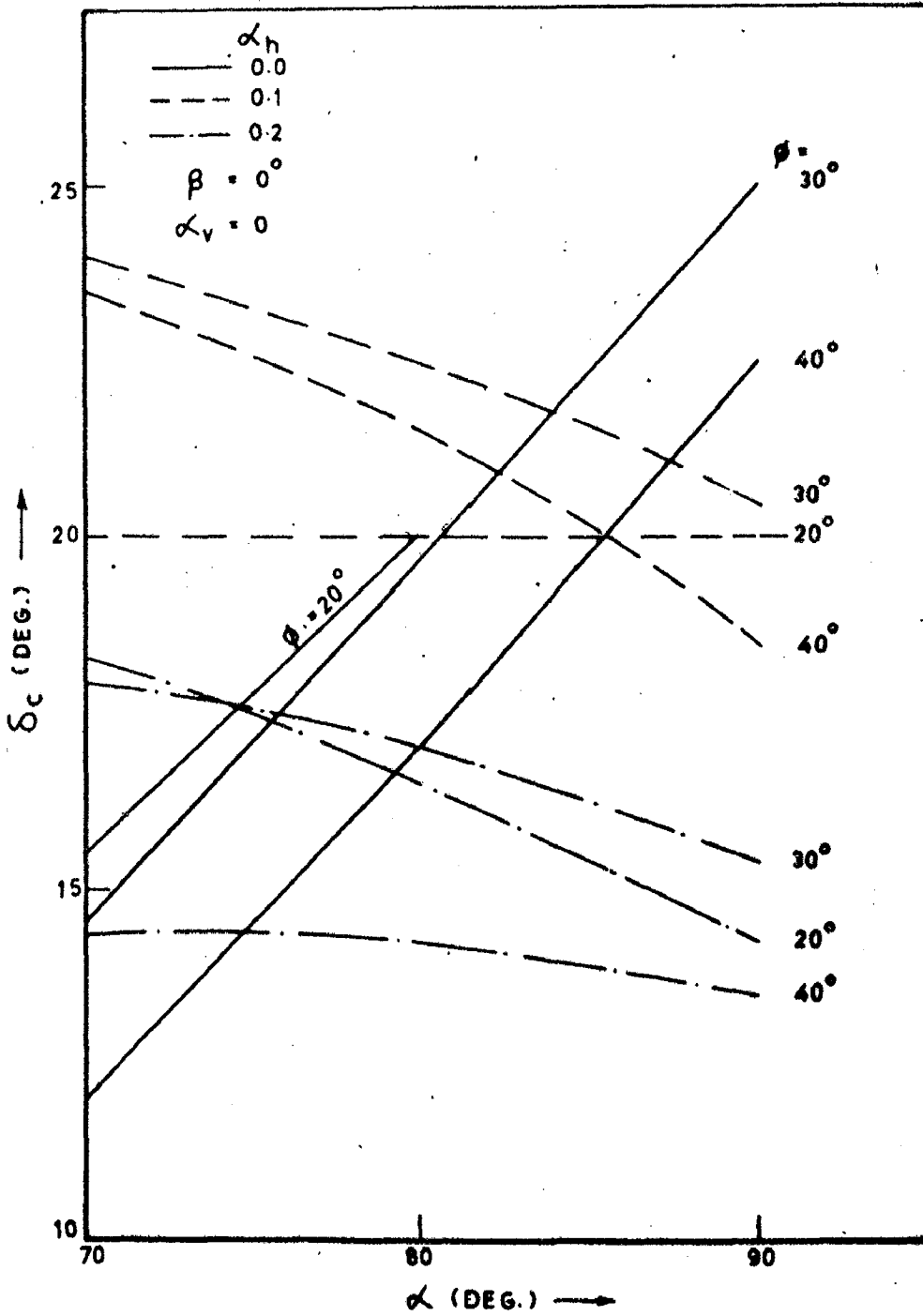


FIG. 4.7.7. VARIATION OF δ_c WITH α FOR VARIOUS VALUES OF ϕ AND α_h

The variation of δ_c with β for different values of ϕ and α_h for vertical wall back is shown in Fig.4.7.8. It may be observed from this figure that the value of δ_c falls very sharply with β for dynamic case. This decrease in value of δ is more pronounced for higher values of α_h and lower values of ϕ . The values of δ_c for different cases have been listed in Tables 4.7.1 and 4.7.2.

From the discussions cited above it is clear that the common practice for relating δ_c with ϕ only is considerably in error. Besides the common notion that the value of δ_c for dynamic case is less than that for static case is also not always correct. It is more rational to relate the value of δ_c to α , ϕ , β and α_h . For the static case simple analytical relationship has been proposed between δ_c , α and ϕ . It is not feasible to develop similar expression with β and α_h as additional parameters. Therefore, it is recommended that analytical investigations on the lines suggested in this section may be carried out for evaluation of appropriate value of δ_c .

4.8 EFFECT OF ANGLE OF SHEARING RESISTANCE

The angle of shearing resistance of the backfill material is a source of resisting force along the rupture surface. It, therefore, tends to reduce the earth force on the wall back for increase in values of ϕ . The values of different non-dimensional factors obtained for different

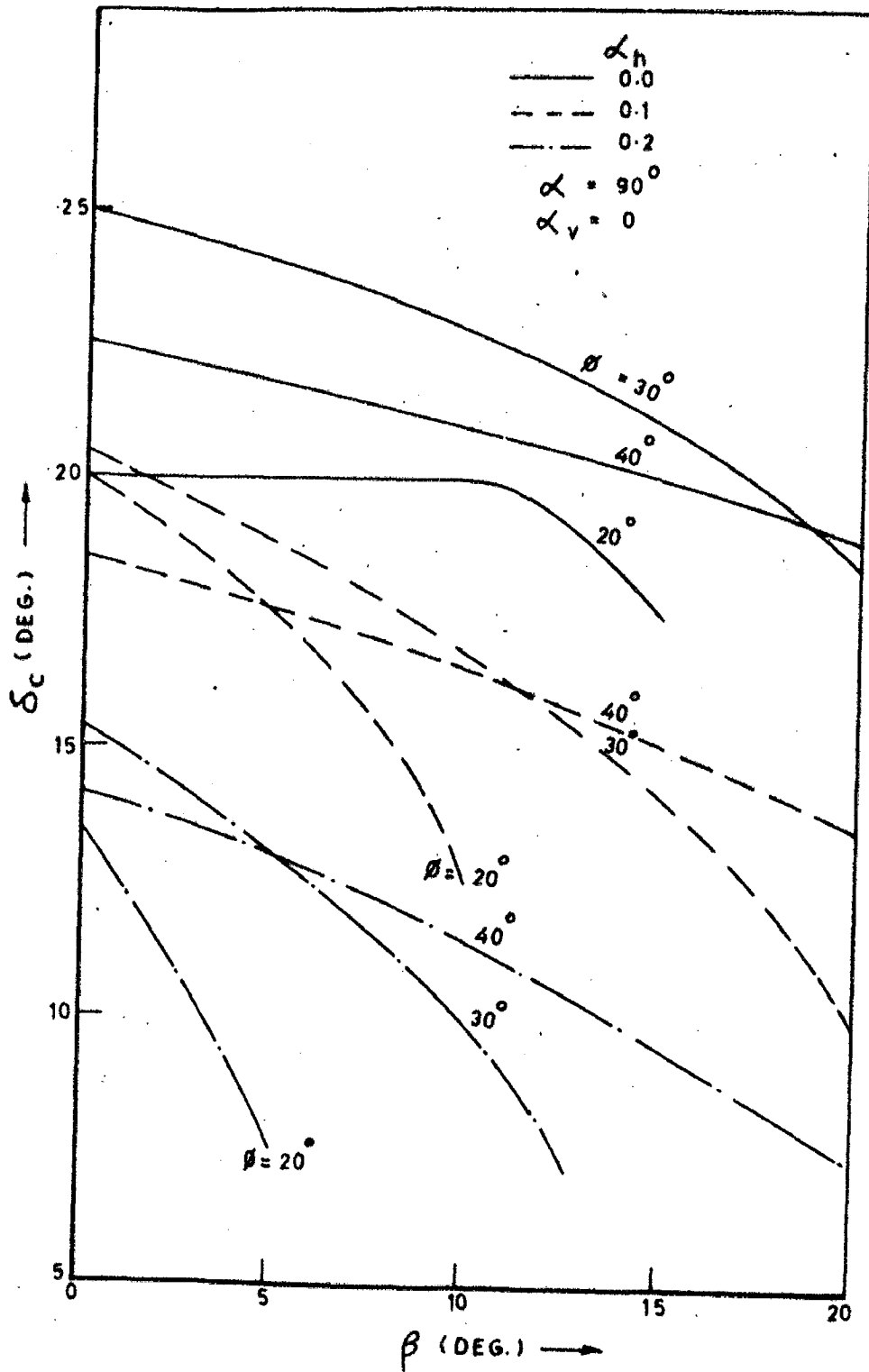


FIG. 4.7.8 - VARIATION OF δ_c WITH β FOR VARIOUS VALUES OF ϕ AND α_h

TABLE 4.7.1 VALUES OF δ_c FOR VARIOUS VALUES OF α AND α_h
($\beta = 0^\circ$ and $\alpha_v = 0$)

		δ_c (IN DEG.)				
α	α_h	$\phi = 20^\circ$	$\phi = 25^\circ$	$\phi = 30^\circ$	$\phi = 30^\circ$	$\phi = 35^\circ$
90°	0.0	20.00	25.00	25.00	24.00	22.50
	0.1	20.00	21.00	20.50	19.65	18.50
	0.2	13.50	15.00	15.40	15.00	14.25
80°	0.0	20.00	20.45	19.65	18.50	17.00
	0.1	20.00	22.50	22.50	22.00	21.25
	0.2	14.25	16.25	17.00	17.00	16.50
70°	0.0	15.50	15.25	14.50	13.50	12.00
	0.1	20.00	23.50	24.00	23.75	23.25
	0.2	14.35	16.68	17.95	18.15	18.30

TABLE 4.7.2 VALUES OF δ_c FOR VARIOUS VALUES OF β AND α_h AND
 $\alpha = 90^\circ$, AND $\alpha_h = 0$

		δ_c (IN DEG.)					
ϕ	α_h	$\beta = 0^\circ$	$\beta = 5^\circ$	$\beta = 10^\circ$	$\beta = 15^\circ$	$\beta = 20^\circ$	$\beta = 25^\circ$
20°	0.0	20.00	20.00	20.00	17.50	-	-
	0.1	20.00	17.50	12.50	-	-	-
	0.2	-	7.00	-	-	-	-
30°	0.0	25.00	24.00	22.75	21.00	18.50	15.00
	0.1	20.50	18.75	16.75	14.25	10.00	-
	0.2	15.40	13.00	10.00	-	-	-
40°	0.0	22.50	21.75	20.09	20.00	18.90	17.50
	0.1	18.50	17.60	16.50	15.15	13.60	-
	0.2	14.15	13.00	11.40	-	-	-

values of ϕ and other parameters are listed in Table 4.8.1. Figure 4.8.1 shows the variation of C_{ma} , C_{ha} and C_{fah} from which it may be observed that both C_{ma} and C_{fah} continuously decrease with increase in ϕ for all values of α_h , which is in agreement with observations cited above. On the other hand C_{ha} increases with ϕ . Eventhough, this increase is insignificant for $\alpha = 90^\circ$, $\beta = 0^\circ$ and $\delta = 7.5^\circ$; it may be significant for $\alpha < 90^\circ$ and $\beta > 0^\circ$ for higher values of α_h . The decrease in C_{fa} with increasing ϕ may be attributed to corresponding increase in ρ and associated decrease in weight of the failure wedge. Since C_{fa} decreases much faster than increase in C_{ha} , the C_{ma} value decreases with increasing ϕ , for the range of parameters considered in this investigation.

The distribution of pressure factor with depth shown in Fig.4.8.2 indicates a contineous decrease in intensity of pressure with increasing values of ϕ for any given depth factor, which is in agreement with the discussion cited above. Similar observations may be made from this figure for the dynamic case also.

The values of C_a and N for different values of ϕ and α_h shown in Fig.4.8.3 also support these observations.

4.9 EFFECT OF SEISMIC COEFFICIENTS

Horizontal seismic accelerations cause inertia forces which, when directed towards the wall, will produce additional dynamic earth forces on the retaining wall. Because of

TABLE 4.8.1: EFFECT OF ANGLE OF SHEARING RESISTANCE OF SOIL, ϕ ,
 ($\alpha = 90^\circ$, $\beta = 0^\circ$, $\delta = 7.5^\circ$ and $\alpha_v = 0$) (ρ IN DEG.)

ϕ	20°	25°	30°	35°	40°	
$\alpha_h = 0$	C_{fah}	0.4511	0.3757	0.3105	0.2541	0.2051
	ρ	51.9121	55.2348	58.3033	61.2163	64.0271
	C_{ha}	0.3137	0.3163	0.3184	0.3202	0.3218
	C_{ma}	0.4245	0.3565	0.2966	0.2441	0.1981
	N	1.24963	1.22198	1.19980	1.18105	1.16464
	C_a	0.38902	0.32991	0.27661	0.22904	0.18688
$\alpha_h = 0.05$	C_{fah}	0.4896	0.4097	0.3408	0.2811	0.2292
	ρ	48.6800	52.5665	55.9051	59.0497	62.0307
	C_{ha}	0.3397	0.3444	0.3490	0.3537	0.3586
	C_{ma}	0.4989	0.4234	0.3569	0.2982	0.2466
	N	0.99417	0.95169	0.91207	0.87288	0.83242
	C_a	0.49556	0.42527	0.36198	0.30528	0.25464
$\alpha_h = 0.1$	C_{fah}	0.5336	0.4478	0.3743	0.3108	0.2556
	ρ	44.9745	49.4712	53.2903	56.7220	59.9104
	C_{ha}	0.3675	0.3733	0.3795	0.3861	0.3935
	C_{ma}	0.5882	0.5015	0.4262	0.3600	0.3018
	N	0.7624	0.71792	0.67282	0.62576	0.5755
	C_a	0.61567	0.52887	0.45238	0.38442	0.32379
$\alpha_h = 0.15$	C_{fah}	0.5846	0.4907	0.4116	0.3436	0.2846
	ρ	40.6737	46.0743	50.4311	54.2181	57.6597
	C_{ha}	0.3982	0.4036	0.4102	0.4180	0.4270
	C_{ma}	0.6984	0.5941	0.5066	0.4309	0.3646
	N	0.5442	0.50997	0.46827	0.42140	0.36955
	C_a	0.75112	0.64022	0.54661	0.46507	0.39296
$\alpha_h = 0.2$	C_{fah}	0.6456	0.5400	0.4534	0.3799	0.3165
	ρ	35.5969	42.2455	47.2944	51.5209	55.2636
	C_{ha}	0.4343	0.4361	0.4418	0.4496	0.4593
	C_{ma}	0.8411	0.7064	0.6009	0.5124	0.4362
	N	0.32888	0.31905	0.28861	0.24775	0.19944
	C_a	0.90441	0.7590	0.64373	0.54626	0.46136

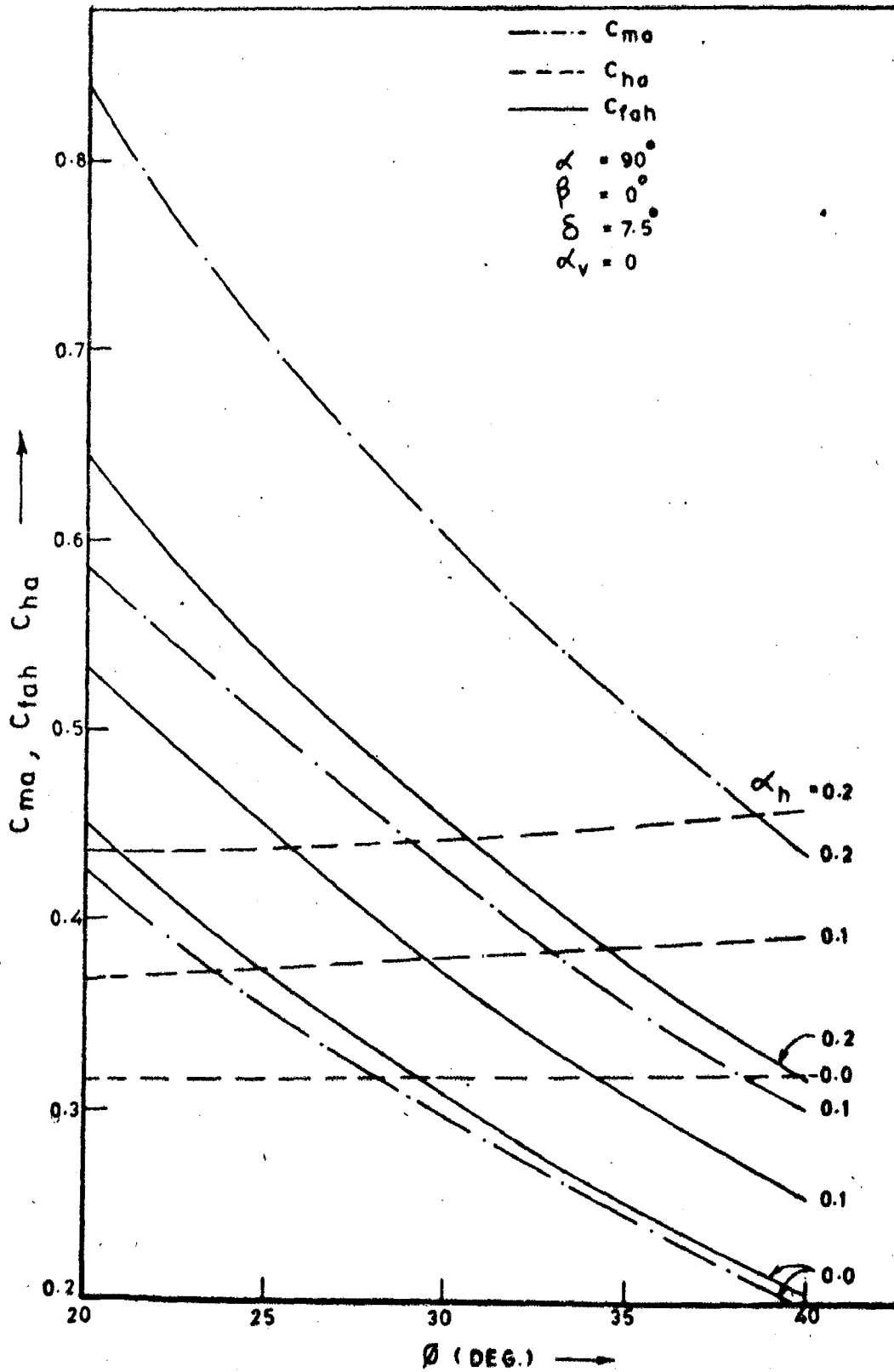


FIG. 4.8.1 - VARIATION OF C_{ma} , C_{ha} , C_{fah} WITH θ FOR VARIOUS VALUES OF α_h

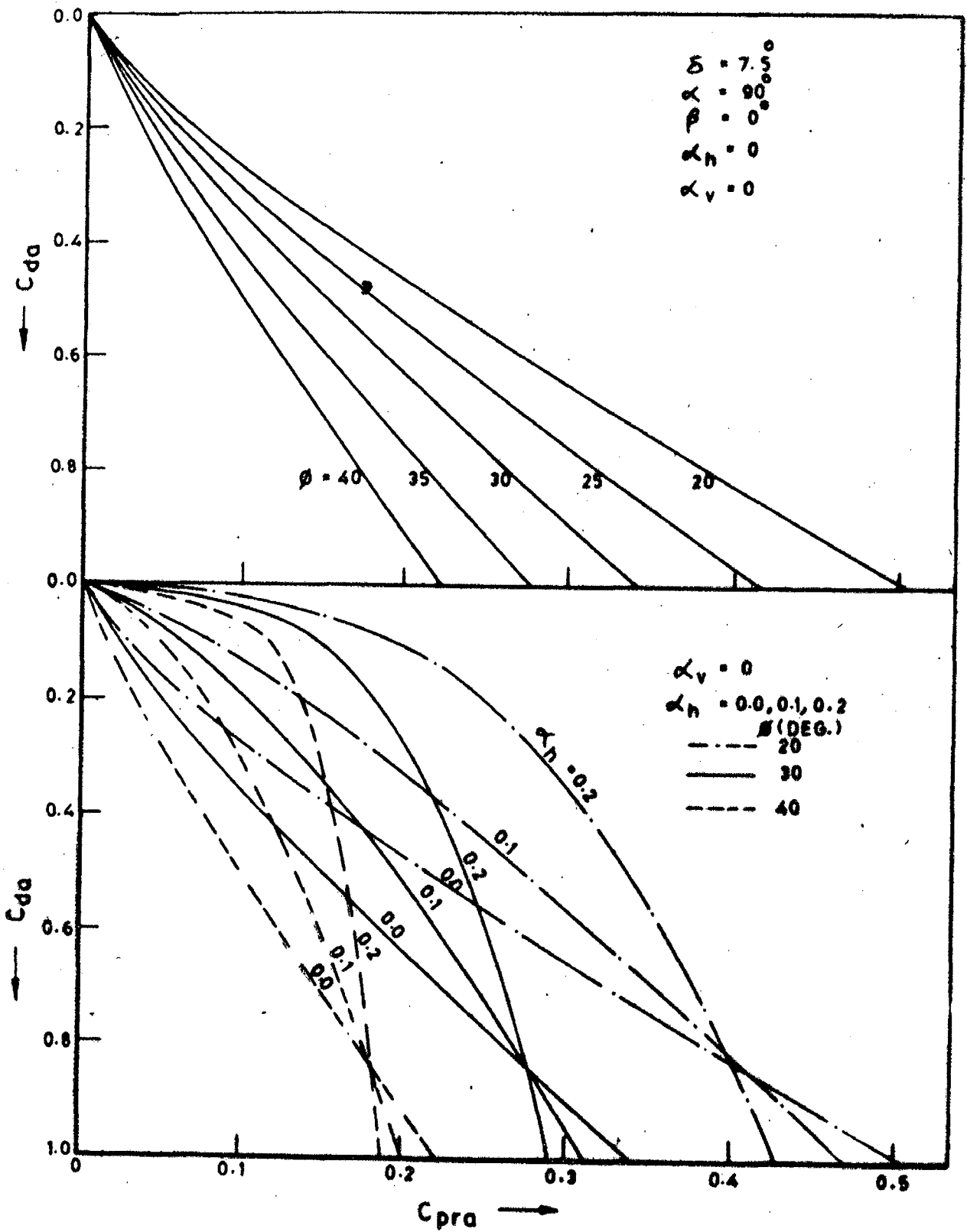


FIG. 4.8.2 - VARIATION OF C_{pra} WITH DEPTH FOR DIFFERENT VALUES OF ϕ AND α_h

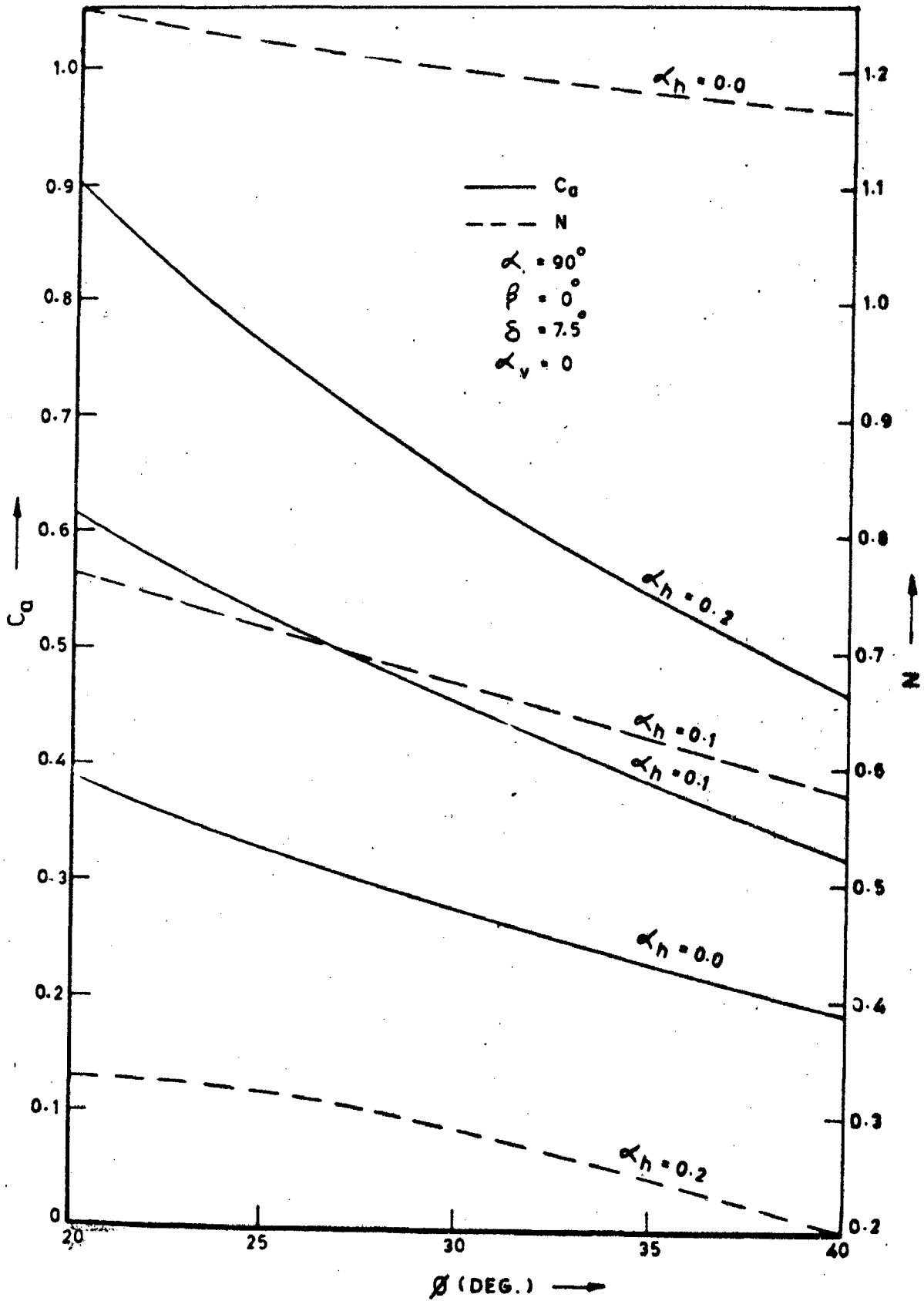


FIG. 4.8.3 - VARIATION OF C_d AND N WITH θ FOR DIFFERENT VALUES OF α_h

this additional disturbing force, additional soil mass is enabled to slip down. Therefore, the angle of failure plain with horizontal decreases with increasing value of α_h . This leads to increase in the mass of the rupture wedge which is basically responsible for increasing the dynamic earth force against the wall.

The width of the rupture wedge is obviously larger at the top and gradually reduce to zero at the base. Therefore, inertial force being proportional to mass, for a given seismic acceleration, it follows that the contribution of inertial force by the sliding wedge is greater near the top compared to that near the base. This results into increase in intensity of earth pressure near the top end of the wall for the dynamic case. This results into increase in the value of C_{ha} . Figures 4.9.1, 4.9.2 and 4.9.3 support these observations.

It may be observed from Fig. 4.9.1 that C_{ha} , C_{ma} and C_{fah} increase with increasing α_h . For any α_h these quantities decrease with increasing values of α . Similar observations can be made from Fig. 4.9.2 for increasing values of δ also. In the case of ϕ , even though the values of C_{ha} , C_{ma} and C_{fah} increase with increasing α_h , C_{ma} and C_{fah} increase and C_{ha} decreases with decreasing ϕ for any given value of α_h .

So far the effect of α_v has not been considered. Figure 4.9.4 shows variation of C_{ha} with α_h for different values of α_v , from which it may be observed that for a given value of α_h ,

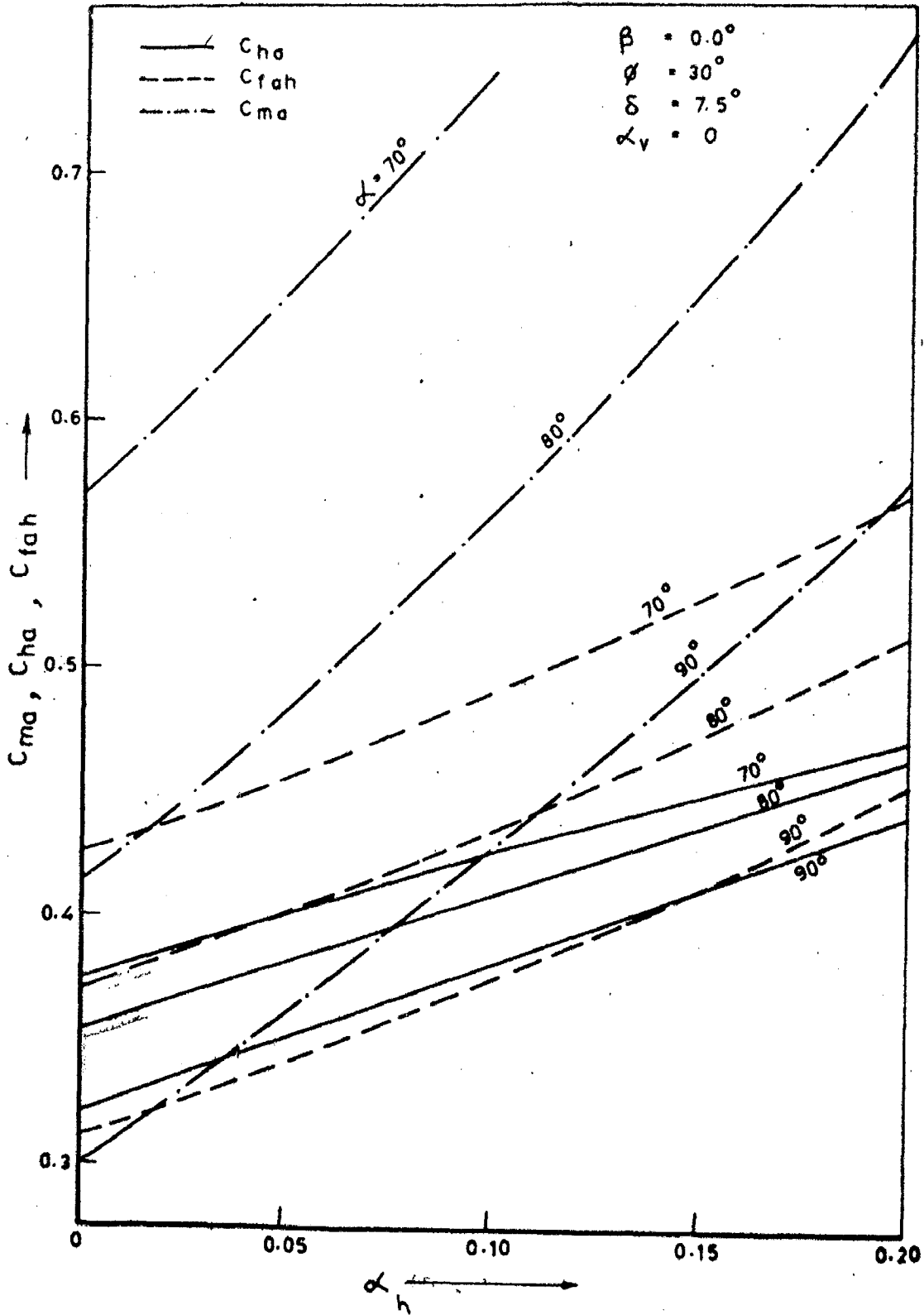


FIG. 4.9.1 - EFFECT OF HORIZONTAL SEISMIC COEFFICIENT, α_h ON MOMENT FACTOR, POINT OF ACTION FACTOR AND FORCE FACTOR FOR DIFFERENT VALUES OF α

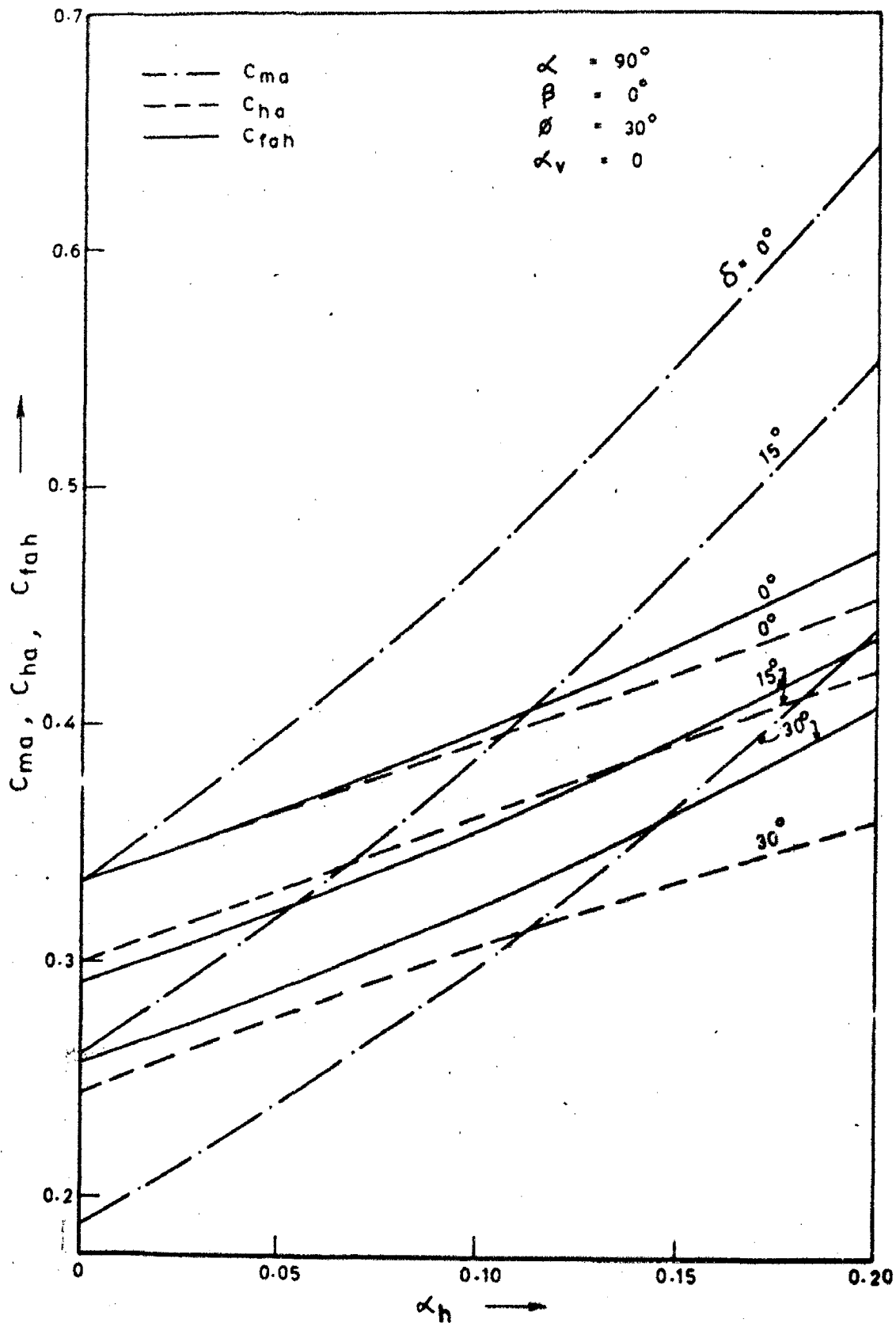


FIG. 4.9.2 - VARIATION OF C_{ma}, C_{ha}, C_{tah} WITH α_h FOR VARIOUS VALUES OF δ

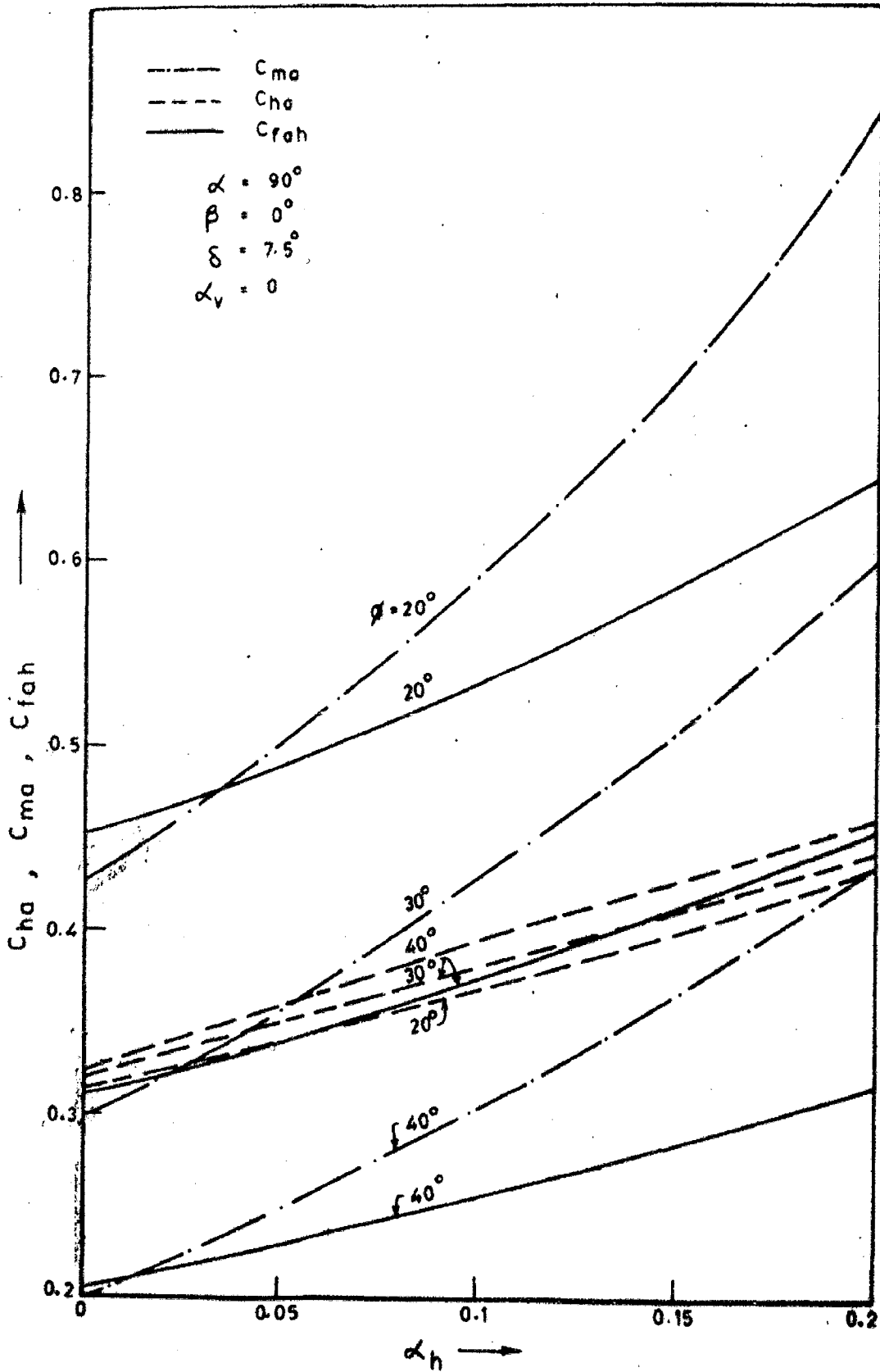


FIG. 4.9.3 - VARIATION OF C_{ma}, C_{ha}, C_{tah} WITH α_h FOR VARIOUS VALUES OF ϕ

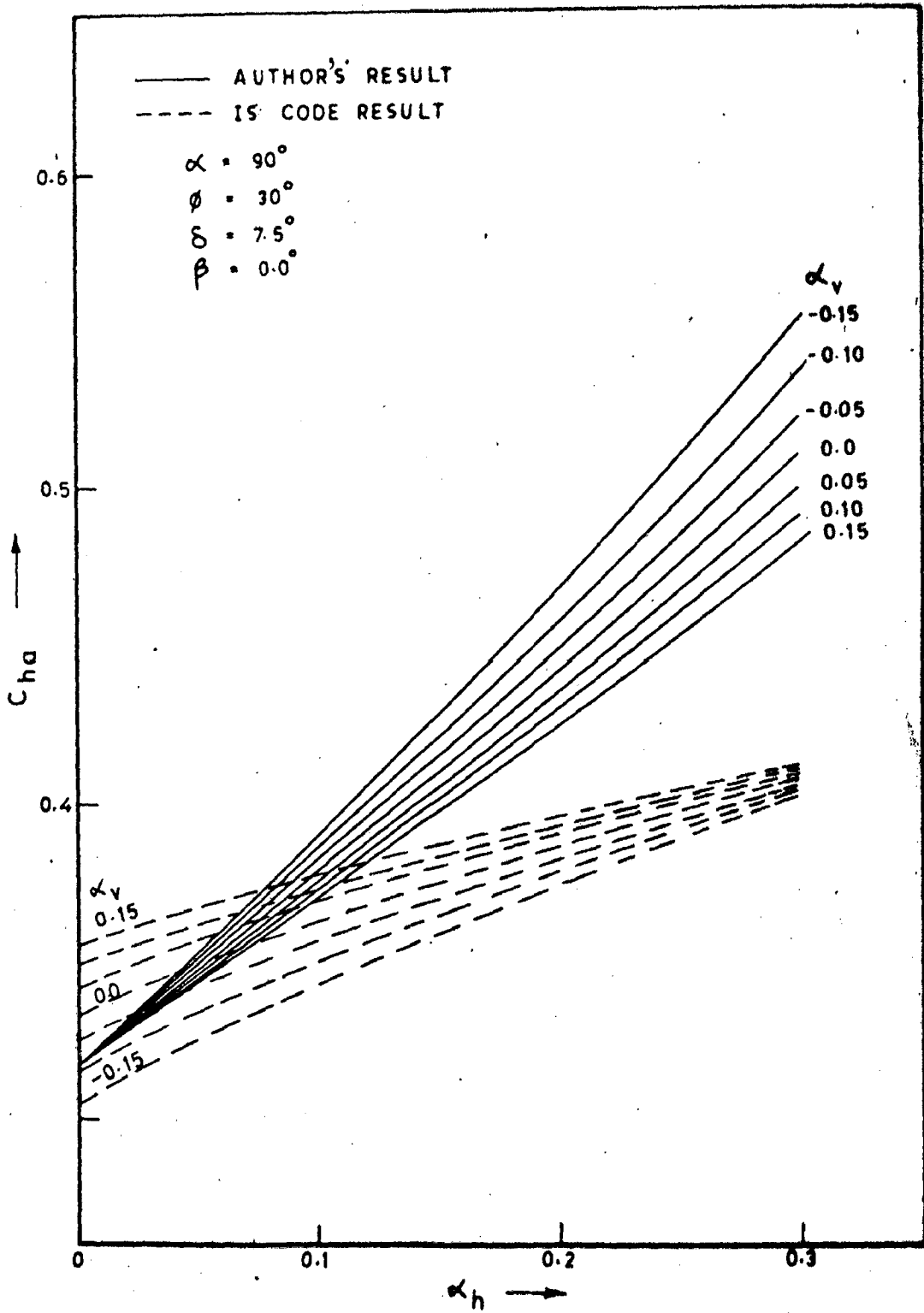


FIG. 4.9.4 - VARIATION OF C_{ha} WITH α_h AND α_v FOR $\beta = 0^\circ$

changes in values of α_v cause significant changes in C_{ha} particularly for higher values of α_h . Similar details for $\beta = 5^\circ$ and $\beta = 10^\circ$ are presented in Fig.4.9.5 and 4.9.6 from which it may be noticed that C_{ha} increases, rather sharply for higher values of α_h and α_v with increasing β . In fact for $\beta = 10^\circ$, $\phi = 30^\circ$, $\delta = 7.5^\circ$, $\alpha = 90^\circ$, $\alpha_h = 0.3$ and $\alpha_v = -0.15$, the value of C_{ha} obtained is 1.329 which is not physically possible. This is so because, the value of $\beta = 10^\circ$ is permissible by Mononobe-Okabe formula (for this set of data) which considers only $\Sigma H = 0$ and $\Sigma V = 0$. The formula has not accounted for moment equilibrium condition. This example clearly shows that the Mononobe-Okabe formula does not always stand the test of moment equilibrium condition.

It is, therefore, desirable to limit the permissible values of β to much smaller values than that indicated by Mononobe-Okabe formula. The recommendations proposed in Fig. 4.5.6 in which permissible β is 5° (five degrees) below that recommended by Mononobe-Okabe formula is safe with respect to moment equilibrium condition also, for the range of ϕ , α_h and α_v considered.

The effect of vertical seismic coefficient on the pressure distribution may be studied from Fig.4.9.6. It may be observed that positive values of α_v cause increase in pressure intensity and negative values cause decrease at any depth. This is observed to be so for other values of α , β , ϕ and δ .

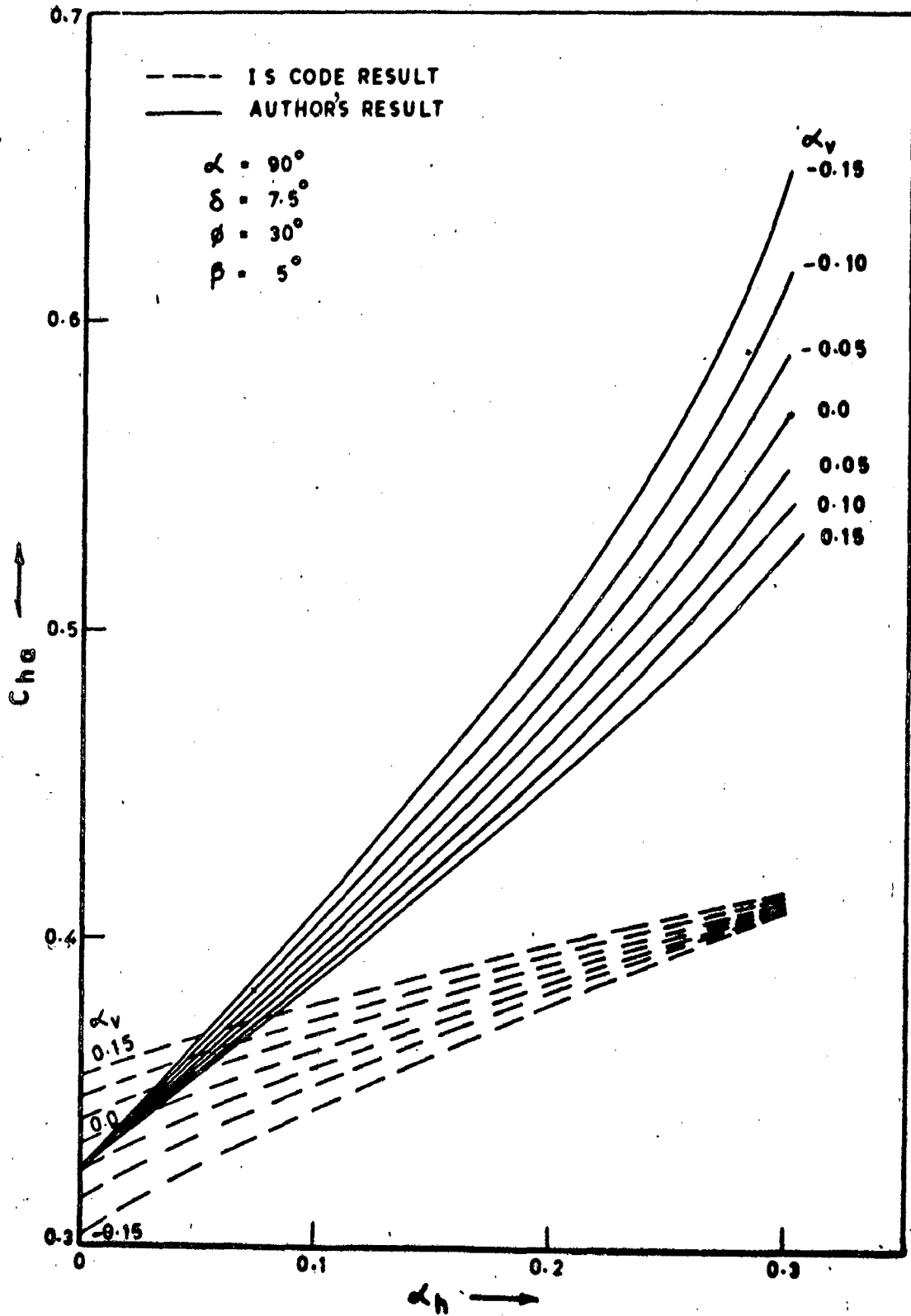


FIG. 4.9.5 - VARIATION OF C_{ha} WITH α_h AND α_v FOR $\beta = 5^\circ$

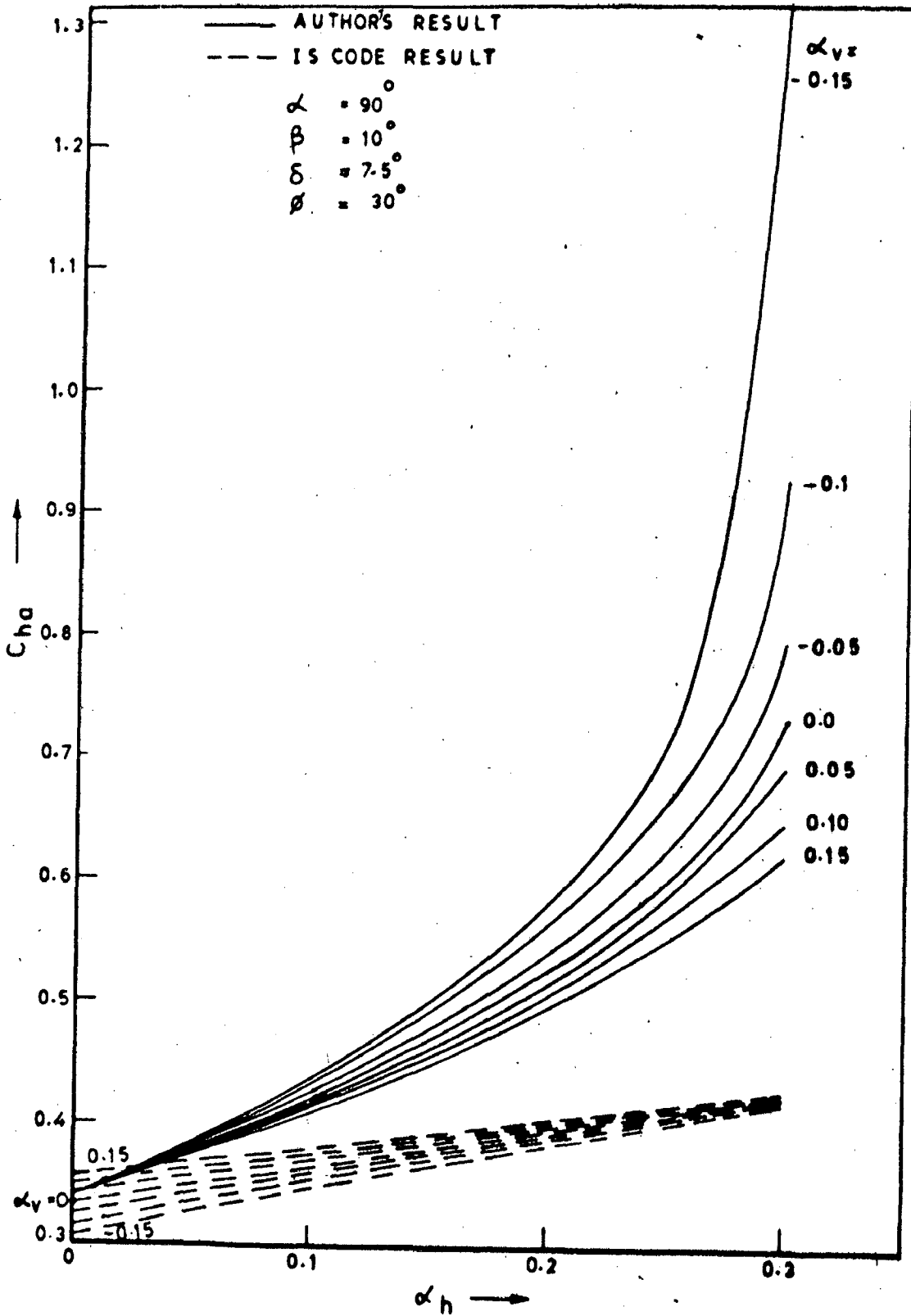


FIG. 4.9.6 - VARIATION OF C_{ha} WITH α_h AND α_v FOR $\beta = 10^\circ$

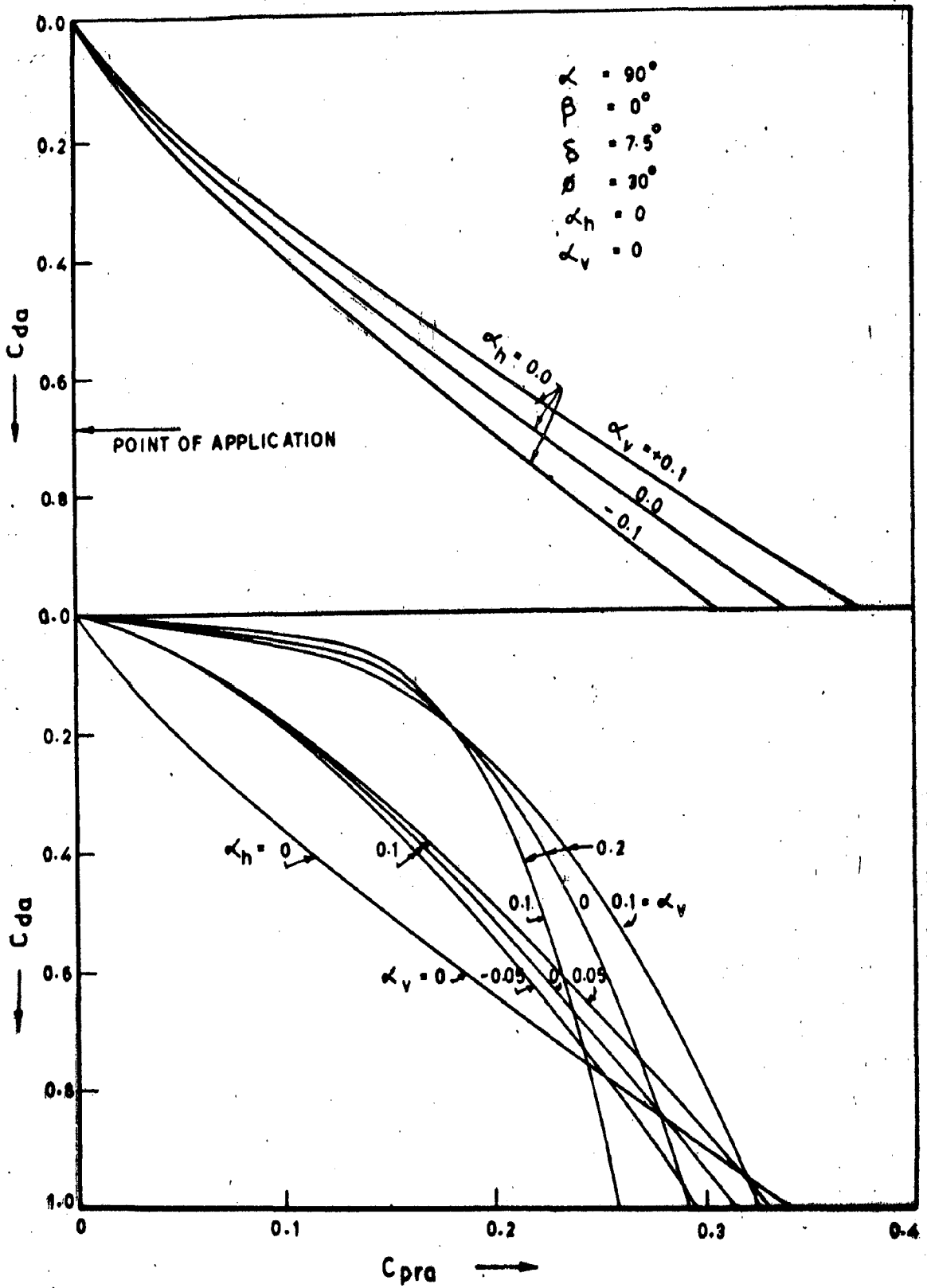


FIG. 4.9.7 - VARIATION OF C_{pra} WITH DEPTH FOR VARIOUS VALUES OF α_h AND α_v

The pressures for static case and for dynamic case with $\alpha_h = 0.1$ and 0.2 with $\alpha_v = \pm \alpha_h/2$ are also shown in this figure. It may be observed from this figure that the curve for dynamic pressure for a given α_h at $\alpha_v = 0$ is very close to the corresponding plots with $\alpha_v = \pm \alpha_h/2$ for the top one third height of the wall. The effect of α_v on the pressure gradually increases there onwards with depth reaching a maximum at the base. This is logical, because, the vertical inertia forces will reach maximum for the vertical slice close to the wall and, therefore, produce a maximum effect near the base of the wall. On the other hand the horizontal seismic coefficient has greater influence in the upper portion of the wall, because, it will be producing higher horizontal inertia force near the upper end of the rupture wedge where the width is maximum.

4.10 ADVANTAGES AND LIMITATIONS OF THIS INVESTIGATION

: As assumed in Chapter III, the use of Mononobe-Okabe rupture wedge is in agreement with the experimental results reported by many investigators. This is a point in favour of this investigation. Similarly, the assumption of same acceleration coefficient throughout the rupture mass also appears to be in good agreement with the experimental evidence. These findings give reasonable respectability to the results reported in this investigation.

The variation in measured seismic acceleration given by Ishii et al.(1960) has been listed in the following Table:

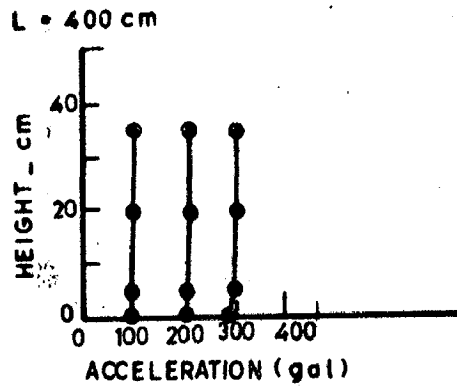
TABLE 4.10.1 DISTRIBUTION OF ACCELERATION WITHIN THE RUPTURE WEDGE. FOR ACTIVE CASE (Ishii et al.,1960)

L = 400 cm (NEIGHBOURHOOD OF WALL)

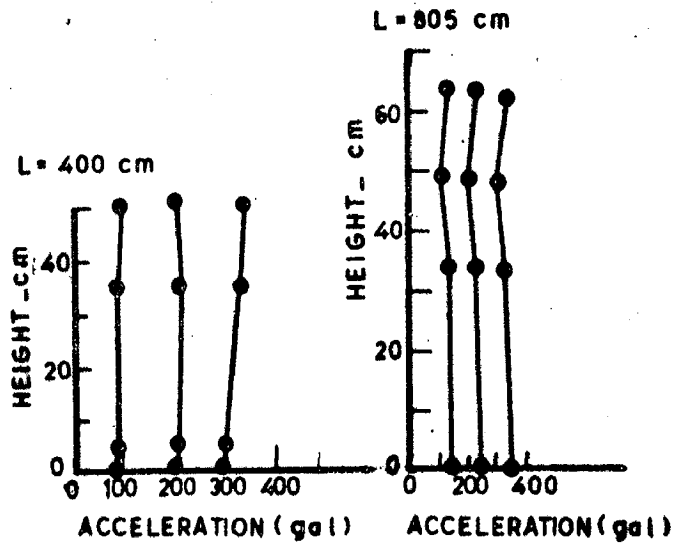
H in cm.	$\alpha_h.g$	Variation (percent)	$\alpha_h.g$	Variation (percent)	$\alpha_h.g$	Variation (percent)
0	82.857	-	192.56	-	274.286	-
05	84.286	1.7	192.56	0.0	285.714	4.2
20	84.286	1.7	200.00	3.9	292.857	6.8
35	84.286	1.7	200.00	3.9	292.857	6.8
50	-	-	-	-	-	-

(CENTRAL PART OF THE BOX)

00	82.857	-	192.56	-	285.714	-
04	82.857	0.0	200.0	3.9	297.143	4.0
35	78.57	5.2	207.14	7.6	321.43	12.5
50	85.714	3.8	200.00	3.9	328.57	15.0



ACCELERATION NEAR THE WALL



ACCELERATION AT CENTER OF THE BOX

FIG. 4.10.1 - DISTRIBUTION OF ACCELERATION WITHIN THE RUPTURE WEDGE (ISHII ETAL, 1960)

The numerical approach for obtaining the stress distribution due to soil reaction is of great help in accounting for moment equilibrium condition without making unreasonable assumptions to carryout the analysis. This is yet another point in favour of this investigation. The pressure distribution obtained by the method used in this investigation for a vertical wall back, retaining level backfill with $\phi = 30^\circ$ for the static case are shown in Fig.4.10.3 by curve (A) for $\delta = 7.5^\circ$ and curve B for $\delta = 22.5^\circ$. The pressure distribution obtained by the method proposed by Basavanna (1970) is also shown in this figure by curve C. It may be observed from this figure that for $\delta = 7.5^\circ$ the pressure ordinates of curve C are larger along the upper portion of the wall back and smaller along the lower portion compared with those of curve A. This is logical, because, the assumptions made in Basavanna's theory, that the vertical stress at a point within the rupture wedge is given by the weight of the soil column at that point is in error. This drawback has been rectified in this investigation. Therefore, the curve obtained for this investigation appears to be more reasonable. Terzaghi (1936 and 1941), based on his experimental investigations, has reported that the pressures close to the base of the wall approach the at rest earth pressures. Obviously with such a situation the higher pressure ordinates near the base of the wall bring the resultant earth force closer to the base of the wall. This is in agreement with the results obtained in this investigation.

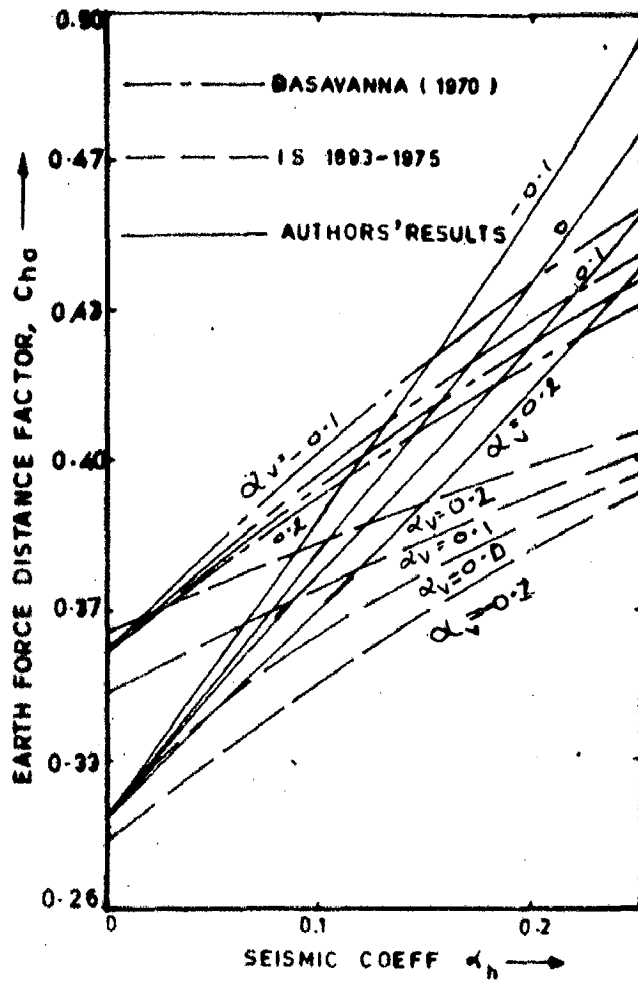


FIG. 4.10.2 - VARIATION OF C_{hd} WITH α_v AND α_h
BY DIFFERENT METHOD

The coefficient of at rest earth pressure by Jaky's method is given by :

$$K_0 = 1 - \sin \phi \quad (4.10.1)$$

The at rest pressures using this expression are also shown in this figure by line D. It may be observed that pressure curve predicted by Basavanna's method moves away from the plot of pressure obtained by Jaky's method which is contrary to Terzaghi's observation cited above. Besides, for a wall tilting about its base, the movement of the wall at base^{is} negligible. Therefore, pressures close to at rest pressure near the base are quite logical. Curve A and B obtained in this investigation are in agreement with these observations of Terzaghi. It may be recalled that for $\phi = 30^\circ$ critical value of angle of wall friction, δ_c , is equal to 25° . The curve C obtained for $\delta = 22.5^\circ$ is pretty close to this condition and which predicts pressure at the base practically identical with that predicted by Jaky's formula. This is another point in support of this investigation.

Figure 4.10.2 shows the point of action factor, C_{ha} , obtained by Basavanna's theory as well as those obtained in this investigation. Besides, C_{ha} values obtained by the method recommended by Indian Standard Code of Practice (IS: 1893 - 1975) are also shown in this figure. It may be observed from this figure that all curves obtained by Basavanna's theory and the results of this investigation with

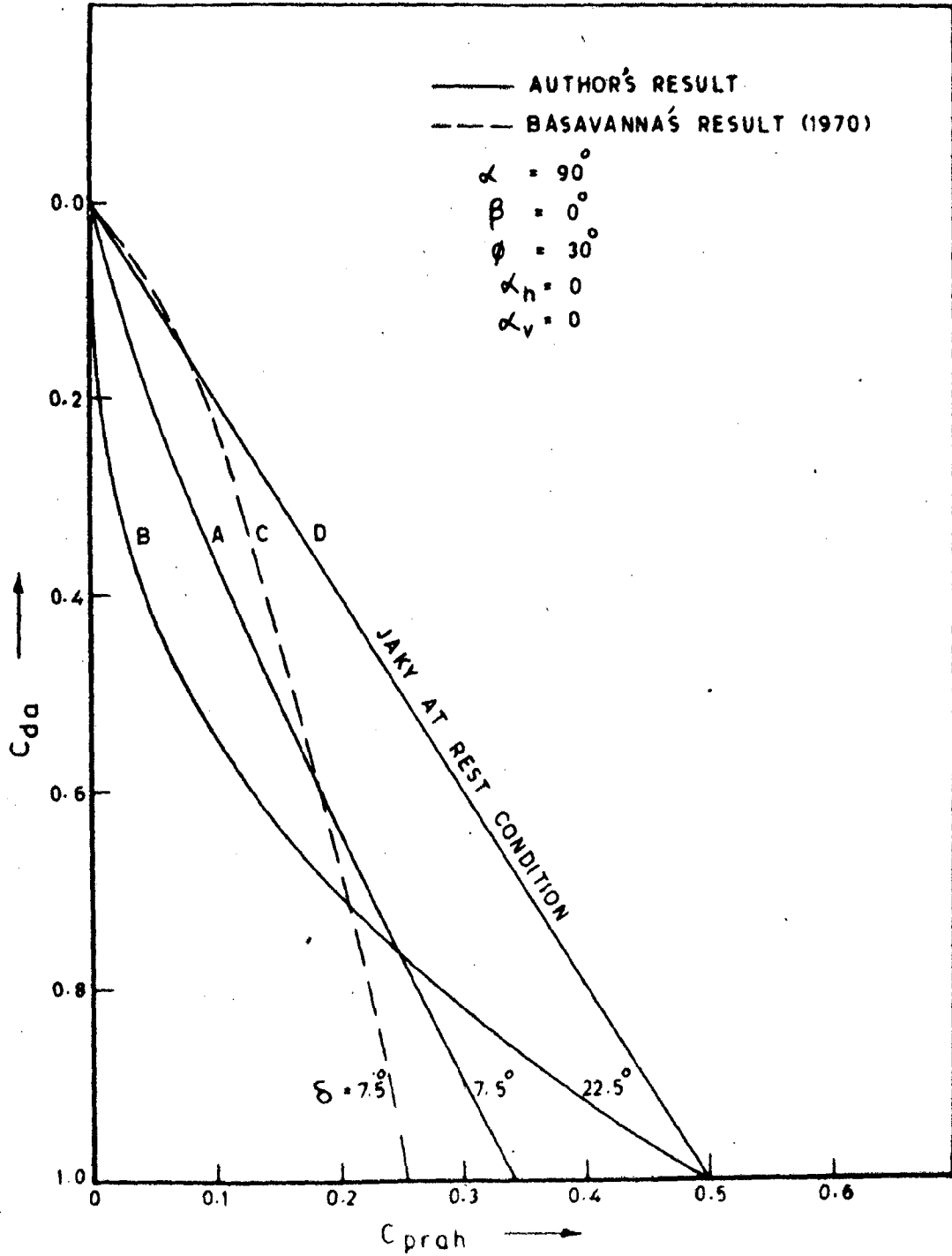


FIG. 4 103 - VARIATION OF C_{prah} WITH C_{da} FOR STATIC CASE BY DIFFERENT PROPOSALS

different vertical seismic coefficients converge to a single point when $\alpha_h = 0$. This is a reasonable finding, because, the vertical accelerations only change the net weight of the soil and as such will not be influencing the pattern of pressure distributions. The vertical acceleration will increase or decrease the pressure ordinates along the wall back. On the other hand, the curves obtained as per IS Code of Practice show a wide scatter at $\alpha_h = 0$ for various values of α_v . This indicates that the recommendation of the IS Code is not based on sound logical theoretical practice. This finding is another point in favour of this investigation.

It may also be observed from Fig. 4.10.2 that at higher values of α_h the scatter between C_{ha} values for various values of α_v also increases as per results obtained in this investigation and those by Basavanna's method. At any value of α_h other than $\alpha_h = 0$, the increase in positive value of α_v decreases the value of C_{ha} and increase in value of negative α_v increases C_{ha} . This is logical, because, the vertical inertia force will be more strongly felt near the base of the wall where the depth of the rupture wedge is more than near the top end of the rupture surface where the depth of the rupture wedge is relatively small. This results into shifting of the point of action of the soil reaction along the rupture surface closer to the base of the wall and hence a corresponding increase in C_{ha} . The trend of the curves obtained as per IS Code of Practice is opposite to this finding. This again

proves that the IS Code of Practice is not based on a sound theoretical background.

The method of analysis adopted in this investigation is very simple. Even when the numbers of discrete wedges is as small as five, the results of this analysis are accurate enough for all engineering practice for both static and dynamic conditions. This method of analysis is simple enough to be carried out even with the help of hand calculators. This is a significant advantage for field engineers as well as design engineers who do not have sophisticated computer facilities or highly trained technical manpower at their disposal for carrying out a more sophisticated analysis. This is particularly a significant advantage for a developing country like India, where it is the responsibility of the engineering community engaged in research and development to device suitable methods which are simple and yet reasonably accurate for all engineering purposes. It is believed that the work reported in this investigation is a right step in this direction.

The computed active dynamic earth force will be utilised in designing the wall properly. For this purpose, the equilibrium of the wall acted upon by this dynamic active earth force, inertia forces due to wall mass and the resisting forces at the base and in front of the wall should be considered. Richards and Elms (1979) have recommended the following expression for the weight of wall, W_w , given by :

$$W_w = \frac{\sin(\alpha - \delta) - \cos(\alpha - \delta) \tan \phi_b}{(1 - \alpha_v) (\tan \phi_b - \tan \theta)} \cdot E_a \quad (4.10.2)$$

where,

ϕ_b = angle of friction at the base of the retaining wall.

However, it may be noticed that this relationship is developed with the help of force equilibrium conditions only.

Like in Mononobe-Okabe theory, this relationship also neglects moment equilibrium condition which is required to be satisfied for proper design of the retaining wall. Since the proposed method successfully predicts that the overturning moments have a considerable significance in evaluating the stability of the retaining wall, it would be more logical to provide adequate moment of resistance in addition to the weight of the wall. If necessary, the weight of the wall may be increased suitably to satisfy this requirement. Expression cited above for the weight of the wall recommended by Richards and Elms has also neglected the passive resistance in front of the retaining wall which is not an insignificant quantity. As a result, the weight of the wall thus predicted is likely to be overestimated. Besides, the counterbalancing moment provided by passive earth force tends to reduce the resisting moment required to be mobilized at the base of the wall which may also lead to a further reduction in the base width and possibly the weight also of the retaining wall.

For any given earthquake, there will be many frequencies simultaneously acting. Therefore, the chances of occurrence of resonance or quasi resonance for a given soil wall system are rather remote. Seed et al (1970) have reported that the difference in seismic coefficients at the top and bottom levels of the wall may be of the orders of ten percent only for the dynamic conditions. Therefore, the assumption of same seismic coefficient for the entire soil wedge does not appear to be a source of significant errors.

Some of the recent methods reported which deal with the dynamic interaction with soil wall system have adopted method of analysis in elastic domain. The results of such investigation for the active earth pressure problem is questionable since the soil along the rupture surface has reached the plastic state. Further research is needed to throw considerable light on this topic. Till such date, the method of analysis adopted for this investigation and hence the results obtained may be considered to be reasonable.

CHAPTER - V

CONCLUSIONS AND SUGGESTIONS FOR FUTURE RESEARCH

5.1 CONCLUSIONS

The numerical method proposed by Joshi and Prajapati (1982) was used in this investigation to carry out extensive parametric studies. The highlight of this method is its ability to obtain pressure distribution due to soil reaction along the rupture surface and hence account for the moment equilibrium of the rupture wedge. The method is very general and many more applications are required to be studied in detail by additional parametric studies, discussed in detail in the next section. The results of the investigation have been presented in the form of dimensionless parameters. It is highly desirable that this practice be popularly used so that the results are independent of the units of the system as well as the size of the problem.

The following significant conclusions have been brought out based on the results of the parametric studies reported in this investigation :

- (1) The direction of interslice force defined by Eqn. 4.3.1 appears to be reasonable, because, the distribution of earth pressure and the soil reaction do not appear to be sensitive enough to the pattern of variation of this quantity.

- (2) Even the use of five discrete wedges appears to be accurate enough for all engineering purposes to obtain pressure distribution for static and dynamic cases. This makes the method ideally suited for solution with minicomputers as well as by ~~long~~ hand Calculators. Design engineers as well as field engineers who may not have computing facilities at their disposal will find this method very helpful particularly in a developing country like India.
- (3) It is not desirable to consider wall back leaning away from the fill, because, it invariably results into higher values of earth force and overturning moments. Therefore, it is strongly recommended that walls with vertical back or back slightly leaning towards the fill may be favoured.] Construct
- (4) The angle of surcharge should be designed in such a way that under dynamic conditions it does not fail due to inadequate slope stability. The limiting value of β predicted by Eqn. 3.2.1 is based on force equilibrium only. It is recommended that to provide adequate safety with respect to moment equilibrium condition this limiting value of β may be further reduced by five degrees. It may be more economical in certain cases to reduce the angle of surcharge to economise the wall design against overturning moments. With increasing angle of surcharge

static and dynamic earth forces and overturning moments increase sharply.

- (5) When sufficient wall motion takes place to develop active condition in the field, the relative motion between the rupture wedge and the wall back is large enough to mobilize optimum value of wall friction. The common practice of relating wall friction to angle of shearing resistance only is inadequate. It is also influenced by angle of surcharge but more significantly by angle of wall back. Simple relationship has been developed in this investigation relating angle of shearing resistance of back fill, the angle of wall back and angle of wall friction for static case with level backfill. The common notion that wall friction for dynamic condition is less than that with static case is always not true.
- (6) With increasing value of angle of shearing resistance of soil the earth force and overturning moment decrease appreciably even though the point of action of earth force moves slightly away from the base. This is true for both static as well as dynamic case.
- (7) As the horizontal seismic coefficient increases the inertia force due to upper portion of the rupture wedge ~~causes considerable~~ increase in earth pressure on the upper portion of the wall. This leads to an

increase in earth force and a more significant increase in the overturning moment. Positive value of the vertical seismic coefficient tends to lower the overturning moments and the negative value shows the opposite trend. This is more pronounced at higher values of horizontal seismic accelerations.

- (8) Basavanna's theory for obtaining pressure distribution does not appear to be reasonable. The recommendations cited in IS Code of Practice (IS: 1893 : 1975) for obtaining point of application of dynamic earth force do not appear to be based on sound theoretical background as the relationship between point of application and the horizontal seismic coefficient recommended by the Code shows tendencies opposite to those obtained in this investigation and also by Basavanna's theory.
- (9) The common concept of linear variation of earth pressure behind the wall is inadequate even for the static case and especially for the dynamic case. To represent the nature of pressure distribution adequately, use of C_a and N is very strongly recommended.

5.2 SUGGESTIONS FOR FUTURE RESEARCH

Eventhough the parametric studies have indicated that the earth pressure is relatively insensitive to variation pattern of orientation of inter-slice forces, it would be desirable to establish this quantity experimentally through measurement of internal stresses.

Most of the experimental evidence reported is based upon tests on small retaining wall models. It would be highly desirable to obtain test data from large scale tests under static and dynamic conditions to eliminate scale errors, if any. Of particular interest would be the study of internal stresses and deformations within the rupture wedge.

Eventhough this investigation has covered most of the significant parameters influencing the earth pressures, some of the parameters not included are : effect of partial submergence of the backfill and influence of concentrated and distributed surcharge loads.

The wall movements required to reach active state in the backfill are specified arbitrarily as per present day state of art . It is very much desirable that suitable relationships are established to predict the wall motion required in terms of material properties of the soil-wall system that can be obtained by laboratory tests.

R E F E R E N C E S

- Aggour, M.S. and C.B. Brown(1973), 'Retaining Wall in Seismic Areas', Proc., 5th World Conference on Earthquake Engg. Rome.
- Arya, A.S. and Y.P. Gupta(1966), 'Dynamic Earth Pressures on Retaining Walls due to Ground Excitations', Bull. Indian Society of Earthquake Technology, Roorkee, Vol. III, No. 2.
- Basavanna, B.M.(1970), 'Dynamic Earth Pressure Distribution behind Retaining Walls', Proc., 4th Symposium on Earthquake Engg., University of Roorkee, Roorkee.
- Coulomb, C.A.(1776), 'Essai sur une application des regles des maximis et minimis a quelque problems de statique relalifs a l' architecture', Mem. acad. roy. pres. diverssavants, Vol. 7, Paris.
- Culmann, C.(1886), Graphische Static, Zurich.
- Franzius (1924), Refer Prakash, Ranjan and Saran (1979).
- Fulton (1920), Refer Prakash, Ranjan and Saran (1979).
- Indian Standard Recommendations for Earthquake Resistant Design of Structures, IS:1893-1975(Third Revision).
- Ishii, Y., H. Arai and H. Tsuchida(1960), 'Lateral Earth Pressure in an Earthquake', Proc., 2nd World Conference in Earthquake Engineering, Tokyo, Vol. 1, p. 211.
- Jacobsen, L.S.(1951), 'Kentucky Project Report No. 13', TVA Series 1951, Appendix D.
- Janbu, N.(1957), 'Earth Pressures and Bearing Capacity Calculation by Generalized Procedure of Slices', 4th International Conference on Soil Mechanics and Foundation Engineering, London, pp 207-212.

- Jaky, J. (1944), 'The Coefficient of Earth Pressure at Rest', Journal of the Society of Hungarian Architects and Engineers, Budapest, Hungary, pp. 355-358.
- Johnson (1953), Refer Prakash, Ranjan and Saran (1979).
- Joshi, V.H. and S. Mukherjee (1981), 'Seismic Displacement Analysis for Surface Hydrel Power Stations in Cohesionless Soil', Bull. ISET, Vol. 18, No. 3, Sept. 1981, pp. 125-130.
- Joshi, V.H. and G.I. Prajapati (1982), 'Active Pressure Distribution due to Cohesionless fills', VII Symp. on Earthquake Engineering, University of Roorkee, Vol. I.
- Joshi, V.H. (1982), 'Earth Pressures for Aseismic Design of Retaining Walls', VII Symp. on Earthquake Engineering, University of Roorkee, Vol. I.
- Joshi, V.H. and G.K. Panigrahy, (1985), 'Active Earth Pressure Distribution for Design of Retaining Structures', Accepted for Publication, Computer 85, Second Int. Conf. on Computer Aided Analysis and Design in Civil Engg.
- Kapila, I.P. (1962), 'Earthquake Resistant Design of Retaining Walls', 2nd Symposium on Earthquake Engineering, University of Roorkee, Roorkee, pp. 97-108.
- Krishna, J., S. Prakash and P. Nandakumaran (1974), 'Dynamic Earth Pressure Distribution Behind Flexible Retaining Walls', Journal, Indian Geotechnical Society, Vol. 4, No. 3, July, pp. 207-224.
- Madhav, M.R. and N.S.K. Rao (1969), 'Earth Pressures under Seismic Conditions', Soils and Foundations, Japan, Vol. IX, No. 4.
- Matsuo, H. (1941), 'Experimental Study on the Distribution of Earth Pressure Acting on a Vertical Wall During Earthquakes', Journal, Japanese Society of Civil Engg. Vol. 127, No. 2.

- Matsuo, H. and S. Ohara (1960), 'Lateral Earth Pressure and Stability of Quay Wall during Earthquakes', Proc., 2nd World Conference on Earthquake Engineering, Tokyo, Vol. 1, pp. 165-183.
- Mononobe, N. and H. Matsuo (1940), 'On the Determination of Earth Pressures during Earthquakes', Proc. World Engineering Conference, Vol. 9, p. 176.
- Muller and Breslau (1916), Refer Prakash, Ranjan and Saran (1979).
- Nadim, F. and Whitman, R. V. (1983), 'Seismically Induced Movement of Retaining Walls', Journal of ASCE, Geotechnical Division, July, pp. 915-919.
- Nandkumaran, P. (1973), 'Behaviour of Retaining Walls under Dynamic Loads', Ph.D. Thesis, Roorkee University, Roorkee, India.
- Nandkumaran, P. and V. H. Joshi (1973), 'Static and Dynamic Active Earth Pressures Behind Retaining Walls', Bull. Indian Society of Earthquake Technology, Sept., Vol. 10, No. 3.
- Okabe, S. (1926), 'General Theory of Earth Pressures', Journal Japanese Society of Civil Engineers, Tokyo, Japan, Vol. 12, No. 1.
- Prakash, S. and S. Saran (1966), 'Static and Dynamic Earth Pressures Behind Retaining Walls', Proc. 3rd Symposium on Earthquake Engineering, University of Roorkee, Roorkee, India, Vol. 1, pp. 277-288.
- Prakash, S. and B. M. Basavanna (1969), 'Earth Pressure Distribution Behind Retaining Walls During an Earthquake', Proc., 4th World Conference in Earthquake Engineering, Santiago, Chile.
- Prakash, S. and P. Nandkumaran (1969), 'Earth Pressure Distribution on Flexible Walls with Rigid Foundations During Earthquakes' (unpublished) Earthquake Engineering Studies, University of Roorkee, Roorkee, India.

- Prakash, S. and P.Nandakumaran(1973), 'Dynamic Earth Pressure Distribution on Rigid Walls', Proc., Symposium on Earth and Earth Structures Subjected to Earthquakes and other Dynamic Loads, Roorkee, March, Vol.1, pp.11-16.
- Prakash, S. and P.Nandakumaran(1979), 'Earth Pressures during Earthquakes', Proc., 2nd U.S.National Symposium on Earthquake Engineering, Stanford, pp.613-622, August.
- Prakash, S., G.Ranjan and S.Saran(1979), 'Analysis and Design of Foundations and Retaining Structures', Sarita Prakashan, Meerut, India.
- Prakash, S., P.Nandakumaran and J.Krishna (1981), 'Displacement Analysis of Rigid Retaining Walls during Earthquakes', Unpublished Report, Univ.of MO-Rolla, Rolla, MO.
- Prakash, S., V.K.Puri and J.U.Khandoker (1981), 'Rocking Displacements of Rigid Retaining Walls during Earthquakes', Companion Paper to Conference on Recent Advances in Geotechnical Earthquake Engineering and Soil Dynamics, Vol.3, St.Louis, MO, April-May.
- Rankine, W.J.M.(1857), 'On the Stability of Loose Earth', Phi. Trans.Royal Soc., London.
- Richards, R.Jr. and D.G.Elms (1979), 'Seismic Behavior of Gravity Retaining Walls', Journal, Geotech.Eng.Div., ASCE, Vol.105, No.GT4, April, pp.449-464.
- Sano, R. (1916), 'Theory of Aseismic Design of Buildings', Report of Imperial Earthquake Investigation Committee, Vol. 83, A.
- Scott, R.F.(1973), 'Earthquake Induced Earth Pressures on Retaining Walls', Proc.5th World Conference on Earthquake Engg. Rome, Vol.2, pp.1611.

Seed, H. B. and R. V. Whitman (1970), 'Design of Earth Retaining Structures for Dynamic Loads', ASCE Specialty Conference on Lateral Stresses in the Ground and Design of Earth Retaining Structures, pp.103-147, Ithaca, NY.

Sim, L. C. and J. B. Berrill (1979), 'Shaking Table Tests on a Model Retaining Wall', Paper presented to the South Pacific Regional Conference on Earthquake Engineering, Wellington New Zealand, May.

Terzaghi, K. (1928-29), Refer Prakash, Ranjan and Saran (1979).

Terzaghi, K. (1936), 'A Fundamental Fallacy in Earth Pressure Computations', Contributions to Soil Mechanics 1925 to 1940, Boston Society of Civil Engineers.

Terzaghi, K. (1941), 'Theoretical Soil Mechanics', John Wiley and Sons, New York, NY.

B I O D A T A

Name	Gopal Krishna Panigrahy	
Born	24th March, 1955, at Berhampur, Orissa	
Education	Panchayat U.P.School, Bendalia, Orissa	1960-65
	M.H.School, Berhampur, Orissa	1965-71
	College of Basic Science and Humanities Bhubaneswar, Orissa	1971-72
	Khalikot College, Berhampur	1972-73
	University College of Engg. Burla	1973-78
	University of Roorkee	1981-83
	Degree	B.Sc. Engg. (Civil), Sambalpur University
Experience	Irrigation Department, Orissa	1978 onwards
Membership of Professional Society	1. Life Member, Indian Geotechnical Society	
	2. Life Member, Indian Society of Earthquake Technology.	
Publications	Joshi, V.H. and Panigrahy, G.K (1985), 'Active Earth Pressure Distribution for Design of Retaining Structures', Accepted for Publication, Computer 85, Second International Conference on Computer Aided Analysis and Design in Civil Engineering, 1985.	